UNIVERSITA' DEGLI STUDI DELL'INSUBRIA

DOTTORATO DI RICERCA IN SCIENZE DELLA VITA E BIOTECNOLOGIE

XXXIII CICLO

Shwachman Diamond Syndrome: a multidisciplinary approach to better understand the pathogenesis and clinical implications.

Docente guida: **Prof. Roberto Valli**

Tesi di dottorato di:

Abdul Waheed Khan

Matricola: 735309

DBSV- Università degli Studi dell'Insubria

Anno accademico 2020-2021

Acknowledgements

Praises be to Allah Almighty who bestowed upon me his grace and blessings to eventually compile my PhD study. In this whole journey despite challenges, I got the opportunity of interacting with nice people that made this overall journey much easier and joyous.

First and foremost, I am profoundly thankful to my mentor Prof. Roberto Valli for his supportive and friendly company, ease of access and useful suggestions that always motivated me to sustain the track leading toward my goals, especially in unfortunate harsh moments of failure.

I was fortunate to work with Prof. Emanuela Maserati, Emeritus Prof. Francesco Pasquali and Prof. Giovanni Porta whose age long experience and supervision was highly fruitful and is greatly appreciated. I am grateful to PhD coordinators, Prof. Silvia Sacchi (incumbent) and Prof. Loredano Pollegioni (ex) for their timely administrative and courses associated guidance in general, and for arranging courses in English in particular.

I express my gratitude toward our collaborators, Dr. Annalisa Frattini, Dr. Marianna Penzo, Dr. Marco Cipolli, Dr. Valentino Bezzerri and Dr. Greta Forlani and team members (Mariam, Fabrizio and Alessendra).

Thanks to all our workplace staff members, especially Giuseppe Montalbano and Paola, and workplace colleagues (Ilaria Caon, Elena Carava, Giovanni Micheloni, Michella Bistoletti, Barbara Bartolini, Giorgia, Annalisa Bosi, Arianna Parnigoni, Davide, Vittoria and Pamela) as well as my PhD class mates (Valentina, Elisa, Elenora, Elena and all other fellows) who deserve a special mention for being always supportive whenever needed. Not to forget, my neighbors, Evangelia Pantelaki, Tiziana

Romanazi and Nicholas Delfrate, along with Collegio Carlo Cattaneo staff who made my stay at the college extremely pleasant and memorable.

At this mesmerizing moment, I have to remember my parents who endure my absence, teachers who laid the foundation of my research career (Prof. Abid Ali, Prof. Ijaz Ali, Prof. Aqib Iqbal, Prof. Iqbal Munir, Prof. Muhammad Fahim and Prof. Israr ud Din), friends (Dr. Zeeshan Nasim, Dr. Fazli Zahir, Dr. Sadia Nawab and Dr. Saba Gul), siblings, family members and all well-wishers for their prayers and endorsement. I supplicate that may our Lord Almighty guide us all in our future endeavors.

Thank you Italy!

Regards,

Abdul Waheed Khan.

CONTENTS

Abstract

Introduction: Shwachman Diamond syndrome (SDS) is an autosomal recessive condition that is attributed to mutations in *SBDS* gene. Due to the functionally versatile nature of SBDS protein, the effects due to mutations in *SBDS* gene are reflected at cellular level and clinically as diverse phenotypes.

Material and Methods: In this study, we analyzed karyotype instability and chromosomal aberrations that take place in SDS patients' bone marrow (BM) by techniques like karyotyping, fluorescent in situ hybridization and comparative genomic hybridization array. We also carried out a comparative BM and osteoblasts gene expression pattern of SDS patients with healthy controls using expression arrays. Lastly, we exploited the ability of ataluren to restore *SBDS* nonsense mutation.

Results: We found that all twenty five SDS patients that we studied for karyotype instability carried del(20)(q) in their BM, where *EIF6* gene was lost unanimously and interstitially. The gene expression pattern of the SDS patients BM and osteoblasts was quite different than the healthy controls. The use of ataluren apparently restored the nonsense mutation in *SBDS* gene.

Conclusion: We highlighted the loss of *EIF6* in del(20)(q) by SDS patients that acts as a mechanism to compensate the deficiency of SBDS. It was also established that the gene expression pattern of SDS patients is different than the healthy controls. We also demonstrated the apparent potential of ataluren as a therapeutic option for SDS.

Keywords: Shwachman Diamond syndrome, del(20)(q), genomic instability, expression array, ataluren.

1. INTRODUCTION

1.1 General background and basic features

Shwachman–Diamond syndrome (SDS, OMIM #260400) is a rare autosomal recessive disorder that manifests diverse symptoms including exocrine pancreatic deficiency, hematological disorders, bone marrow irregularities and neurodevelopmental complications (Dror 2005). Historically, the syndrome was reported by Bodian and Schwachman in 1964 for the first time (Bodian et al. 1964; Shwachman et al. 1964). With an estimated incidence of 1 out of 76000 individuals (Goobie et al. 2001), the condition is considered to be the 3rd most common cause of bone marrow failure (BMF) following Diamond-Blackfan anemia and Fanconi anemia (Ginzberg et al. 1999a). The Italian SDS registry assumes the incidence of SDS to be 1 out of 153000 births (Cesaro et al. 2020).

The age of SDS diagnosis may fluctuate largely among individuals, families and ethnic groups (Donadieu et al. 2012). However, the disorder is commonly ascertained in the first few years of the person facing the condition (Ginzberg et al. 1999b) as indicated by symptoms like growth abnormalities, steatorrhea, and vulnerability to recurrent infections. Additionally, hepatomegaly, behavioral and neural abnormalities may also be observed in such individuals (Rothbaum et al. 2002; Kerr et al. 2010). The symptoms of SDS are wide, heterogeneous and overlapping with other disorders. Therefore, they may sometime cause difficulties in the diagnostic process.

In genetic terms, SDS patients contain biallelic mutations in the *SBDS* gene (Shwachman–Bodian–Diamond syndrome gene) in 90% of clinically diagnosed patients (Boocock et al. 2003). *SBDS* gene is positioned on the long arm of chromosome 7. It was discovered in 2003 and retains physiologically crucial mutations in the exon 2 region of the *SBDS* gene (Boocock et al. 2003). Among these mutations, the most critical mutation is c.183_184TA>CT, that causes an in-frame

introduction of premature termination codon (PTC). The second mutation of *SBDS* is a substitution mutation defined as c.258+2T>C. This mutation disrupts the donor splice site of intron 2 which results in the use of an upstream cryptic donor splice site at position 251_252 as an alternative. The c.258+2T>C may be considered a hypomorphic mutation as some quantity of normal protein is still produced that is available to the cell for its use (Valli et al. 2017a). The exact role of SBDS is not fully known, however, it is believed that it helps in cell division and ribosomal biogenesis (Austin et al. 2008; Finch et al. 2011; Wong et al. 2011). Due to its importance in ribosomal biogenesis and function, sometimes SDS is classified as a ribosomopathy. In addition to *SBDS* gene*, DNAJC21, SRP54, EIF6* and *EFL1* genes have been also recently added to the group of causative genes (Dhanraj et al. 2017; Stepensky et al. 2017; Tan et al. 2019; Koh et al. 2020).

2. Clinical profile of SDS patients

SDS comprises of a diverse range of symptoms and abnormalities that may vary among individuals. However, there are some parameters that are common up to a greater extent in the affected individuals.

2. 1. Hematological features

Primarily, bone marrow failure is a big risk faced by SDS patients. Generally, one or more hematopoietic stem cell line may be suppressed due to the disorder, and can give rise to hematological abnormalities, as identified by multiple studies carried on SDS patients (Ginzberg et al. 1999b; Donadieu et al. 2012). Neutropenia (neutrophil count less than 1,500 × 10^9/L) is one of the leading indicators exhibited by 88–100% of patients with SDS (Ginzberg et al. 1999b). Another study estimated neutropenia to be about 81% whereas neutropenia together with steatorrhea in 51% of SDS patients (Myers at al. 2014). Neutropenia may be persistent or intermittent, making SDS patients vulnerable to a wide range of infections (Cipolli et al. 1999). Neutrophils may have defective functions including impaired chemotaxis (Cipolli et al. 1999). Due to undermined neutrophils, vulnerability to recurrent infections such as otitis media,

osteomyelitis, respiratory tract problems, and septicemia etc., may be increased (Ginzberg et al. 1999a; Mack et al. 1996). According to an estimate, 42% SDS patients show anemia, whereas thrombocytopenia (platelet count <150 × 10^9/L) is reported in 34% of the patients (Ginzberg et al. 1999b). Further, elevated level of hemoglobin F has been commonly observed in SDS patients (Dror and Freedmen 1999).

Generally, SDS patients exhibit pancytopenia, bone marrow hypoplasia, fats deposition and compromised progenitor cells (Bidou et al. 2012). Abnormal levels of granulocyte-monocyte colony-forming units and erythrocyte burst-forming units (BFU-E) have been highlighted precisely. Moreover, in comparison to healthy individuals, bone marrow CD34+ cells of SDS patients are substantially reduced, which eventually contribute toward decreased clonogenic ability (Mercuri et al. 2015). These observations provide the fundamental evidence that origin of SDS is linked to preliminary malfunctioning at the hematopoietic stem cells level.

There is an increased risk associated with SDS patients to progress toward myelodyplastic syndrome (MDS) and undergo malignant changes, acute myeloid leukemia (AML) particularly. AML-6 which is a subtype of AML, is the most prevalent form observed in SDS. It is noticed in approximately 30% cases suffering from leukemic condition. The probability of leukemia and dysplastic condition may be seen between 14% to 30% cases (Dror et al. 2011) that can increase with age. The risk of developing MDS in general population is comparatively substantially less, and especially rare in young individuals. According to an estimate, the median age at onset of MDS in general population is 71 years (Bannon et al. 2016). Moreover, SDS patients with AML or MDS show poor prognosis and response to therapeutic interventions (Myers et al. 2019).

2.2. Exocrine pancreatic malfunction

Exocrine pancreatic dysfunction is a pivotal indicator in SDS along with other signs (Mack et al. 1996). Prior to the discovery of *SBDS* gene, exocrine pancreatic malfunction was considered as a vital factor in clinical diagnosis of SDS. Insufficient

quantity of pancreatic digestive enzymes is observed constantly in the early years of development, however, in the later ages, it is partially resolved. Improper digestion and absorption of nutrients along with steatorrhea could be the result of this disorder. Inadequate levels of digestive enzymes are generally ascertained by reduced serum trypsinogen and isoamylase (Ip et al. 2002). Examination of pancreatic tissue demonstrates scarcity of pancreatic acini overwhelmed by fatty accumulation (Nicolis et al. 2005). Shortage of digestive enzymes in SDS patients is compensated by exogenous supply of digestive enzymes formulations. However, such enzymes supplements may not be a perfect alternative for digestive enzymes to ensure normal health conditions, especially in children. A report by Pichler et al. (2015) demonstrated the discrepancy of vital vitamins such as vitamin A and E and other important trace elements like zinc, copper and selenium in children despite provision of pancreatic enzyme supplements in their diet.

2. 3. Skeletal and neuro-developmental abnormalities

SDS is accompanied by clinical or subclinical level bone and skeletal framework issues of variable degree (Mack et al. 1996). Generally, defects in the rib-cage, thoracic dystrophy and metaphyseal problems are common signs in SDS (Aggett et al. 1980; Ginzberg et al. 1999b). Other skeletal parts that are most likely affected comprise of regions of vertebrae, knees, wrists and ankles etc. As a result of reduced nutrients and minerals mal-absorption, bone dysostosis, osteoporosis and osteomalacia may also be observed (Makitie et al. 2004). These factors enhance the thinning of cartilages, deformation of joints and shortening of ribs. Skeletal dysplasia, reduced ossification and low turnover are the reasons for the irregularities in the bones framework (Toiviainen-Salo et al. 2007).

In addition to skeletal abnormalities, complications related to brain morphology and performance is reported. Overall cognitive efficiency is undermined which is characterized by behavioral issues and learning inefficacy compared to healthy subjects. A small scale study revealed that SDS patients had reduced skull

circumference and small brain volumes (Toiviainen-Salo et al. 2008). Further, those patients also showed less white and grey matters and slow myelination process compared to controls. In a similar study that included SDS patients, cystic fibrosis patients and corresponding healthy controls, it was evident that patients with SDS were confronted with cognitive and behavioral deficiencies (Kerr et al. 2010). The most noticeable indicators were intellectual level, attention and interpretation, memorization, communication and ability to socialize with people. These abnormalities were apparently attributed to SDS as demographic parameters like age, gender and family status had no influence on the outcome of the study.

2.4. Liver and other organs

The presence of enlarged liver (hepatomegaly) and elevated liver enzymes are mostly observed in young subjects (Aggetti et al. 1980; Ginzberg et al. 1999b; Ip et al. 2002). However, this tends to normalize with growing age. Other organs such as kidneys may also show compromised renal function due to renal tubular acidosis and problems in urinary tract (Donadieu et al. 2005).

Dental issues may be also observed. SDS patients exhibit dental dysplasia and are prone to dental caries and other periodontal complications (Dror et al. 2011)

3. Criteria for diagnosis, management and treatment

3. 1. Diagnosis

SDS patients are generally noticeable for their symptoms in the initial years of life. Cesaro et al. (2020) estimated the median diagnosis age for SDS patients of Italian registry to be 1.3 years (range, 0-35.6 years). As SDS symptoms may overlap with other health conditions like cystic fibrosis, Johanson–Blizzard syndrome, Fanconi anemia etc., misdiagnosis or delayed diagnosis was possible previously. However, due to advancement in genomics, the molecular diagnosis has overcome this barrier to a large extent.

In general, the clinical criteria for declaration of SDS is comprised of: (1) proof of exocrine pancreatic insufficiency which includes suboptimal trypsinogen and isoamylase in the serum, decreased fat-soluble enzymes quantity, extraordinary 72-hours fecal fats amount in together with pancreatic imaging abnormalities and (2), demonstration of BMF, that is achieved by the presence of neutrophils < 1500 $\times 10^6$/L, hemoglobin < 10 g/dL, or platelets < 150 × 10^6/L accompanied by elevated hemoglobin F proportion and pancytopenia (Mark et al. 1996; Rothbaum et al. 2002; Woloszynek et al. 2004). Nevertheless, multiple indicators among these parameters are considered supportive and are not strictly considered only in the case of SDS diagnosis.

Since the discovery of *SBDS* gene in 2003 by Boocock et al. (2003), the molecular diagnosis has become more reliable tool for SDS diagnosis. The presence of biallelic mutations in the *SBDS* gene have been regarded crucial in the revised updated criteria for SDS diagnosis now (Dror et al. 2011). In approximately 10% patients, SDS-like condition was found even in the presence of a normal *SBDS* gene (Boocock et al. 2003). This observation remained a mystery until recently conducted studies where few diagnosed cases revealed the existence of SDS despite lack of mutations in the *SBDS* gene. Upon detailed sequencing, those mutated genes were identified as *DNAJC21* (Dhanraj et al. 2017), *EFL1* (Stepensky et al. 2017), *SPR54* (Carapito et al. 2017) and *EIF6* gene (Koh et al. 2020). These results indicated that *SBDS* gene might be the causative mutant gene in most but not in all SDS cases. Therefore, SDS validated its heterogeneity both at phenotypic and genomic levels.

3. 2. Post diagnosis clinical surveillance

Once an individual is diagnosed with SDS, it is important to initiate the follow-up programs of clinical surveillance. The recommended protocol for such individuals is comprised of series of periodic monitoring procedures for hematological, pancreatic and other related aspects such as gastrointestinal and skeletal framework (Dror et al. 2011).

Hematological assessment is carried out regularly every 3-6 months to examine full peripheral blood counts. Bone marrow condition is determined by biopsy and cytogenetic monitoring every 1-3 years for evaluation of possible karyotypic changes and risk of AML/MDS (Dror et al. 2011). Similarly, information about the status of exocrine pancreatic functionality is also recommended during the follow-up period. It has been reported that with growing age the performance of exocrine pancreatic parameters may improve in most patients (Mack et al. 1996). Additionally, keeping check on the levels of various vitamins notably, vitamin A, D and E are also considered vital to oversee vitamins scarcity due to compromised absorption of fats (Dror et al. 2011). Moreover, sessions of counseling with experts are proposed to understand the communication, social and behavioral status of SDS patients for alleviating mental and cognitive problems (Dror et al. 2011).

3.3. Treatment

Treatment options for SDS are limited and mostly consist of symptoms-based supportive interventions. Pancreatic insufficiency is addressed by provision of supplements containing pancreatic enzymes. The formulation can be administered orally and the dosage should be carefully regulated. It has been established that response to exogenously supplied enzyme supplements is outstanding in SDS unlike patients suffering from cystic fibrosis. Nutritional deficiencies could be settled by vitamins supply. Peripheral blood hematological conditions may need blood transfusions while infection due to bacterial/fungus in the circumstances of neutropenia should be controlled by granulocyte colony stimulating factor (GCS-F) doses in conjunction with antibiotics (Dror et al. 2011).

Hematopoietic stem cells transplantation (HSCT) is another treatment option for SDS patients under defined conditions as it has its own limitations. The chances of HSCT success is 80% in the case of aplastic anemia (Dror et al. 2011). However, this percentage lies between 30%-40% in the case of patients with MDS or acute leukemia (Dror et al. 2011). A recent study concluded that a major determining factor in the

success of HSCT in various inherited bone marrow failure syndromes including SDS is associated to the timing of the transplant and stage of the disease (Dalle and de Latour 2016). Hence, HSCT may prove more fruitful in the early stage of a disease before development of complications. Hence there is a need to use better surveillance strategies including computer algorithms and risk assessment tools, as well as timely intervention, to reduce the chances of bone marrow malignant transformation and development of complications in SDS patients (Myers et al. 2019)

4. Molecular genetics and pathogenesis of SDS

4. 1. Structure and mutations of *SBDS* gene

Despite the identification of SDS in year 1964 (Bodian et al. 1964; Shwachman et al. 1964), limited knowledge existed about genetics of the syndrome. In 2003, a breakthrough highlighted SBDS (Shwachman Diamond Bodian Syndrome) gene to be the responsible gene for SDS (Boocock et al. 2003). Orthologues of *SBDS* have been reported in all major kingdoms of life including eukaryotes, plants and archea (Boocock et al. 2003).

In humans, *SBDS* resides on chromosome 7 at locus 7q11. It encodes a transcript of 1.6 Kb size which is translated into a highly conserved protein of 250 amino acids. The *SBDS* gene is composed of five exons that stretch over a length of 7.9 Kb. Interestingly, a pseudogene copy of *SBDS* is also present in the genome on the distal side at a distance of 5.8 Mb from the normal *SBDS* gene known as *SBDSP.* The pseudogene copy has accumulated various mutations during evolutionary process that impair its coding ability. However, with about 97% sequence similarity to the actual *SBDS* gene, the *SBDSP* remains a leading reason for disease-related mutations due to gene conversion (Boocock et al. 2003) (Fig 1).

Mutations that accumulate in the *SBDS* gene are mostly localized within the exon 2 region. Two mutations in the exon 2 region of *SBDS* are substantially important (Boocock et al. 2003). The first and the most critical mutation is a dinucleotide

substitution mutation c.183_184TA>CT that causes an in-frame placement of PTC. This mutation does not exist in homozygous form due to its lethality, as demonstrated in mouse model (Zhang et al. 2006). The second mutation is a substitution mutation c.258+2T>C that disrupts the donor splice site of intron 2 which results in the use of an upstream cryptic donor splice site at position 251_252 as an alternative. In the case of c.258+2T>C mutation, it is speculated that limited quantity of normal SBDS protein is still produced that is available to the cell for its use. Valli et al. (2017a) has highlighted this mechanism in a schematic manner (Fig 2).

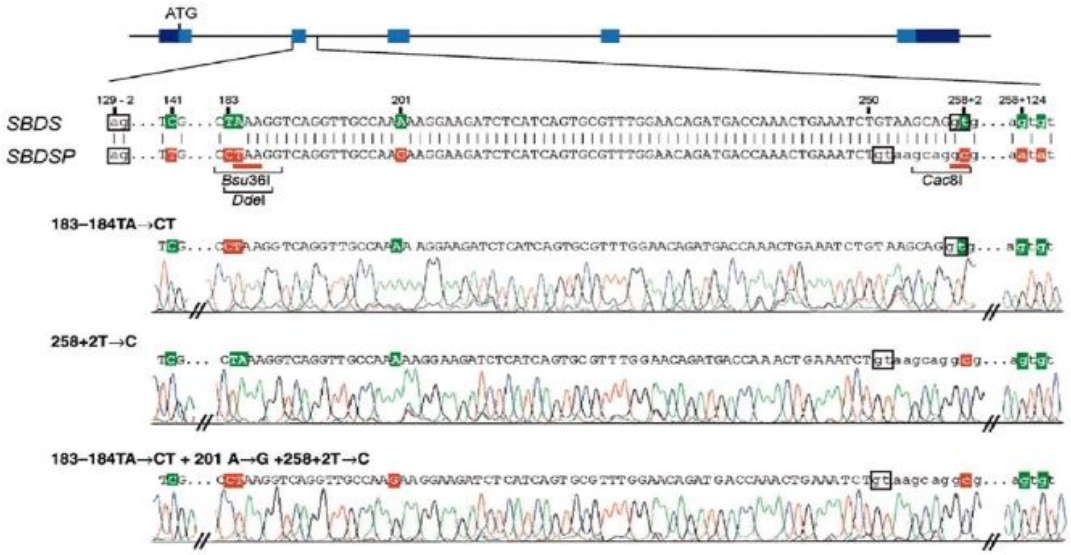

Figure 1. Sequence comparison based map of *SBDS* and *SBDSP* shows position of various important mutations (Boocock et al. 2003). Image available under Creative Commons Attribution License.

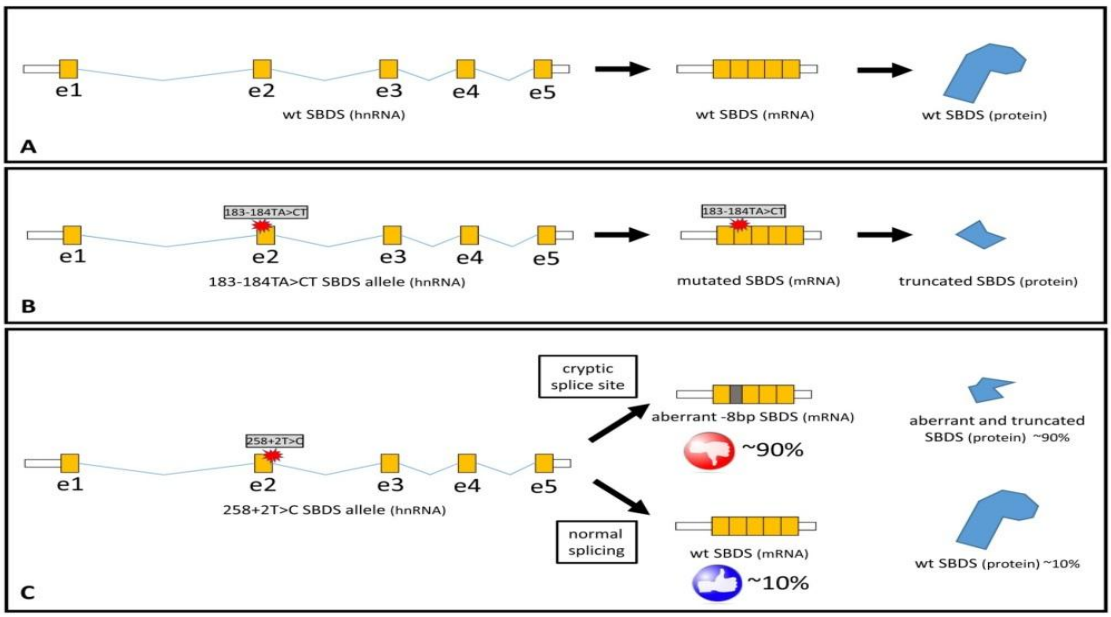

Figure 2. (a) Wild-type *SBDS* gene generates wild-type mRNA and wild-type functional SBDS protein. (b) *SBDS* allele with c.183-184TA>CT mutation generates premature stop codon that give rise to truncated non-functional protein. This allele is lethal in homozygous condition (c) SBDS allele carrying c.258+2T>C mutation impairs splice-site in the start of the intron 2. A cryptic splice-site within the exon 2 is utilized to create an aberrant mRNA with 8bp deleted frameshift sequence in 90% circumstances, encoding truncated non-functional protein. In 10% events, normal splicing produces normal SBDS mRNA and consequently normal SBDS protein. Compromised SBDS protein in this case attribute towards SDS pathogenesis (Valli et al. 2017a). Image available under Creative Commons Attribution License.

4. 2. SBDS function and interaction with EIF6

SBDS has been known for its versatile function in multiple cellular processes. Mainly, SBDS is reported to facilitate cell division events like spindle formation (Austin et al. 2008), DNA replication (Ball et al. 2009) plus ribosomal biogenesis (Finch et al. 2011; Wong et al. 2011). These studies have shown that SBDS deficiency give rise to issues during cell division and ribosome associated cellular operations. Hence, chromosomal instability and ribosomal defects may be the aftermath in such individuals. However, the threshold amount of SBDS needed for proper functioning of cellular machinery may vary in different cells and setups (Wong et al. 2010).

Finch et al. (2011) established that SBDS is required to interact with elongation factor-like 1 (EFL1) for the removal of eukaryotic translation initiation factor 6 (eIF6) from

pre-60S subunits. The attachment of eIF6 to the pre-60S subunit hinders the ribosomal subunits joining, hence, eIF6 acts as an anti-association factor during the ribosomal assembly. On the contrary, SBDS exploits EFL1 GTP hydrolysis to ensure the release of eIF6 and facilitate the association between pre-60S and 40S ribosomal subunits.

Apart from *SBDS* gene, *DNAJC21* (Dhanraj et al. 2017), *EFL1* (Stepensky et al. 2017), *SRP54* (Carapito et al. 2017) and *EIF6* (Koh et al. 2020) genes have been also recently identified to cause SDS in the absence of *SBDS* mutations (Table 1). The discovery of *DNAJC21, SRP54, EFL1* and *EIF6* implies that the association of other currently unknown genes which could cause SDS or SDS-like condition cannot be ruled out.

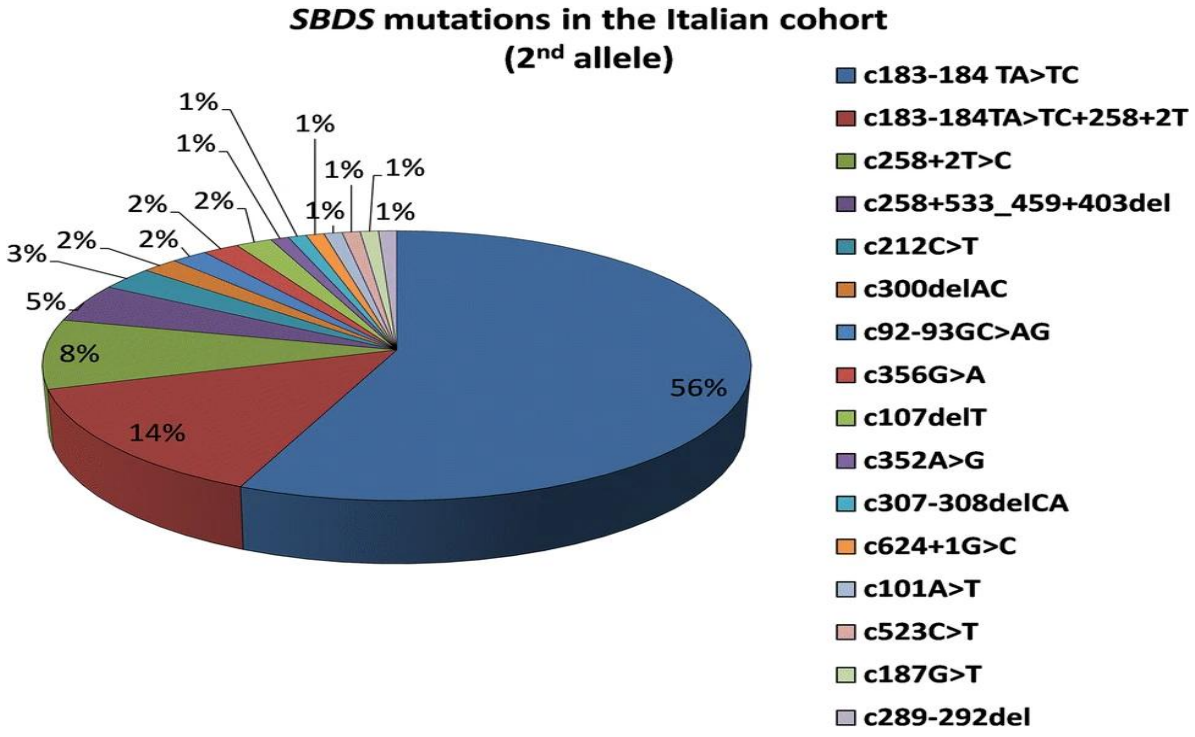

Figure 3. Percent prevalence of various mutations in *SBDS* gene of Italian SDS patients. The diagram illustrates the mutation percentage in single allele, supposing the other allele with mutation c.258+2T>C (Bezzerri et al. 2019). Image available under Creative Commons Attribution License.

Gene	Known mutations	Amino acid change	References
SBDS	c.24C>A	p.N8K	(Boocock et al. 2003; Shammas et al. 2005; Delaporta et al. 2017;Bezzerri et al. 2019; Morini et al. 2018)
	c.56G>A	p.R19Q	
	c.93C>G	p.C31W	
	c.97A>G	p.K33E	
	c.101A>T	p.N34I	
	c.123delC	p.S41fs17	
	c.131A>G	p.E44G	
	c.183-184TA>CT	p.K62X	
	c.183-184TA>CT+258+2T>C	p.K62X	
	c.199A>G	p.K67E	
	c.212T>C	p.L71P	
	c.279_284delTCAAGT	p.Q94_V95del	
	c.258+1G>C	p.84Cfs3	
	c.258+2T>C	p.84Cfs3	
	c.258+533_459+40del	p.99Efs20	
	c.260T>G	p.I87S	
	c.291_293delTAAinsAGTTCAAGTATC	p.D97-K98delinsEVQVS	
	c.300delAC	p.K118N	
	c.377G>C	p.R126T	
	c.458A>G	p.Q153R	
	c.460-1G>A	Splice site mutation	
	c.505C>T	p.R169C	
	c.506G>T	p.R169L	
	c.624+1G>C	Splice site mutation	
	c.523C>T	-	
	c.635T>C	p.I212T	
DNAJC21	c.100A>C	-	(Dhanraj et al. 2017; Morini et al. 2018)
	c.438-?_894+?del	-	
	c.520C>T	-	
	c.862G>A	-	
	c.1024G>A	-	
EFL1	c.1486C>T	-	(Stepensky et al. 2017; Morini et al. 2018)
	c.1849A>G	-	
	c.2132A>G	-	
	c.2645T>A	-	
	c.3284G>A	p.R1095Q	
SRP54	c.343A>G	p.T115A	(Carapito et al. 2017)
	c.343_351del	p.T117del	
	c.677G>A	p.G226E	
EIF6	c.182G>T	p.R61L	(Koh et al. 2020)

Table 1. Summary of identified genes and their known mutations associated with SDS till date (Bezzerri et al. 2019). Data partially retrieved from image available under Creative Commons Attribution License.

4. 3. Genomic instability and cytogenetics in SDS

Patients suffering from SDS may acquire clonal alterations in their bone marrow karyotype. These chromosomal changes are generally nonrandom. Among the observed chromosomal changes, an isochromosome of the long arm of chromosome 7, i(7)(q10), and an interstitial deletion of the long arm of chromosome 20, del(20)(q) occur commonly (Presato et al. 2012). The interstitial deletion of long arm of chromosome 20, del(20)(q) may encompass the *EIF6* gene (Eukaryotic Initiation Factor 6). As already described that in normal bone marrow cells, SBDS protein interacts with EFL1 (Elongation Factor-like 1) to ensure the removal of EIF6 (Eukaryotic Initiation Factor 6) from the premature-60S ribosomal subunit and promote the biogenesis of mature 80S ribosome (Finch et al. 2011). Therefore, the removal of *EIF6* is vital for normal biogenesis of mature and fully functional ribosomes. Valli et al. (2017a) has postulated the deletion of *EIF6* in del(20)(q) as a rescue mechanism for compensation of the depleted SDS protein in affected cells to promote ribosomal biogenesis and decline the risk of developing MDS and /or AML. The study proposes various ribosomal conditions that may arise due to the presence or absence of clonal chromosomal anomalies and their possible outcome (figure 4). Hence, the i(7)(q10) and del(20)(q) are considered important for their prognostic relevance in clones where they emerge. The del(20)(q) has been observed in other disorders involving chromosomal instability (Bench et al. 2000). On the contrary, the loss of *EIF6* by the deleted long arm of chromosome 20 is exclusively observed in SDS, which makes the scenario interesting. Pressato et al. (2015) has demonstrated that i(7)(q10) was absent in dysplastic or neoplastic clones derived from patients already in the MDS/AML phase. Similarly, del(20)(q) is seen in the same manner, nevertheless, probability of advancement towards MDS/AML cannot be fully avoided. Apart from these two prognostically beneficial chromosomal anomalies, other less known chromosomal anomalies have been reported as well (Valli et al. 2017b).

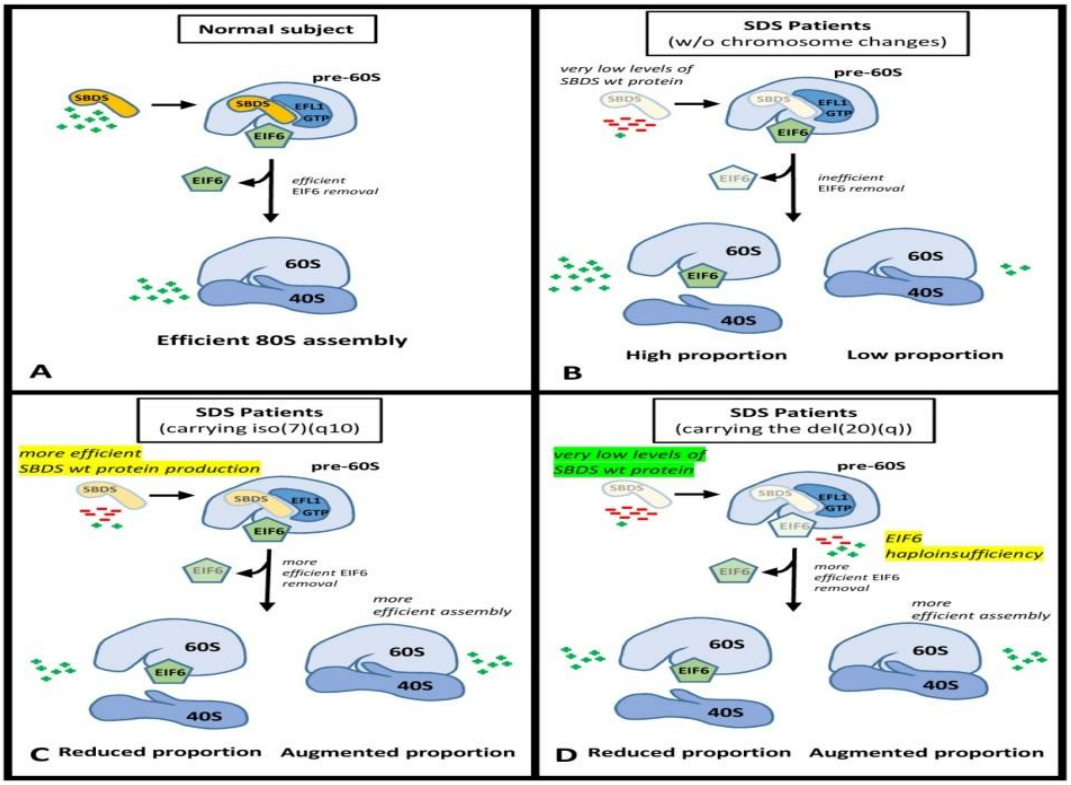

Figure 4. +' and "-" signs determine the quantity of available protein. a) Normal healthy individuals with normal SBDS quantity and normal ribosomal assembly. B). SDS patients with frequently known mutations but no chromosomal anomalies show less SBDS quantity and poor ribosomal assembly. C). Patients with frequently known mutations and i(7)(q10) chromosome: an additional copy of SBDS on the i(7)(q10) with the mild mutation c.258+2T>C enhance SBDS quantity and improved ribosomal assembly. D) SDS patients with frequently known mutations and del(20)(q) chromosome: loss of *EIF6* gene causes compromised EIF6 protein and fairly better ribosomal assembly in EIF6 partial absence (Valli et al 2017a). Image available under Creative Commons Attribution License.

5. Nonsense mutations and genetic disorders

Nonsense mutations in functionally vital genes are the underlying reason for many genetic disorders. Generally, cells have a mechanism of regulation for the PTC, called none sense mediated decay (NMD) (Celik et al. 2015). By this mechanism, the ribosomes perceive a PTC located at least 50 nucleotides ahead of an exon junction causing to trigger the NMD pathway. Consequently, NMD directed protein complex commences the decay of the defective mRNA. According to an estimate, there are approximately 2400 various genetic disorders attributed to the presence of a

minimum of one nonsense mutation (Mort et al. 2008). For example, patients who suffer from Hurler Syndrome acquire a nonsense mutation in the *IDUA* gene, which results in skeletal and cognitive problems (Sakuru et al. 2020). Similarly, *CFTR* gene in cystic fibrosis (Fanen et al. 2014) and *USH2A* gene in Usher syndrome (Samanta et al. 2019) are also listed in the same category. Moreover, some oncogenes may also be deteriorated by a similar phenomenon (Bykov et al. 2018).

5.1. Strategies to combat effects due to nonsense mutations

Given the importance of nonsense mutations to substantially impair genes expression and function, multiple counter strategies have been established to overcome this phenomenon (Morias et al. 2020). These strategies involve the suppression of nonsense mutations by "read through" process where a sense codon substitutes a stop codon (Bidou et al 2012). Some examples of suppression approaches against nonsense mutations include the use of aminoglycoside antibiotics, particularly gentamicin and a small molecule called ataluren. Emerging innovative options in this regards are nucleic acid-derived alternatives such as antisense technology, suppressor tRNA, RNA editing approaches and CRISPR based gene editing. In general, all the available nonsense suppression options have their merits and demerits and conditions to apply.

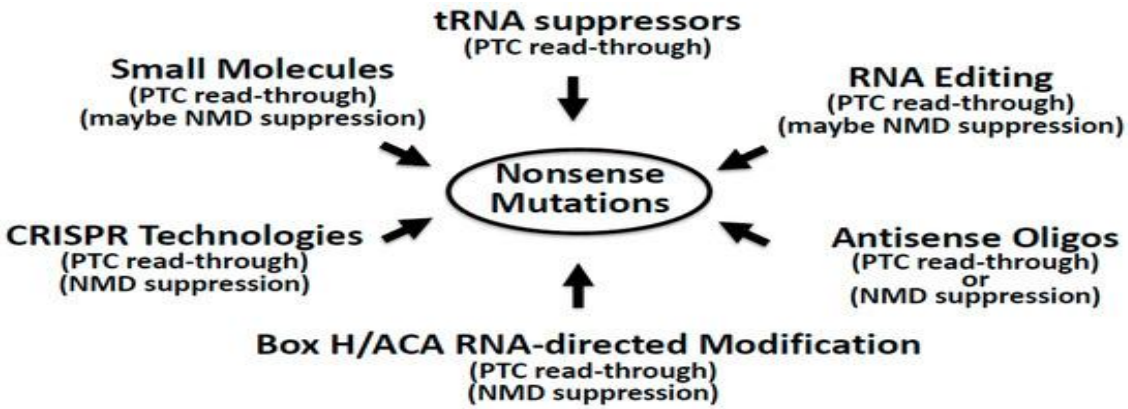

Figure 5. Various available options against nonsense suppression (Morias et al. 2020). Image available under Creative Commons Attribution License.

Among the established nonsense suppression options, gentamycin and ataluren are relatively better known as their efficacy has been reported frequently in literature (Lentini et al. 2014; Samanta et al. 2019; Tutone et al. 2019; Morias et al. 2020). However, the association of gentamycin with nephrotoxicity and ototoxicity is a renowned side effect of this drug (Linde and Kerem, 2008), hence making it inappropriate for prolonged use.

6. Study objectives

In Shwachman Diamond syndrome (SDS), *SBDS* gene acquires mutations that contribute to the reduced level of normal SBDS protein. Due to the functionally versatile nature of SBDS protein for its role in various cellular processes like DNA replication, spindle formation and ribosomal biogenesis etc., it is understandable that in the case of its depletion, the affected individuals have to bear multipronged effects and complications both at cellular and overall phenotype level. Taking into consideration the aforementioned scenario, we devised the central idea of this PhD project to illustrate the pathogenesis, pathophysiology and clinical aspects of SDS for better understanding of this relatively less understood disorder by the use of advanced and state of the art molecular techniques.

In line with the central hypothesis of this study, we specify the study goals as the following major points:

1. Characterization of SDS bone marrow samples and assessment of clones with *EIF6* gene deletion by fluorescence in situ hybridization (FISH) and comparative genomic hybridization array (aCGH).

2. Study of patients-derived bone marrow and osteoblasts for transcriptome analysis.

3. Assessment of ribosomal profiles in SDS patients and effect of ataluren treatment on ribosomal assembly.

RESULTS (SECTION 1)

Specific contribution

"*Abdul Waheed Khan contributed in the experimental work, helped in analyzing experimental data and revision of the manuscript for important intellectual content*"

bjh research paper

Shwachman-Diamond syndrome with clonal interstitial deletion of the long arm of chromosome 20 in bone marrow: haematological features, prognosis and genomic instability

Roberto Valli,[1] Antonella Minelli,[2] Marta Galbiati,[3] Giovanna D'Amico,[3] Annalisa Frattini,[1,4] Giuseppe Montalbano,[1] Abdul W. Khan,[1] Giovanni Porta,[1] Giorgia Millefanti,[1] Carla Olivieri,[2] Marco Cipolli,[5] Simone Cesaro,[6] Francesco Pasquali,[1] Cesare Danesino,[2] Gianni Cazzaniga[3] and Emanuela Maserati[1]

[1]*Genetica Umana e Medica, Dipartimento di Medicina e Chirurgia, Università dell'Insubria, Varese,* [2]*Genetica Medica, Fondazione IRCCS Policlinico S. Matteo and Università di Pavia, Pavia,* [3]*Immunology and Cell Therapy, Centro Ricerca Tettamanti, Paediatric Clinic, University of Milan Bicocca/MBBM, Monza,* [4]*Istituto di Ricerca Genetica e Biomedica, CNR, Milano,* [5]*Cystic Fibrosis Center, AOU Ospedali Riuniti, Ancona, and* [6]*Oncoematologia Pediatrica, Azienda Ospedaliera Universitaria Integrata, Verona, Italy*

Received 1 August 2018; accepted for publication 28 September 2018
Correspondence: Emanuela Maserati, Dipartimento di Medicina e Chirurgia, Università dell'Insubria, Via J. H. Dunant, 5, I 21100 Varese, Italy.
E-mail: emanuela.maserati@uninsubria.it

Summary

In Shwachman-Diamond syndrome (SDS), deletion of the long arm of chromosome 20, del(20)(q), often acquired in bone marrow (BM), may imply a lower risk of developing myelodysplastic syndrome/acute myeloid leukaemia (MDS/AML), due to the loss of the *EIF6* gene. The genes *L3MBTL1* and *SGK2*, also on chromosome 20, are in a cluster of imprinted genes, and their loss implies dysregulation of BM function. We report here the results of array comparative genomic hybridization (a-CGH) performed on BM DNA of six patients which confirmed the consistent loss of *EIF6* gene. Interestingly, array single nucleotide polymorphisms (SNPs) showed copy neutral loss of heterozygosity for *EIF6* region in cases without del(20)(q). No preferential parental origin of the deleted chromosome 20 was detected by microsatellite analysis in six SDS patients. Our patients showed a very mild haematological condition, and none evolved into BM aplasia or MDS/AML. We extend the benign prognostic significance of del(20)(q) and loss of *EIF6* to the haematological features of these patients, consistently characterized by mild hypoplastic BM, no or mild neutropenia, anaemia and thrombocytopenia. Some odd results obtained in microsatellite and SNP-array analysis demonstrate a peculiar genomic instability, in an attempt to improve BM function through the acquisition of the del(20)(q).

Keywords: Shwachman Diamond syndrome, del(20)(q), genomic instability, *EIF6* gene, risk of MDS/AML/BM aplasia.

Shwachman-Diamond syndrome (SDS) is an autosomal recessive disorder (Online Mendelian Inheritance in Man identification 260400) that is caused by mutations of the *SBDS* gene in at least 90% of cases (Maserati *et al*, 2009). It implies a wide spectrum of clinical signs and is characterized by exocrine pancreatic insufficiency, skeletal and neurodevelopmental abnormalities, bone marrow (BM) failure with peripheral cytopenias and an increased risk to develop myelodysplastic syndromes (MDS) and/or acute myeloid leukaemia (AML) (Dror, 2005). SDS is a ribosomopathy, as SBDS protein cooperates with the GTPase EFL1 to catalyse the removal of factor EIF6 from nascent 60S ribosomal subunit during ribosome biogenesis (Valli *et al*, 2017a; Warren, 2018). In a small proportion of cases, biallelic mutations of two other genes involved in ribosome biogenesis may cause SDS, or an SDS-like condition: *DNAJC21* (Dhanraj *et al*, 2017; D'Amours *et al*, 2018) and *EFL1* (Stepensky *et al*, 2017). Further, an SDS-like phenotype may be caused by monoallelic mutations of the gene *SRP54*, which produces a protein that is a key member of the cotranslational protein-targeting pathway (Carapito *et al*, 2017).

The most frequent clonal chromosome anomalies in BM of patients with SDS are an isochromosome of the long arm of chromosome 7, i(7)(q10), and an interstitial deletion of the long arm of chromosome 20, del(20)(q) (Pressato *et al*,

First published online 26 December 2018
doi: 10.1111/bjh.15729

2012). Since 1999, we have followed a cohort of 96 Italian patients with SDS, including 18 patients with the exclusive del(20)(q) and two other patients who retain this abnormality in combination with i(7)(q10). We previously demonstrated by array-based comparative genomic hybridization (a-CGH) on DNA from BM, the loss of the Eukaryotic Initiation Factor 6 (*EIF6*) gene in all 6 of the patients tested patients from this group of 20 patients (Valli *et al*, 2013). EIF6 protein is necessary for ribosome biogenesis, and in mammals it is required for insulin and growth factor-stimulated translation; its physiological significance impacts on cancer and SDS (Brina *et al*, 2015). We postulated that *EIF6* hemizygosity in SDS patients permits more efficient ribosome biogenesis, leading to a lower risk of developing MDS and/or AML (Valli *et al*, 2013). The indirect evidence that *EIF6* hemizygosity affects ribosome biogenesis, has been demonstrated by polysomal profiles in knock-out heterozygous mice for the orthologue eIF6 gene (Gandin *et al*, 2008).

The genes *L3MBTL1* and *SGK2* are located in a cluster of imprinted genes on chromosome 20, and their loss might be related to dysregulation of erythropoiesis and megakaryopoiesis (Aziz *et al*, 2013). In six patients with del(20)(q) (five of which were included in our aforementioned a-CGH analysis), a possible preferential parental origin of the deleted chromosome 20 was excluded (Nacci *et al*, 2017). However, the authors noted that the haemoglobin concentration (Hb) and red blood cell count were higher in their SDS patients carrying del(20)(q) in comparison with 20 SDS patients without clonal del(20)(q) (Nacci *et al*, 2017).

We here report the results of a-CGH of six more patients, all with biallelic mutations of *SBDS* and del(20)(q). In addition, the analysis of parental origin of the deleted chromosome 20 in six patients was also examined. The overall results were compared with essential haematological data.

Furthermore, investigations on single nucleotide polymorphisms (SNPs) in arrays were performed on 14 patients with the del(20)(q) and/or other chromosome changes, to obtain further evidence of chromosome anomalies and instability.

Materials and methods

All the patients of this study presented the main typical phenotypic signs of SDS, and the diagnosis was confirmed by mutation analysis of *SBDS*. The BM of six patients of our cohort was used to perform chromosome and a-CGH analyses (Unique Patient Number (UPN) 1, 6, 35, 82, 84 and 85). Microsatellite study was performed to identify the parental origin of the deleted chromosome 20 in patients UPN 1, 14, 35, 82, 84 and 85. SNP-arrays were performed on 14 cases (UPN 1, 2, 13, 14, 20, 24, 29, 35, 36, 40, 54, 58, 65 and 84), seven of whom carry del(20)(q), two carry del(20)(q) in combination with i(7)(q10), six with i(7)(q10) alone and one exhibited an unbalanced translocation t(1;16)(q21;q23) (Table I). Results of chromosome analysis and/or a-CGH of patients UPN 1, 2, 6, 13, 14, 17, 20, 24, 29, 35, 36, 40, 65 and 68 have already been partially reported (Maserati *et al*, 2006, 2009; Pressato *et al*, 2010; Valli *et al*, 2013) (Table I).

Informed consent for this study was obtained according to the principles of the Declaration of Helsinki from the patients or their parents.

Chromosome analyses were performed on BM with routine methods. Fluorescence *in situ* hybridization (FISH) on BM nuclei was carried out according to standard techniques with the following BAC probes, informative for the deletion detected in each patient: RP11-17F3 (UPN 6, 13, 17, 20, 35, 65, 82), CTD-2559C9 (UPN 13, 17), CTD-3092L7 (UPN 14) and XL Del(20q) probe (Metasystems, Altlussheim, Germany) (UPN 68, 84).

The a-CGH was performed on DNA from BM samples with the 244 K genome-wide system (Agilent Technologies Inc., Santa Clara, CA, USA), according to the manufacturer's instructions. All map positions in the results refer to the genome assembly map hg19.

The parental origin of the deleted chromosome 20 was determined by microsatellite analysis, as described by Nacci *et al* (2017), on the same DNA used for a-CGH. The short tandem repeat (STRs) polymorphisms used were chosen based on their heterozygosity (always above 80%): D20S484, D20S195, D20S890, D20S601, D20S847, D20S884, D20S891.

Table I. Bone marrow clonal anomalies of the patients studied in this report and the a-CGH/SNP arrays performed.

UPN	Clonal anomalies	a-CGH*	SNP array*
1	i(7)(q10)/del(20)(q)†	+¶/present paper	+
2	i(7)(q10)†	+¶	+
6	del(20)(q)†	+ present paper	−
13	del(20)(q)†	+**	+
14	i(7)(q10)/del(20)(q)†	+**	+
17	del(20)(q)‡	+**	−
20	del(20)(q)‡	+**	+
24	i(7)(q10)‡	+¶	+
29	i(7)(q10)‡	+ not informative ‡	+
35	del(20)(q)‡	+ present paper	+
36	i(7)(q10)‡	+¶	+
40	i(7)(q10)§	+§	+
54	i(7)(q10)	+¶	+
58	der(1)t(1;16)(q21;q23)	+ not informative	+
65	del(20)(q)	+**	+
68	del(20)(q)	+**	−
82	del(20)(q)	+ present paper	−
84	del(20)(q)	+ present paper	+
85	del(20)(q)	+ present paper	−

a-CGH, array comparative genomic hybridization; SNP, single nucleotide polymorphism; UPN, unique patient number.
*+ = performed; − = not performed.
†Cytogenetic analysis results reported in Maserati *et al* (2006).
‡Cytogenetic analysis results reported in Maserati *et al* (2009).
§Chromosome analysis and a-CGH results reported in Pressato *et al* (2010).
¶a-CGH confirms the i(7)(q10) (Maserati *et al*, 2009 and unpublished data).
**Valli *et al* (2013).

SNP-array analysis was performed on the DNA samples of 14 patients listed in Table I, genotyped by the Affymetrix® Cytogenetics Whole-Genome 2.7M Array (6 cases) or Affymetrix CytoScan HD Array (8 cases) (Affymetrix, Santa Clara, CA, USA) according to the manufacturer's protocol. Analysis of copy number variations and copy number neutral loss of heterozygosity (cnLOH) regions was performed with the Chromosome Analysis Suite (Affymetrix®, Santa Clara, CA, USA) software v.3.1.0.15 and based on hg19 assembly. Amplifications ≥20 kb and deletions ≥15 kb, containing a minimum of 20 markers in the region, were considered as significant. Detection of cnLOH was limited to aberrations longer than 2000 kb. Unfortunately, UPN 20 was analysed only for gains and losses, and not for cnLOH.

Results

Chromosome analysis on BM of the 12 patients used here for a-CGH (monitored at least once per year) showed the presence of the clonal interstitial deletion of chromosome 20.

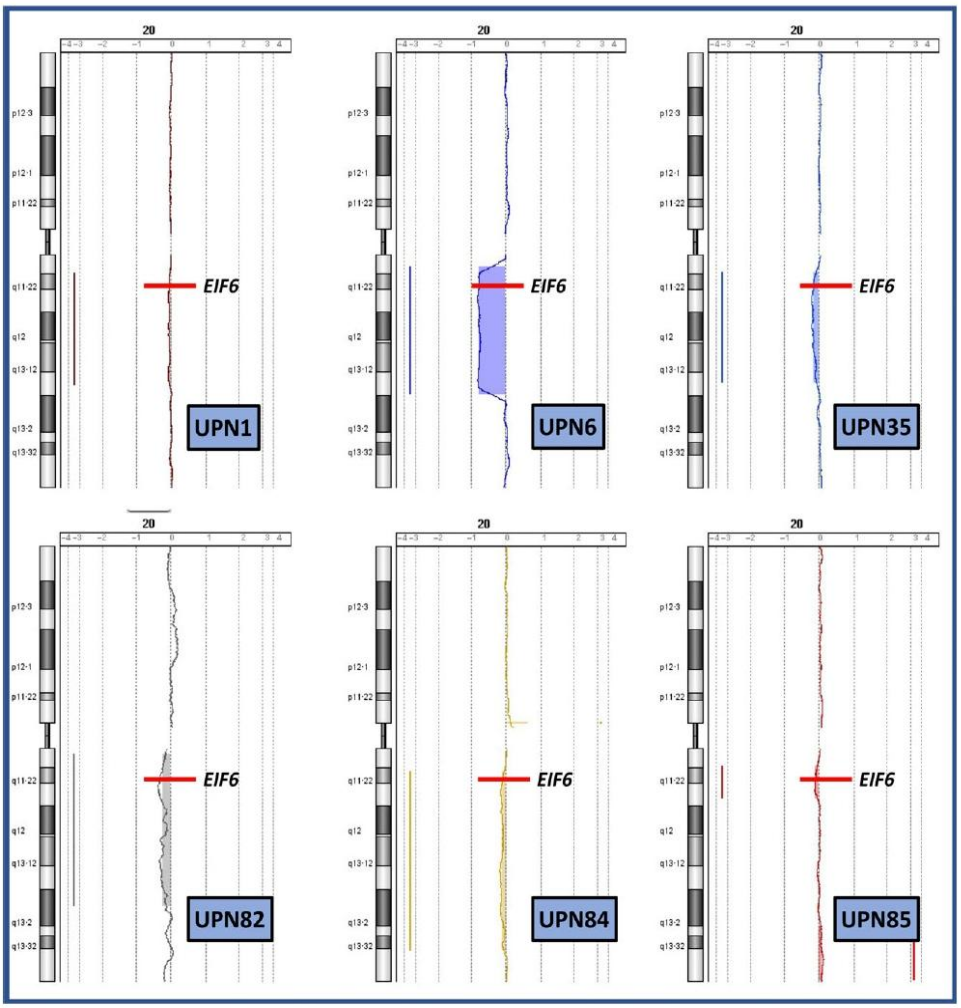

Fig 1. Array comparative genomic hybridization profiles of chromosome 20 in the newly investigated six patients with del(20)(q). Patients are identified by a Unique Patient Number (UPN). The profiles show extension of the interstitial deletion and the loss of the *EIF6* gene. [Colour figure can be viewed at wileyonlinelibrary.com]

The a-CGH results of the newly analysed six patients UPN 1, 6, 35, 82, 84 and 85 are shown in Fig 1. The positions of the breakpoints leading to the deletions are listed in Table II, which also gives the proportion of BM abnormal cells, as calculated with the formula suggested by Valli *et al* (2011). The proportion of cells containing the deletion was consistent with the evaluations obtained by FISH on nuclei with informative long arm probes (data not shown). The value of these proportions, variable at the time of our analyses, ranged from 9·5% to 82% (Table II).

SNP-array genotyping was performed on 14 SDS patients (Tables I and SI with raw data). Copy number variation analysis confirmed the presence of i(7)(q10) and del(20)(q), already identified by chromosome analyses and a-CGH (Maserati *et al*, 2009; Pressato *et al*, 2010; Nacci *et al*, 2017) (Table III). Interestingly, cnLOH regions involving the long arm of chromosome 20 were detected in three patients, namely UPN 1, 40 and 54. Two of them (UPN 40 and 54) were without del(20)(q) (Table I) and one case (UPN 1) showed del(20)(q) in a small proportion of cells (Table IV).

Microsatellite analysis on BM of the newly analysed patients with del(20)(q) (UPN 1, 14, 35, 82, 84 and 85) showed a different dosage of the paternal and maternal alleles in nine patients, providing evidence of the parental chromosome 20 deletion. The origin was paternal in two of these new cases, and maternal in one. In three patients (UPN 35, 82 and 85), unexpected discordant results were obtained, with some STRs indicating a paternal origin and others a maternal origin (Table IV).

There were some discordances between SNP array and cytogenetic/a-CGH results with regard to the start/stop points of the del(20)(q) and the abnormal cell proportion (Tables II, III, and SI). These differences are probably due to a different sensitivity of the technologies. Moreover, in some patients (UPN 1, 14, 20, 24 and 84) the material used for SNP array and a-CGH analyses was sampled at different dates, when the size of the abnormal clone might have changed.

Discussion

The results obtained from a-CGH of the 12 patients listed in Table II confirm that all deletions of the long arm of chromosome 20 in SDS are interstitial, that their proximal breakpoints are clustered in a rather small region of about 2600 kb, while the distal breakpoints are more variable. Excluding patients UPN 14 and 85, who presented very small deletions with the loss of 4150 and 4700 kb respectively, the distal breakpoints in the other 10 patients cluster in a segment of 11 227 kb, and the material lost is in the range 14 008 (UPN 68)–26 863 kb (UPN 13). One of these 10 patients (UPN 68) had two interstitial deletions present, with a segment of 2103 kb conserved between them.

The *EIF6* gene was lost in all 12 patients with the del(20)(q); moreover, three additional patients out of 14 analysed by SNP-array showed cnLOH encompassing the region containing *EIF6* (UPN 1, 40 and 54). These data on cnLOH further extend the involvement of this region in instability events; indeed, the minimal cnLOH region length was about 2200 kb and included the *EIF6* gene in all cases (Fig 2). Other recurrent cnLOH were identified, although their involvement in the disease could not be ascertained (Table III).

The *L3MBTL1* and *SGK2* genes were lost in all cases except UPN 14 and 85, i.e., the patients with the smallest deletions. The imprinted genes *L3MBTL1* and *SGK2* are expressed normally only if paternal in origin, thus suggesting possible differences in the BM status among SDS patients with either maternal (UPN 14, 20, 65, and 68) or paternal (UPN 1, 6, 13, 17, and 84) deleted chromosome. Considering the 12 available informative patients altogether, including those already reported (Nacci *et al*, 2017), the deleted chromosome 20 was of paternal origin in five cases and maternal

Table II. Results of array comparative genomic hybridization on bone marrow samples from the 12 patients with Shwachman-Diamond syndrome and acquired del(20)(q) listed in Table I. The bands involved and the start/stop points of the deletion provided by the bp positions give the details of the chromosome anomaly (genome assembly hg19).

UPN	Band	Deletion start (bp)	Deletion stop (bp)	% abnormal cells
1	q11.21–q13.13	31891819	48287277	9·50%
6	q11.21–q13.13	30922628	49497969	82%
13	q11.21–q13.32	30876455	57739620	55%
14	q11.21–q11.23	31163090	35309412	18·20%
17	q11.21–q13.31	31205853	55894884	47%
20	q11.21–q13.32	31294381	57252363	66·57%
35	q11.21–q13.13	31798183	47884947	20%
65	q11.21–q13.13	30157286	49497910	43%
68	q11.21–q13.12	31262228	43141623	16%
	q13.12–q13.13	45244728	47373188	
82	q11.21–q13.2	30020250	52206444	31·13%
84	q11.22–q13.33	32620650	58600338	15·50%
85	q11.21–q11.23	31814242	36538658	13·90%

UPN, unique patient number.

Table III. Recurring gains, losses (A) and copy number neutral loss of heterozygosity (B), found in ≥2 patients, derived from single nucleotide polymorphism-array analysis of 14 patients (Table I). Minimal common regions have been listed.

Patients	CN	Type of genomic variation	Chr	Bands	Size (kb)	Genomic location
(A) Recurring gains and losses						
1, 24, 36, 40, 54	1	Loss (mosaic)	7	whole p arm		
1, 24, 36, 40, 54	3	Gain (mosaic)	7	whole q arm		
13, 14, 20, 65, 84	1	Loss (mosaic)	20	q11.22–q11.23	3055	chr20:32758000-35813438
(B) Recurring cnLOH regions						
1, 13	2	LOH	2	p13.2–p12	3·061	chr2:72502269-75563148
13, 54	2	LOH	6	p22.1–p22.1	1·912	chr6:27363586-29275298
58, 84	2	LOH	3	p21.31–p21.2	2·189	chr3:49685591-51874275
1, 84	2	LOH	7	q11.21–q11.21	2·444	chr7:64140053-66583570
4, 13	2	LOH	8	p12–p12	2·022	chr8:32803572-34825223
2, 14, 24	2	LOH	8	q11.1–q11.21	2·091	chr8:46944404-49035329
14, 24, 36	2	LOH	10	q22.1–q22.2	2·369	chr10:74480275-76849397
29, 36	2	LOH	11	p11.2–p11.12	3·545	chr11:48018354-51563636
14, 29	2	LOH	14	q23.3–q24.1	2·055	chr14:65865670-67920573
1, 40, 54*	2	LOH	20	q11.22–q11.23	2·230	chr20:32738611-34968575
54, 40	2	LOH	X	q11.1–q12	5·140	chrX:62018109-67158519
36, 24, 54	2	LOH	X	q13.1–q21.1	6·336	chrX:71523649-77859592

Chr, chromosome; CN, copy number state; cnLOH, copy number neutral loss of heterozygosity; LOH, loss of heterozygosity.
*cnLOH 20q: see also Fig 2.

Table IV. Basic haematological data of the Shwachman-Diamond syndrome cohort included in Table I, and parental origin of the del(20)(q).

UPN	Age (years)	% abnormal cells	BM morphology	Neutropenia‡	Anaemia§	Thrombocytopenia¶	Parental origin of del(20)(q)
1*	9	9·5%	Almost normal	Mild	No	Mild	Maternal
6	18	82·7%	Almost normal	No	No	Mild	Paternal
13	11	55%	Almost normal	Mild	Mild	Mild	Paternal
14*	11	18.2%	Mild hypoplasia	Mild	No	No	Paternal
17†	23	48·5%	Mild hypoplasia	No	No	Mild	Paternal
20†	31	66%	Mild hypoplasia	Mild	No	Mild	Maternal
35	13	20%	Mild hypoplasia	Mild	Mild	No	Discordant
65	12	43%	Normal	No	No	Mild	Maternal
68	20	13·9%	Severe hypoplasia	No	No	Mild/No	Maternal
82	15	31·1%	Mild hypoplasia	Mild	Mild	Mild	Discordant
84	14	15·5%	Mild hypoplasia	Severe	No	Mild	Paternal
85	20	13·9%	Almost normal	Mild	No	Mild	Discordant

BM, bone marrow; UPN, unique patient number.
*Patient also had an independent clone with i(7)(q10).
†Patient also had a subclone with a rearrangement of the del(20)(q), with deleted and duplicated portions of chromosome 20 (Valli *et al*, 2017b).
‡Mild: neutrophil count 0·5–1·5 × 10^9/l, severe <0·5 × 10^9/l.
§Mild: Haemoglobin concentration 80–120 g/l, severe <70–80 g/l.
¶Mild: platelet count 50–150 × 10^9/l, severe <50 × 10^9/l.

in four (Table IV). So, no preferential parental origin of the deleted chromosome 20 was detected, and, therefore, the expression of these genes may be hardly relevant to the haematological phenotype of the patients with the del(20)(q).

In three patients (UPN 35, 82, 85) it was not possible to establish the parental origin of the deleted chromosome 20, because microsatellite analysis gave unexpectedly discordant results (Table IV). The simplest explanation may be a mitotic recombination between the two chromosomes 20 in the region of, or near to *EIF6*.

Both the discordant results obtained by microsatellite analysis and the cnLOH found by SNP-array may represent attempts to rearrange the chromosome, aiming to delete *EIF6* on chromosome 20. We hypothesize that the BM cells of SDS patients tend to attempt an improvement of their function, impaired by the defective SBDS protein, through the acquisition of the del(20)(q). Their attempt is successful when the deletion arises, while cnLOH might represent an unsuccessful attempt. The discordant microsatellite results might also represent attempts to rearrange chromosome 20,

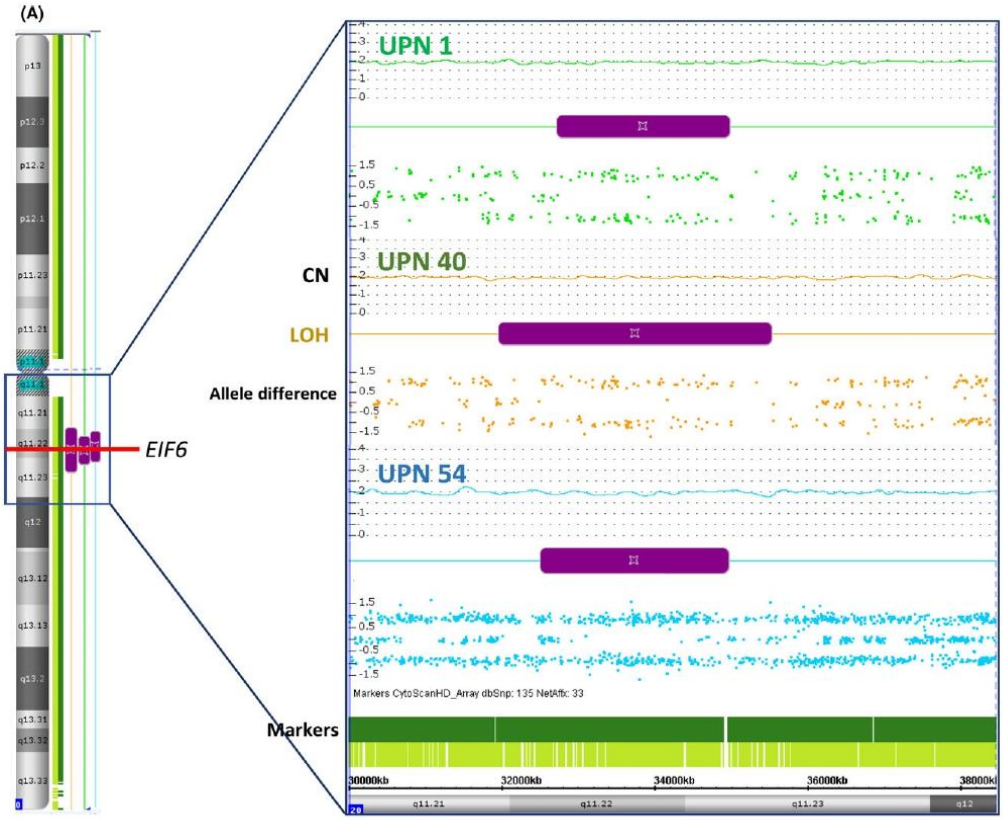

(B)

Minimal Common LOH Region	Genes
Chr20:32738611-34968575 (2230 Kb)	*ASIP, AHCY, ITCH, MIR644A, DYNLRB1, MAP1LC3A,PIGU, TP53INP2, NCOA6, HMGB3P1,GGT7, ACSS2, GSS, MYH7B, MIR499A, MIR499B, TRPC4AP, EDEM2, PROCR, MMP24, MMP24OS, EIF6, FAM83C, UQCC1, GDF5, CEP250, C20orf173, ERGIC3, SPAG4, CPNE1, RBM12, NFS1, ROMO1, RBM39, PHF20, SCAND1, CNBD2, NORAD, EPB41L1, AAR2*

Fig 2. Copy number neutral loss of heterozygosity (cnLOH) of chromosome 20. (A) Detail of 20q cnLOH in UPN 1, 40 and 54. (B) List of genes included in minimal common LOH region. CN, copy number state; LOH, loss of heterozygosity; UPN, unique patient number. [Colour figure can be viewed at wileyonlinelibrary.com]

even in cases in which the *EIF6* gene was then successfully deleted. We previously postulated a peculiar kind of karyotype instability in the BM of SDS patients many years ago, when molecular data were not available (Maserati *et al*, 2000). We also reported evidence that several different cell lines, with different chromosome changes, can be found in BM of SDS patients (Pressato *et al*, 2015). This is case when the i(7)(q10) and the del(20)(q) are acquired subsequently in different clones, or clones with further rearrangements of del (20)(q), or together with i(7)(q10) or del(20)(q), other different anomalies in independent clones (Pressato *et al*, 2015; Valli *et al*, 2017b).

Table IV provides some basic information about the haematological condition of our patients with del(20)(q) at the time of a-CGH analysis, the criteria used to consider the level of severity of the condition, together with their age and proportion of BM cells bearing the del(20)(q). The definitions used to describe BM morphology come from the pathologists who analysed the preparations. In particular, "normal" and "almost normal" BM are based on standard generally accepted criteria (Greer *et al*, 2013). The benign prognostic significance of del(20)(q) and loss of *EIF6* may be sustained by the haematological features of these patients: BM picture and peripheral blood counts give evidence of a very mild condition in all our patients, both with regard to the BM morphology and the absent or mild peripheral blood cytopenias. Nevertheless, exceptions are represented by two borderline patients, with some more severe symptoms: patient UPN 68, with severely hypoplastic BM, but with no neutropenia, no anaemia and almost no thrombocytopenia (platelet count 143×10^9/l), and patient UPN 84, who had an almost normal BM morphologically, with neutropenia which may be considered severe (neutrophil count $0{\cdot}46 \times 10^9$/l), but no anaemia and mild thrombocytopenia (platelet count 127×10^9/l). Interestingly, these two patients are among those showing lower percentages of BM cells with the del (20)(q) (Table IV). Although some other patients with similar low percentages are present in our cohort (e.g. UPN 1 and 85), we do not know in which BM cell lineages the clonal anomaly is present, and this could vary from case to case.

We postulate that the loss of the *EIF6* gene due to the del(20) (q), as confirmed by the results reported here, is a good prognostic sign in general, in addition to the already suggested lower risk of transformation into MDS/AML (Pressato *et al*, 2012). To date, none of our 12 patients have encountered either this complication or evolution to severe BM aplasia. More extensive study on larger samples of patients, possibly with analysis of their follow-up, may further confirm this conclusion.

The 12 patients with del(20)(q) reported here are quite old for a disorder that is usually diagnosed in infants or children (Dror, 2005), as their age range is (in 2018), 14–44 years, with an average of 23 years. Also, this fact should be taken into account with regard to the risk of MDS/AML evolution, as it is well known that this risk increases with age (Maserati *et al*, 2006; Shimamura, 2006; Maserati *et al*, 2009; Pressato *et al*, 2010). Similarly, it is noteworthy that none of our patients showed haematogical features indicating progression towards BM severe aplasia. The lower risk of SDS patients with del(20)(q) to develop MDS/AML and to become frankly aplastic is further supported by these considerations concerning their age.

A comparison between the haematological data of the cohort of patients with del(20)(q) reported here and patients without this anomaly is not really feasible. Several facts would make it not convincing. First, the BM morphology and the cytopenias in SDS are quite variable. Second, the haematological condition varies considerably over time. Third, all patients with important cytopenias are transfused and treated, even for long periods. Nevertheless, in order to attempt a rough comparison, we randomly chose 25 patients from our entire cohort of 96 Italian patients, without any criteria besides the absence of del(20)(q). This cohort comprised 11 females and 14 males, with an age range of <1–38 years. The BM karyotype was normal in 20/25 patients, whereas a clonal i(7)(q10) was present in five of them at the time of blood sampling. Neutropenia was present in all but four patients and, among the other 21 patients, it was severe in 10 (neutrophil count $0{\cdot}058–0{\cdot}4 \times 10^9$/l and mild in 11 cases (neutrophil count $0{\cdot}5–1{\cdot}24 \times 10^9$/l). Hb was normal in 3/25 patients: anaemia was severe in two (53–71 g/l) and mild in 20 (79–129 g/l). Thrombocytopenia was present in 15/25 patients: severe in four (platelet count $9{\cdot}0–42 \times 10^9$/l) and mild in 11 ($81–143 \times 10^9$/l). Although these data are not statistically evaluable, they certainly show some relevant differences from the cohort of patients that have del(20)(q).

Acknowledgements

This work was supported by grants from the Associazione Italiana Sindrome di Shwachman (AISS), and from Fondazione Banca del Monte di Lombardia. Abdul Waheed Khan is a PhD student enrolled in the Life Sciences and Biotechnology program of the XXXIII cycle. The authors warmly thanks clinicians who contributed with haematological data to the work: Rita Maria Pinto and Franco Locatelli (Oncoematologia Pediatrica, Ospedale Pediatrico Bambino Gesù, Roma), Marco Zecca (Oncoematologia Pediatrica, IRCCS Policlinico S. Matteo, Pavia), Carla Cerri (Oncoematologia Pediatrica, Azienda Ospedaliera, Perugia), Grazia Iaria (Ematologia, Azienda Ospedaliera, Reggio Calabria).

Conflict of interest

The authors declare that they have no conflict of interest.

Author contributions

RV, AM, MG, GD, AF, GM, AWK, GP, CO performed the research and analyzed the data. MC, SC, FP, CD, GC, EM designed the research, analyzed the data, and wrote the paper.

Supporting Information

Additional supporting information may be found online in the Supporting Information section at the end of the article.

Table SI. Raw SNP array data: data from SNParray analysis of SDS patients by Affymetrix® Cytogenetics Whole-Genome 2.7M Array and Affymetrix CytoScan HD Array.

References

Aziz, A., Baxter, E.J., Edwards, C., Cheong, C.Y., Ito, M., Bench, A., Kelley, R., Silber, Y., Beer, P.A., Chng, K., Renfree, M.B., McEwen, K., Gray, D., Nangalia, J., Mufti, G.J., Hellstrom-Lindberg, E., Kiladjian, J.J., McMullin, M.F., Campbell, P.J., Ferguson-Smith, A.C. & Green, A.R. (2013) Cooperativity of imprinted genes inactivated by acquired chromosome 20q deletions. *The Journal of Clinical Investigation*, **123**, 2169–2182.

Brina, D., Miluzio, A., Ricciardi, S. & Biffo, S. (2015) eIF6 anti-association activity is required for ribosome biogenesis, translational control and tumor progression. *Biochimica et Biophysica Acta*, **1849**, 830–835.

Carapito, R., Konantz, M., Paillard, C., Miao, Z., Pichot, A., Leduc, M.S., Yang, Y., Bergstrom, K.L., Mahoney, D.H., Shardy, D.L., Alsaleh, G., Naegely, L., Kolmer, A., Paul, N., Hanauer, A., Rolli, V., Müller, J.S., Alghisi, E., Sauteur, L., Macquin, C., Morlon, A., Sancho, C.S., Amati-Bonneau, P., Procaccio, V., Mosca-Boidron, A.L., Marle, N., Osmani, N., Lefebvre, O., Goetz, J.G., Unal, S., Akarsu, N.A., Radosavljevic, M., Chenard, M.P., Rialland, F., Grain, A., Béné, M.C., Eveillard, M., Vincent, M., Guy, J., Faivre, L., Thauvin-Robinet, C., Thevenon, J., Myers, K., Fleming, M.D., Shimamura, A., Bottollier-Lemallaz, E., Westhof, E., Lengerke, C., Isidor, B. & Bahram, S. (2017) Mutations in signal recognition particle SRP54 cause syndromic neutropenia with Shwachman-Diamond-like features. *The Journal of Clinical Investigation*, **127**, 4090–4103.

D'Amours, G., Lopes, F., Gauthier, J., Saillour, V., Nassif, C., Wynn, R., Alos, N., Leblanc, T., Capri, Y., Nizard, S., Lemyre, E., Michaud, J.L., Pelletier, V.-A., Pastore, Y.D. & Soucy, J.-F. (2018) Refining the phenotype associated with biallelic *DNAJC21* mutations. *Clinical Genetics*, **94**, 252–258.

Dhanraj, S., Matveev, A., Li, H., Lauhasurayotin, S., Jardine, L., Cada, M., Zlateska, B., Tailor, C.S., Zhou, J., Mendoza-Londono, R., Vincent, A., Durie, P.R., Scherer, S.W., Rommens, J.M., Heon, E. & Dror, Y. (2017) Biallelic mutations in *DNAJC21* cause Shwachman-Diamond syndrome. *Blood*, **129**, 1557–1562.

Dror, Y. (2005) Shwachman-Diamond syndrome. *Pediatric Blood & Cancer*, **45**, 892–901.

Gandin, V., Miluzio, A., Barbieri, A.M., Beugnet, A., Kiyokawa, H., Marchisio, P.C. & Biffo, S. (2008) Eukaryotic Initiation Factor 6 is rate-limiting in translation, growth and transformation. *Nature*, **455**, 684–688.

Greer, J.P., Arber, D.A., Glader, B., List, A.F., Means, R.T., Paraskevas, F. & Rodgers, G.M. (2013) Wintrobe's Clinical Hematology, 13th edn. Wolters Kluver Health/Lippincott Williams and Wilkins Publ., Alphen Aan den Rijn/Philadelphia, pp. 12–14.

Maserati, E., Minelli, A., Olivieri, C., Bonvini, L., Marchi, A., Bozzola, M., Danesino, C., Scappaticci, S. & Pasquali, F. (2000) Isochromosome (7)(q10) in Shwachman syndrome without MDS/AML and role of chromosome 7 anomalies in myeloproliferative disorders. *Cancer Genetics and Cytogenetics*, **121**, 167–171.

Maserati, E., Minelli, A., Pressato, B., Valli, R., Crescenzi, B., Stefanelli, M., Menna, G., Sainati, L., Poli, F., Panarello, C., Zecca, M., Lo Curto, F., Mecucci, C., Danesino, C. & Pasquali, F. (2006) Shwachman syndrome as mutator phenotype responsible for myeloid dysplasia/neoplasia through karyotype instability and chromosomes 7 and 20 anomalies. *Genes Chromosomes & Cancer*, **45**, 375–382.

Maserati, E., Pressato, B., Valli, R., Minelli, A., Sainati, L., Patitucci, F., Marletta, C., Mastronuzzi, A., Poli, F., Lo Curto, F., Locatelli, F., Danesino, C. & Pasquali, F. (2009) The route to development of myelodysplastic sindrome/acute myeloid leukaemia in Shwachman-Diamond syndrome: the role of ageing, karyotype instability, and acquired chromosome anomalies. *British Journal of Haematology*, **145**, 190–197.

Nacci, L., Valli, R., Pinto, R.M., Zecca, M., Cipolli, M., Morini, J., Cesaro, S., Boveri, E., Rosti, V., Corti, P., Ambroni, M., Pasquali, F., Danesino, C., Maserati, E. & Minelli, A. (2017) Parental origin of the deletion del(20q) in Shwachman-Diamond patients and loss of the paternally derived allele of the imprinted L3MBTL1 gene. *Genes Chromosomes & Cancer*, **56**, 51–58.

Pressato, B., Marletta, C., Montalbano, G., Valli, R. & Maserati, E. (2010) Improving the definition of the structure of the isochromosome i(7)(q10) in Shwachman-Diamond Sindrome. *British Journal of Haematology*, **150**, 632–633.

Pressato, B., Valli, R., Marletta, C., Mare, L., Montalbano, G., Lo Curto, F., Pasquali, F. & Maserati, E. (2012) Deletion of chromosome 20 in bone marrow of patients with Shwachman-Diamond syndrome, loss of the EIF6 gene and benign prognosis. *British Journal of Haematology*, **157**, 503–505.

Pressato, B., Valli, R., Marletta, C., Mare, L., Montalbano, G., Lo Curto, F., Pasquali, F. & Maserati, E. (2015) Cytogenetic monitoring in Shwachman-Diamond syndrome: a note on clonal progression and a practical warning. *Journal of Pediatric Hematology and Oncology*, **37**, 307–310.

Shimamura, A. (2006) Shwachman-Diamond syndrome. *Seminars in Hematology*, **43**, 178–188.

Stepensky, P., Chacón-Flores, M., Kim, K.H., Abuzaitoun, O., Bautista-Santos, A., Simanovsky, N., Siliqi, D., Altamura, D., Méndez-Godoy, A., Gijsbers, A., Naser Eddin, A., Dor, T., Charrow, J., Sánchez-Puig, N. & Elpeleg, O. (2017) Mutations in *EFL1*, an *SBDS* partner, are associated with infantile pancytopenia, exocrine pancreatic insufficiency and skeletal anomalies in a Shwachman-Diamond like syndrome. *Journal of Medical Genetics*, **54**, 558–566.

Valli, R., Maserati, E., Marletta, C., Pressato, B., Lo Curto, F. & Pasquali, F. (2011) Evaluating chromosomal mosaicism by array comparative genomic hybridization in haematological malignancies: the proposal of a formula. *Cancer Genetics*, **204**, 216–218.

Valli, R., Pressato, B., Marletta, C., Mare, L., Montalbano, G., Lo Curto, F., Pasquali, F. & Maserati, E. (2013) Different loss of material in recurrent chromosome 20 interstitial deletions in Shwachman-Diamond syndrome and in myeloid neoplasms. *Molecular Cytogenetics*, **6**, 56.

Valli, R., Frattini, A. & Minelli, A. (2017a) Shwachman-Diamond syndrome: diagnosis, pathogenesis and prognosis. *Expert Opinion on Orphan Drugs*, **5**, 753–767.

Valli, R., De Paoli, E., Nacci, L., Frattini, A., Pasquali, F. & Maserati, E. (2017b) Novel recurrent chromosome anomalies in Shwachman-Diamond syndrome. *Pediatric Blood & Cancer*, **64**, e26454.

Warren, A.J. (2018) Molecular basis of the human ribosomopathy Shwachman-Diamond syndrome. *Advances in Biological Regulation*, **67**, 109–127.

RESULTS (SECTION 2)

- Manuscript Draft -

Rescue mechanisms in the bone marrow of patients with Shwachman-Diamond syndrome: overview of deletions of chromosome 20 and novel evidences of karyotype instability

Abdul Waheed Khan,[1§] Alyssa Kennedy,[2] Elissa Furutani,[2] Kasiani Myers,[3] Annalisa Frattini,[1,4] Giuseppe Montalbano,[1] Antonella Minelli,[5] Giovanni Porta,[1] Marco Cipolli,[6] Simone Cesaro,[7] Cesare Danesino,[5] Akiko Shimamura,[2] Francesco Pasquali[1] and Roberto Valli,[1]

[1] *Genetica Umana e Medica, Dipartimento di Medicina e Chirurgia, Università dell'Insubria, Varese, Italy*
[2] *Dana Farber/Boston Children's Cancer and Blood Disorders Center, Boston, MA, USA*
[3] *Cincinnati Children's Hospital and Medical Center, Cincinnati, OH, USA*
[4] *Istituto di Ricerca Genetica e Biomedica, CNR, Milano, Italy*
[5] *Genetica Medica, Fondazione IRCCS Policlinico S. Matteo and Università di Pavia, Pavia, Italy*
[6] *Cystic Fibrosis Center, AOU Ospedali Riuniti, Ancona, Italy*
[7] *Oncoematologia Pediatrica, Azienda Ospedaliera Universitaria Integrata, Verona, Italy*
[§] PhD student enrolled in the Life Sciences and Biotechnology program of the XXXIII cycle

Corresponding author: Roberto Valli, Dipartimento di Medicina e Chirurgia, Università dell'Insubria, Via J. H. Dunant, 5, I 21100 Varese, Italy - e-mail: roberto.valli@uninsubria.it - Phone: ++39 0332 217114; Fax: ++39 0332 217119

ABSTRACT

Background: An interstitial deletion of the long arm of chromosome 20, del(20)(q), and an isochromosome of the long arm of chromosome 7, i(7)(q10), are the most frequent anomalies acquired in the bone marrow (BM) of patients with Shwachman-Diamond syndrome (SDS). These clonal changes imply significantly milder haematological symptoms, and lower risk of developing myelodysplastic syndromes and acute myeloid leukaemia, thanks to the loss of the EIF6 gene in the del(20)(q) and to the mutations of the SBDS gene in the i(7)(q10), as both act as rescue mechanisms in the BM of these patients.

Procedure: Fourteen patients exhibiting either the del(20)(q) or the i(7)(q10) were subjected to chromosome analyses, and FISH on BM nuclei and mitoses with informative bac probes; DNA from BM was also analysed by array-Comparative Genomic Hybridization.

Results: The del(20)(q) was analyzed in 13 patients. For eight patients, del(20)(q) was the sole chromosomal abnormality. Five patients with the del(20)(q) and one with the i(7)(q10) showed more than one clonal abnormality, either within a single BM sample, or across sequential samples.

Conclusions: An analysis of the del(20)(q) deletion was presented for 25 patients (13 reported here and 12 previously reported). All the deletions were interstitial, with loss of material varying from 1.7 to 26.9 Mb, and all resulted in the loss of the EIF6 gene, with a possible rescue effect in BM, that was already postulated. The six patients with unexpected clonal variations of the anomalies provided further evidence of the striking selection pressure exerted by SBDS deficiency driving karyotype instability and specific clonal abnormalities in this ribosomopathy.

INTRODUCTION

Shwachman-Diamond syndrome (SDS) is an autosomal recessive disorder (Online Mendelian Inheritance in Man #260400) characterized by exocrine pancreatic insufficiency, bone marrow failure, peripheral cytopenias and an increased risk of developing aplastic anaemia, myelodysplastic syndrome (MDS) and acute myeloid leukaemia (AML). The patients may also exhibit additional anomalies. SDS is caused by mutations of the *SBDS* gene in at least 90% of cases.[1] In addition to other functions, SBDS protein has a pivotal role in ribosome biogenesis.[1] However, SDS is genetically heterogeneous. Biallelic mutations of two other genes involved in ribosome biogenesis may cause SDS, or an SDS-like condition: *DNAJC21*,[2,3] and *EFL1*.[4] An SDS-like phenotype may be also caused by monoallelic mutations of the gene *SRP54*, which produces a protein that is a key member of the cotranslation protein-targeting pathway.[5] Therefore, SDS may be considered a ribosomopathy.

Clonal chromosome changes are often found in the bone marrow (BM) of patients with SDS. Among them, the most frequently observed clonal abnormalities are an isochromosome of the long arm of chromosome 7, i(7)(q10), and an interstitial deletion of the long arm of chromosome 20, del(20)(q).[6] We have already shown those molecular mechanisms underlying the fact that both these more frequent anomalies are benign prognostic signs, as they are not associated with leukemia progression. The i(7)(q10) results in duplication of mutation c.258+2 t>c of the *SBDS* gene, which is a hypomorphic mutation that allows the production of a scant amount of functional protein.[7] The del(20)(q) results in deletion of the *EIF6* gene.[8,9] Both these anomalies are predicted to result in more efficient ribosome biogenesis in the BM abnormal clone which may lower the risk of MDS/AML[7,8] and result in a milder haematological condition compared to SDS patients with other chromosome changes or with normal karyotype.[10,11,12]

We have demonstrated that SDS is not associated with

an increase of spontaneous chromosome breaks, as in customary breakage syndromes, a possibility that was raised by some previously published reports.[13] Nevertheless, we suggested since 2000 that SDS may be associated with a particular type of karyotype instability resulting in specific anomalies of chromosome 7 and 20: i(7)(q10) and del(20)(q).[14]

We present here an updated overview of available cases with del(20)(q) from a cohort of patients in whom the deletion was defined by array-based comparative genomic hybridization (a-CGH) and fluorescence in situ hybridization (FISH). These findings support the notion that the selection pressures exerted by *SBDS* deficiency result in specific karyotype instability (confirmed by some novel data presented here) and recurrent clonal abnormalities.

MATERIALS AND METHODS

Bone marrow samples were obtained from eight patients from the cohort of the North American Shwachman-Diamond Syndrome Registry (SDSR) and from six patients from the cohort of the Registro Italiano per la Sindrome di Shwachman-Diamond (RI-SDS). In total, samples were analyzed from fourteen patients, three females and eleven males, with age at the time of sampling for the analyses reported here ranging from three to 29 years. All the patients presented the main typical phenotypic signs of SDS. Mutational analysis confirmed the presence of biallelic mutations of *SBDS* gene among all of them (Table 1). These patients were chosen because they bore the more frequent clonal chromosome anomalies in BM, the del(20)(q) in thirteen patients and the i(7)(q10) in one, which were detected by chromosome analysis.

Informed consent for this study was obtained according to the principles of the Declaration of Helsinki from the patients or the patients' parents on protocols approved by the institutional review boards for human subjects research.

Chromosome analyses were performed on BM with routine methods. FISH on BM nuclei and mitoses was carried out according to standard techniques with the following bac probes, informative for the change detected in each patient: RP11-17F3 (Patients 9, 11, 12, 14), RP11-29E13 (Patients 11, 12, 14), RP11-261N10 and CTD-4095D13 (Patient 10).

The a-CGH was performed on DNA from BM samples with the 4x180 K or 244 K genome-wide system (Agilent Technologies Inc., Santa Clara, CA, USA), according to the manufacturer's instructions, as already described.[15] All map positions in the results refer to the genome assembly map hg19.

RESULTS

The del(20)(q) was defined by a-CGH and FISH in the 13 patients in whom it was initially noted on chromosomal karyotype analysis. Eight patients manifested the del(20)(q) as their sole chromosomal anomaly. The positions of the deletion breakpoints, together with the proportion of cells harboring the deletion are listed in Table 2. The a-CGH profiles of six of these patients are shown in Figure 1A. Table 2 includes also the two cases (11 and 12) in whom the paucity of BM abnormal cells did not allow the a-CGH study, and the result derives only from FISH on interphase nuclei (Figure 1B and 1C). The FISH results in these two patients could also indicate a clone with monosomy 20, but we interpreted our findings as due to a large deletion, because standard chromosome analyses, repeatedly performed in them for 14 and 11 years respectively, never showed cells with monosomy 20, but only few cells with del(20)q).

Six patients, five with the del(20)(q) and one with the i (7)(q10), showed more than one abnormal clone, either simultaneously in a single BM sample (cases 2, 4, and 13), or sequentially in two samples drawn in different years (cases 9, 10, and 14). The results concerning these patients are summarized in Table 3. The percentage of abnormal cells in Tables 1 and 2 was calculated from a-CGH data as previously described.[16]

In particular the results in these patients may be described as follows. The a-CGH profile of patient 2 (Table 3, Fig. 2C) showed in the same BM sample not only a large deletion in 43% of the cells but also a second clone with a smaller deletion, inside the region of the first one, in 23% of the cells. The overall percentage of abnormal cells became 66% for this smaller segment. Patient 4 showed a large deletion del(20)(q), a small duplication of 1.9 Mb, dup (20)(q13.32q13.33), and a duplication of the long arm of chromosome 3 (Table 3, Fig. 2A): these anomalies, found in the same BM sample, might be present in the same clone or in independent clones. In patient 9, the deletion was defined by a-CGH in 2009, but it became shorter in 2017 (Table 3, Fig. 2B): the only possible explanation of these results is that two clones with different deletions originated independently, possibly at different times. Similarly, two clones with different deletions of chromosome 20 were identified in patient 13 by comparing the results of standard chromosome analyses and a-CGH performed in 2018 (Table 3). A large del(20)(q) was observed by chromosome analysis (it was already identified one year earlier), however, a-CGH showed only a very small deletion (the smallest we ever found, 1.7 Mb (Table 3, Fig. 2E)). The only explanation for this is the presence of two clones with two different deletions, as the one observed by a-CGH was too small to be identified through chromosome analysis, despite its presence in 35% of the cells. On the contrary, the large deletion identified at standard chromosome analysis should be present in a small clone which escaped identification at a-CGH.

In patient 14, the del(20)(q) was found in 2017, and defined by a-CGH, which also gave evidence of a small duplication of chromosome 20 of 2.8 Mb, dup(20) (q11.33) (Table 3). In 2019 standard chromosome analysis failed to show the deletion, but FISH on nuclei with two different probes demonstrated the presence of two different deleted clones (Table 3, Fig. 2D), as 4% (9/222 nuclei) of the cells lost both the signals of the probes used, while 6% (13/222 nuclei) lost only the one of the probes including the *EIF6* gene. Every del(20)(q) clonal abnormality resulted in a deletion of the *EIF6* gene

The only patient considered here with the i(7)(q10), patient 10, later acquired also a deletion of the short arm of chromosome 7 (Table 3, Fig. 3), which was demonstrated by FISH as present in a clone without the isochromosome. Figure 3A shows the a-CGH profile of thei(7)(q10)in BM samples obtained in 2009 and 2017. An enlarged view of the short arm telomeric region from the sample obtained in 2017 demonstrates the de-

leted segment (Figure 3B). FISH analysis demonstrates that the clones with the i(7)(q10) and with the del(7)(p21.3pter) are independent (Figures 3C, D and E).
Results of chromosome analysis and/or a-CGH of patients 9, 10, and 11 have been previously partially reported.[10,13,17]

DISCUSSION

This study provides a detailed analysis of an additional 13 SDS patients with del(20)(q) which, taken together with the patients previously reported, demonstrate that *EIF6* is deleted in all del(20)(q) clones observed in a total of 25 patients analyzed. Overall, among 23 the result was reached by means of a-CGH, and, in two cases, through FISH analysis with informative probes. In a study on gene expression in BM of SDS patients with del(20)(q), with i(7)(q10), with other clonal anomalies or with normal karyotype, the transcription pattern of the patients with acquired del(20)(q) was similar to that of healthy subjects, at least in cases with a high proportion of abnormal cells, thus supporting a potential positive role of this anomaly[18].
These results confirmed that all the deletions are interstitial, with proximal breakpoints clustered in a region of about 2.6 Mb in bands q11.21-q11.22, while distal breakpoints were variable (Tables 2 and 3, Supplemental Table S1). In the majority of the cases, the deletion was large enough to be identified by standard chromosome analysis (range 14-26.9 Mb in 18 out of 25 patients), though smaller deletions were detectable only by a-CGH or FISH in a minority of cases. Overall, the range of the losses varies from 1.7 Mb (patient 13) to 26.9 Mb (patient 9) (Table 3). All the deletions del(20)(q) observed in the 25 patients analyzed caused the loss of the *EIF6* gene, thus confirming our previous hypothesis.
The six patients with unexpected clonal variations of the anomalies in BM, del(20)(q) in five cases, i(7)(q10) in one, either in a single sample, or in samples obtained in different years (Table 3) deserve a specific comment.
Besides the results concerning these six cases, further evidence of peculiar instability is offered by one patient already reported (UPN 68 in our previous reports),[10] in whom the del(20)(q) consisted in fact of two deletions with a segment of 2.1 Mb conserved between them.
The data regarding these seven patients provide novel evidence of karyotype instability involving mainly chromosomes 7 and 20 in the BM of patients with SDS. As the clonal anomalies found in these patients have specific prognostic significance, playing a role as BM rescue mechanisms,[10,12,18] the demonstrated variability emphasizes the importance of repeated cytogenetic follow-up, performed with all the techniques available.

ACKNOWLEDGEMENTS

This work was supported by grants from the Associazione Italiana Sindrome di Shwachman (AISS). Abdul Waheed Khan is a PhD student enrolled in the Life Sciences and Biotechnology program of the XXXIII cycle, at the University of Insubria, Varese, Italy.

CONFLICT OF INTEREST

The authors declare that there is no conflict of interest.

REFERENCES

1.Warren AJ. Molecular basis of the human ribosomopathy Shwachman-Diamond syndrome. Adv Biol Regul. 2018;67:109-127.
2.Dhanraj S, Matveev A, Li H, et al. Biallelic mutations in DNAJC21 cause Shwachman-Diamond syndrome. Blood. 2017;129:1557-1562.
3.D'Amours G, Lopes F, Gauthier J, et al. Refining the phenotype associated with biallelic DNAJC21 mutations. Clin Genet. 2018;94:252-258.
4.Stepensky P, Chacón-Flores M, Kim KH et al. Mutations in EFL1, an SBDS partner, are associated with infantile pancytopenia, exocrine pancreatic insufficiency and skeletal anomalies in a Shwachman-Diamond like syndrome. J Med Genet. 2017;54:558-566.
5.Carapito R, Konantz M, Paillard C, et al. Mutations in signal recognition particle SRP54 cause syndromic neutropenia with Shwachman-Diamond-like features. J Clin Invest. 2017;127:4090-4103.
6.Myers KC, Davies SM, Shimamura A. Clinical and molecular pathophysiology of Shwachman-Diamond syndrome: an update. Hematol Oncol Clin North Am. 2013;27:117-128.
7.Minelli A, Maserati E, Nicolis E et al. The isochromosome i(7)(q10) carrying c.258+2t>c mutation of the SBDS gene does not promote development of myeloid malignancies in patients with Shwachman syndrome. Leukemia. 2009;23:708-711.
8.Pressato B, Valli R, Marletta C, et al. Deletion of chromosome 20 in bone marrow of patients with Shwachman-Diamond syndrome, loss of the EIF6 gene and benign prognosis. Br J Haematol. 2012;157:503-505.
9.Valli R, Pressato B, Marletta C, et al. Different loss of material in recurrent chromosome 20 interstitial deletions in Shwachman-Diamond syndrome and in myeloid neoplasms. Mol Cytogenet. 2013;6:56.
10.Valli R, Minelli A, Galbiati M, et al. Shwachman-Diamond syndrome with clonal interstitial deletion of the long arm of chromosome 20 in bone marrow: haematological features, prognosis and genomic instability. Br J Haematol. 2019;184:974-981.
11.Nacci L, Valli R, Pinto RM, et al. Parental origin of the deletion del(20q) in Shwachman-Diamond patients and loss of the paternally derived allele of the imprinted L3MBTL1 gene. Genes Chromos Cancer 2017; 56:51-58.
12.Revy P, Kannengiesser C, Fischer A. Somatic genetic rescue in Mendelian haematopoietic diseases. Nat Rev Genet. 2019;20:582-598.
13.Maserati E, Minelli A, Pressato B, et al. Shwachman syndrome as mutator phenotype responsible for myeloid dysplasia/neoplasia through karyotype instability and chromosome 7 and 20 anomalies. Genes Chromos Cancer. 2006;45:375-382.
14.Maserati E, Minelli A, Olivieri C et al. Isochromosome i(7q) in Shwachman Syndrome without MDS/AML and role of chromosome 7 anomalies in myeloproliferative disorders. Cancer Genet Cytogenet. 2000;121:167-171.
15.Valli R, De Bernardi F, Frattini A et al. Comparative genomic hybridization on microarray (a-CGH) in olfactory neuroblastoma: Analysis of ten cases and review of the literature. Genes Chromos Cancer. 2015;54:771-775.
16.Valli R, Maserati E, Marletta C, et al. Evaluating chromosomal mosaicism by array comparative genomic hybridization in haematological malignancies: the proposal of a formula. Cancer Genet. 2011;204:216-218.
17.Maserati E, Pressato B, Valli R, et al. The route to development of myelodysplastic sindrome/acute myeloid leukaemia in Shwachman-Diamond syndrome: the role of ageing, karyotype instability, and acquired chromosome anomalies. Br J Haematol. 2009;145:190-197.
18.Khan AW, Minelli A, Frattini A et al. Microarray expression studies on bone marrow of patients with Shwachman-Diamond syndrome in relation to deletion of the long arm of chromosome 20, other chromosome anomalies or normal karyotype. Mol Cytogenet. 2020;13:1.

TABLE 1 The cohort of patients investigated: age at BM sampling, sex and mutations of the *SBDS* gene

Patient [a]	ID[b]	Age[c]/sex	*SBDS* Mutations
1	SDS1-000016	6/M	c.183_184TA>CT/c.258+2T>C
2	SDS1-000050	4/M	c.258+2T>C/c.258+2T>C
3	SDS1-000056	20/F	c.183_184TA>CT/c.258+2T>C
4	SDS1-000076	5/M	c.183_184TA>CT/c.258+2T>C
5	SDS1-000107	11/M	c.170T>C/258+2T>C
6	SDS1-000108	14/M	c.258+2T>C/c.258+2T>C
7	SDS1-000137	29/M	c.183_184TA>CT/c.258+2T>C
8	SDS1-000187	16/M	c.183_184TA>CT/c.258+2T>C
9	UPN 13	11, 19/M	c.183_184TA>CT+258+2T>C/258+2T>C
10	UPN 24	13, 16/F	c.183_184TA>CT/c.258+2T>C
11	UPN 31	15/F	c.183_184TA>CT/c.258+2T>C
12	UPN 45	M	c.183_184TA>CT/c.258+2T>C
13	UPN 63	13, 14/M	c.183_184TA>CT+258+2T>C/c.258+2T>C
14	UPN 81	3, 5/M	c.183_184TA>CT+258+2T>C/c.258+2T>C

[a] Patients 1-8 from the cohort of the North American Shwachman-Diamond Syndrome Registry (SDSR); patients 9-14 from the cohort of the Registro Italiano per la Sindrome di Shwachman-Diamond (RI-SDS).

TABLE 2 Patients with del(20)(q) as unique anomaly in BM: definition of the deletion by a-CGH (patients 1-8) or FISH (patients 11 and 12). The percentage of abnormal cells is calculated from a-CGH results, except for patients

Patient	Bands	Deletion start (bp)	Deletion stop (bp)	% abnormal cells
1	q11.21-q13.13	31954597	48328296	36%
3	q11.2-q13.2	31720622	53559811	26%
5	q11.21-q13.13	30849566	49398586	29%
6	q11.21-q13.13	30889915	47912299	74%
7	q11.21-q13.13	31412080	49339757	39%
8	q11.21-q13.32	31671222	57911624	36%
11	q11.22-q12[a]	-	-	-[b]
12	q11.22-q12[a]	-	-	-[c]

[a] Result obtained by double color FISH with the bac probes RP11-17F3 and RP11-29E13: the deletion therefore is at least from 33,797,020 to 40,857,566 bp.
[b] % from FISH results: 1/16 mitoses and 18/321 nuclei.
[c] % from FISH result: 9/309 nuclei.

TABLE 3 Patients with more than one different clonal anomalies in BM, either in the same sample or in samples drawn in different years: definition of anomalies by a-CGH and FISH (patients 10 and 14). The percentage of abnormal cells is calculated from a-CGH results, except for the 2nd clone of patient 13 and the 2019 sample of patient 14.

Patient	Sample	Anomaly 1st clone – bands and DNA bp (% cells)	Anomaly 2nd clone – bands and DNA bp (% cells)
2	2009	del(20)(q11.21q13.13) 30,733,183 – 49,339,757 bp (43%)	del(20)(q11.22q11.23) 33,148,327 – 36,779,644 bp (66%)[a]
4	2010	del(20)(q11.21q13.13) 31,954,597 – 49,216,901 bp (17%)[b] dup(20)(q13.32 - q13.33) – 58,349,436 –	dup(3)(q24q29) 143,044,212 – 195,076,511 bp (34%)[b]
9	2009	del(20)(q11.21q13.32) 30,876,455 – 57,739,561 bp (55%)	-
	2017	-	del(20)(q11.21q13.13) 30,904,022 – 49,344,382 bp (52%)
10	2006	i(7)(q10) (24%)[c]	-
	2009	i(7)(q10) (16%)[c]	del(7)(p21.3pter) (10%)[d]
13	2018	del(20)(q11.22q11.23) 32,738,995 – 34,468,385 bp (35%)	del(20)(q11.2q13)[e] 2 out of 6 mitoses
14	2017	del(20)(q11.21q12) 31,814,242 – 40,237,993 bp (12%)[b] dup(20)(q11.33) 58,725,726 – 61,314,465 bp	-
	2019	del(20)(q)[f]	del(20)(q)[f]

[a] This percentage includes also the cells of the 1st abnormal clone; the 2nd clone would be represented by 23% of the cells.
[b] The anomalies may be in independent clones or associated in a single clone.
[c] a-CGH results showed monosomy of the entire short arm and trisomy of the entire long arm.
[d] The anomalies were in two independent clones, as shown by FISH.
[e] Result of chromosome analysis.
[f] Two clones with different del(20)(q), as shown by FISH.

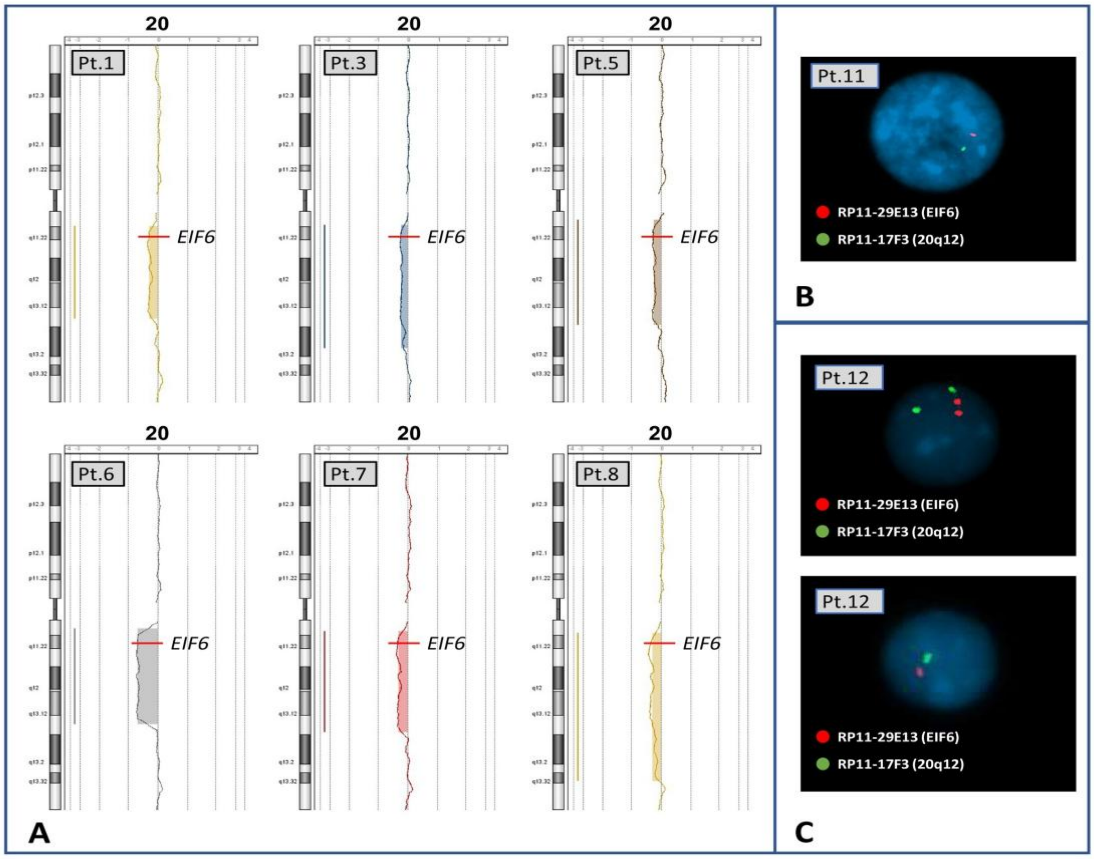

FIGURE 1 Patients with del(20)(q) as sole anomaly: a-CGH profiles of six patients (A), and FISH results on nuclei with probes RP11-29E13 (red signal), which includes the *EIF6* gene, and RP11-17F3 (green), localized in band 20q12. Patient 11, with one single signal of both probes (B), indicating a large deletion; Patient 12, with one normal nucleus with two signals of both probes and one nucleus with one signal for both probes (large deletion) (C). The precise definition of the deletions is in Table 2.

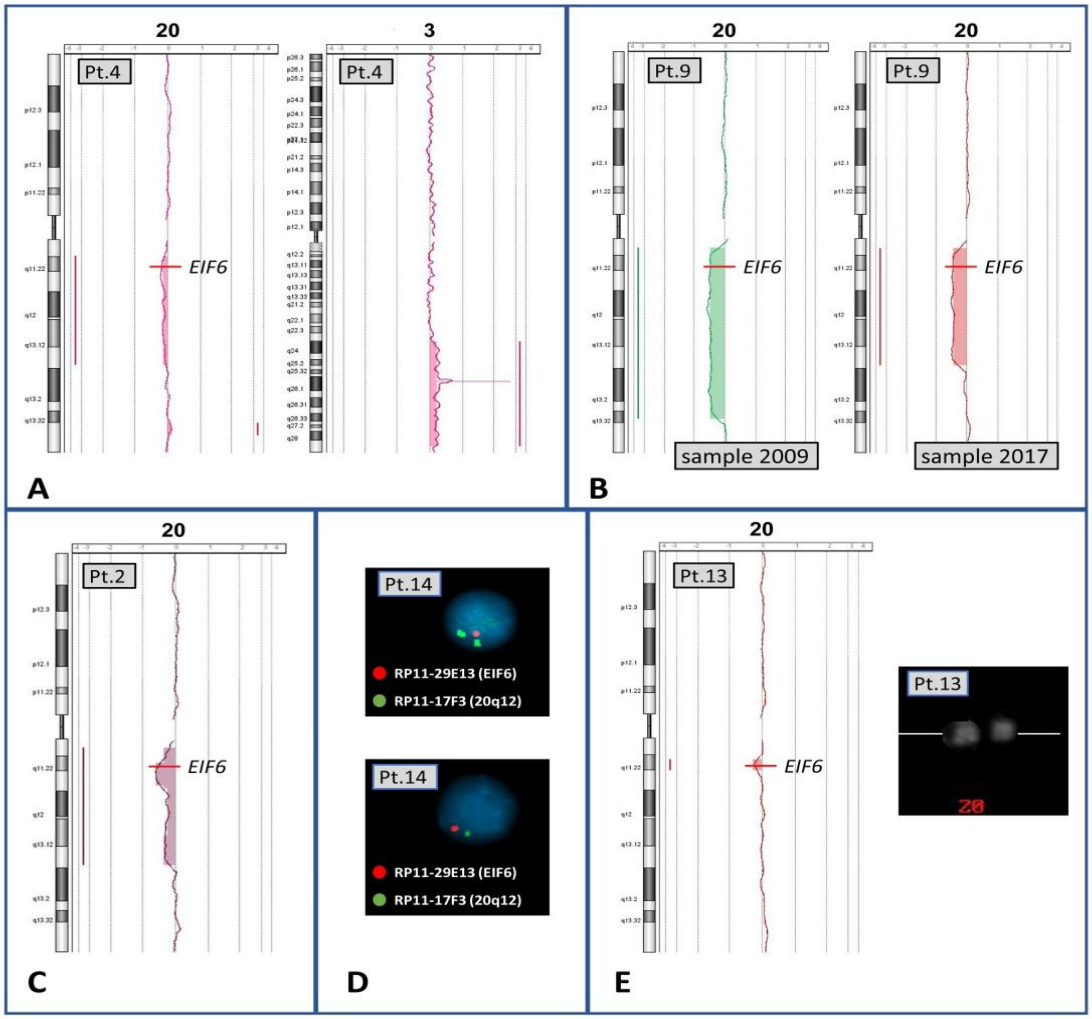

FIGURE 2 Profiles of a-CGH and FISH signals in patients with more than one abnormal clone. The a-CGH profiles of chromosome 20 and chromosome 3 of patient 4 show a large deletion del(20)(q), a small duplication of the long arm of chromosome 20 and a large duplication of chromosome 3 (A). The a-CGH profiles of BM samples from patient 9 drawn in 2009 and 2017 show two distinct sequential clones with deletions of different sizes (B). The a-CGH profile of patient 2 shows two overlapping deletions in (20)(q), one larger and one smaller, included in the first one, and both leading the loss of the *EIF6* gene (C). The double color FISH on nuclei of patient 14 at the BM sample drawn in 2019 (D), with two different probes (indicated in the figure), demonstrates that one clone bear a large deletion (loss of both signals, below), and another clone a smaller deletion, losing only the region of the *EIF6* gene (only one red signal, above). The a-CGH profile of patient 13 with a tiny del(20)(q), and a cut -out of Q-banded chromosomes 20 in which the deletion, although small, is large enough to be detected (E). The precise delineation of the anomalies is summarized in Table 3.

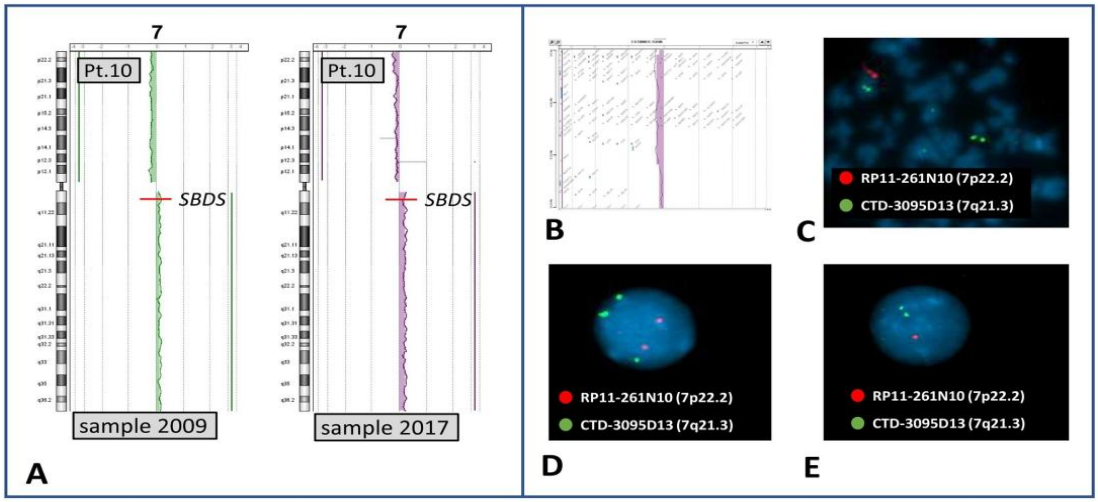

FIGURE 3 Profiles of a-CGH of patient 10 in the BM samples drawn in 2006 and 2009, showing the i(7)(q10), and in 2009 also showing a deletion of the telomeric region of the short arm (A), which is more appreciable in an enhanced image (B). Double color FISH with the probes indicated in the figure (one located in the short arm, the other in the long arm) shows that two different abnormal clones are present: one with the i(7)(q10) (nucleus with three green and two red signals) (D), one without the i(7)(q10) and with the deletion as demonstrated by the mitosis with one normal chromosome 7 and a deleted one, with only the green signal (C), and by the nucleus with two green and one red signal (E).

Supplemental Table S1: The present table lists all the 25 patients who carry the del(20)(q), included in the present report and in two previous papers. The del(20)(q) start/stop breakpoints (obtained by aCGH or FISH) and the extent of the del(20)(q) are indicated. Patients SDS1-000050 and UPN68 carry two separate del(20)(q) deletions as indicated by the breakpoints in the table.

Reference	Patient ID	Year	Deletion Start	Deletion stop	Extent (bp)
Present report	SDS1-000016	2018	31954597	48328296	16,373,699
Present report	SDS1-000050	2009	30733183 33148327	49339757 36779644	18,606,574 3,631,317
Present report	SDS1-000056	2018	31720622	53559811	21,839,189
Present report	SDS1-000076	2010	31954597	49216901	17,262,304
Present report	SDS1-0000107	2016	30849566	49398586	18,549,020
Present report	SDS1-0000108	2011	30889915	47912299	17,022,384
Present report	SDS1-0000137	2018	31412080	49339757	17,927,677
Present report	SDS1-0000187	2017	31671222	57911624	26,240,402
Present report	UPN 13	2009	30876455	57739561	26,863,106
Present report	UPN 13	2017	30904022	49344382	18,440,360
Present report	UPN 31	2019	33797020*	40857566*	7,060,546**
Present report	UPN 45	2019	33797020*	40857566*	7,060,546**
Present report	UPN 63	2017	32738995	34468385	1,729,390
Present report	UPN 81	2017	31814242	40237993	8,423,751
Valli et al, 2013	UPN 14	2004	31163090	35309353	4,146,263
Valli et al, 2013	UPN 17	2008	31205853	55894832	24,688,979
Valli et al, 2013	UPN 20	2004	31294381	57252304	25.957.923
Valli et al, 2013	UPN 65	2012	30157286	49497910	19.340.624
Valli et al, 2013	UPN 68	2013	31262228 45244728	43141564 47373129	11.879.336 2.128.401
Valli et al, 2019[9]	UPN 1	2001	31891819	48287277	16.395.458
Valli et al, 2019[9]	UPN 6	2006	30922628	49497969	18.575.341
Valli et al, 2019[9]	UPN 35	2016	31798183	47884947	16.086.764
Valli et al, 2019[9]	UPN 82	2014	30020250	52206444	22.186.194
Valli et al, 2019[9]	UPN 84	2016	32620650	58600338	25.979.688
Valli et al, 2019[9]	UPN 85	2015	31814242	36538658	4,724,416

* From FISH: approximate minimal evaluation
** minimal evaluation

RESULTS (SECTION 3)

Khan *et al. Molecular Cytogenetics* (2020) 13:1
https://doi.org/10.1186/s13039-019-0466-9

Molecular Cytogenetics

RESEARCH Open Access

Microarray expression studies on bone marrow of patients with Shwachman-Diamond syndrome in relation to deletion of the long arm of chromosome 20, other chromosome anomalies or normal karyotype

Abdul Waheed Khan[1], Antonella Minelli[2], Annalisa Frattini[1,3], Giuseppe Montalbano[1], Alessia Bogni[4], Marco Fabbri[5], Giovanni Porta[1], Francesco Acquati[6], Rita Maria Pinto[7], Elena Bergami[8], Rossella Mura[9], Anna Pegoraro[10], Simone Cesaro[10], Marco Cipolli[11], Marco Zecca[8], Cesare Danesino[2], Franco Locatelli[7], Emanuela Maserati[1], Francesco Pasquali[1] and Roberto Valli[1*]

Abstract

Background: Clonal chromosome changes are often found in the bone marrow (BM) of patients with Shwachman-Diamond syndrome (SDS). The most frequent ones include an isochromosome of the long arm of chromosome 7, i (7)(q10), and an interstitial deletion of the long arm of chromosome 20, del (20)(q). These two imbalances are mechanisms of somatic genetic rescue. The literature offers few expression studies on SDS.

Results: We report the expression analysis of bone marrow (BM) cells of patients with SDS in relation to normal karyotype or to the presence of clonal chromosome anomalies: del (20)(q) (five cases), i (7)(q10) (one case), and other anomalies (two cases). The study was performed using the microarray technique considering the whole transcriptome (WT) and three gene subsets selected as relevant in BM functions. The expression patterns of nine healthy controls and SDS patients with or without chromosome anomalies in the bone marrow showed clear differences.

Conclusions: There is a significant difference between gene expression in the BM of SDS patients and healthy subjects, both at the WT level and in the selected gene sets. The deletion del (20)(q), with the *EIF6* gene consistently lost, even in patients with the smallest losses of material, changes the transcription pattern: a low proportion of abnormal cells led to a pattern similar to SDS patients without acquired anomalies, whereas a high proportion yields a pattern similar to healthy subjects. Hence, the benign prognostic value of del (20)(q). The case of i (7)(q10) showed a transcription pattern similar to healthy subjects, paralleling the positive prognostic role of this anomaly as well.

Keywords: Shwachman-diamond syndrome, Expression analysis, Clonal chromosome anomalies in bone marrow, *EIF6* gene, Risk of MDS/AML, Somatic genetic rescue

* Correspondence: roberto.valli@uninsubria.it
[1]Genetica Umana e Medica, Dipartimento di Medicina e Chirurgia, Università dell'Insubria, Via J. H. Dunant, 5, 21100 Varese, Italy
Full list of author information is available at the end of the article

Background

Shwachman-Diamond syndrome (SDS) is an autosomal recessive disorder (Online Mendelian Inheritance in Man #260400) characterized by bone marrow failure, peripheral cytopenias and an increased risk of developing myelodysplastic syndrome (MDS) and acute myeloid leukaemia (AML). The patients exhibit several other anomalies, including cognitive impairment [1]. SDS is caused by mutations in the *SBDS* gene in at least 90% of cases [1], but it is genetically heterogeneous. In addition to other functions, the SBDS protein has a pivotal role in ribosome biogenesis [1]. Furthermore, biallelic mutations of two other genes involved in ribosome biogenesis may cause SDS or an SDS-like condition: *DNAJC21* [2, 3] and *EFL1* [4]. Moreover, an SDS-like phenotype may be caused by monoallelic mutations in the *SRP54* gene, which produces a protein that is a key member of the cotranslation protein-targeting pathway [5]. Therefore, SDS may be considered a ribosomopathy.

Clonal chromosome changes are often found in the bone marrow (BM) of patients with SDS. Among them, the most frequent ones include an isochromosome of the long arm of chromosome 7, i (7)(q10), and an interstitial deletion of the long arm of chromosome 20, del (20)(q) [6]. We already postulated that the presence of del (20)(q), with the loss of the *EIF6* gene, results in more efficient ribosome biogenesis and implies both a lower risk of MDS/AML [7] and a milder haematological condition compared to SDS patients without del (20)(q) [8, 9].

The literature offers quite a few expression studies on SDS. Some of them concern the expression of specific genes in *SBDS* knocked-down cell lines (HeLa, NIH3T3) or in BM cells of SDS patients. These studies reveal interesting results; however, the scope of the presented work is limited to a few sets of considered genes [10–12]. We also remark that in some cell lines, such as HeLa, the results of expression analysis might be altered due to high variability of genomic instability and expression profiling among different batches, to the point that some results may be not completely reliable [13]. More extensive expression studies on BM from SDS patients and on other modified cell lines led to the detection of a series of genes that are up- or downregulated. Among those gene sets, many are important in leukaemia pathogenesis or ribosome biogenesis and function [14, 15]. Possible chromosome anomalies were not considered in all those studies.

The benign prognostic role of del (20)(q) that is acquired in BM prompted us to perform an expression study on the BM of patients with del (20)(q) even at the level of the whole transcriptome. In these patients, we report the expression analysis of the *EIF6* gene, of the whole genome, and of gene sets selected as relevant in haematopoiesis, myeloid leukaemias, or myeloid differentiation. These results are compared with those obtained from patients who exhibit other clonal chromosome anomalies or show a normal karyotype in relation to healthy controls.

Results

Out of the total 17 patients with SDS, chromosome anomalies were found in eight, and their cytogenetic results, at the date of sampling for RNA study, are summarized in Table 1. All patients are identified by their unique patient number (UPN). The clonal del (20)(q) was present in five patients (UPN 6, 13, 20, 68, 85) encompassing the *EIF6* gene in all samples, as demonstrated by array-based comparative genomic hybridization (a-CGH), the i (7)(q10) in one patient (UPN 24) and a clonal unbalanced translocation t(1;16) in one patient (UPN 58). The a-CGH analysis showed that the del (20)(q) in UPN 13 was smaller in the 2017 sample than that in the 2015 sample. One patient (UPN 92), the only one who developed AML, showed clones with complex abnormal karyotypes, with structural anomalies, not better defined, involving chromosomes 1, 2, 3, 5, 8, 10, 11 and 12. Table 1 also provides the percentage of abnormal cells at the date of BM sampling for transcription analysis. These percentages were inferred either from the results of fluorescent in situ hybridization (FISH)

Table 1 Clonal chromosome anomalies in BM, and percentage of abnormal cells at the date of sampling for RNA study

Patient UPN	Sample[a]	anomaly	% abnormal cells
6	2014	del (20)(q11.21q13.13)	44%[e]
13	2015	del (20)(q11.21q13.32)	12%[e]
	2017	del (20)(q11.21q13.13)	52%[f]
20	2013	del (20)(q11.21q13.32)[b]	68%[f]
	2015		60%[f]
	2017		76%[f]
24	2009	i (7)(q10)	30%[f]
58	2014	der(16)t(1;16)(q21;q23)	17%[f]
	2017		15%[f]
68	2016	del (20)(q11.21q13.12) del (20)(q13.12q13.13)[c]	19%[f]
85	2015	del (20)(q11.21q11.23)	14%[f]
	2016		–
	2017		11%[e]
92	2017	complex karyotype[d]	83%[g]

[a]Sample identified by the year of analysis
[b]Presence of an additional subclone with a rearrangement of the del (20)(q), with deleted and duplicated portions of chromosome 20 [16]
[c]Two interstitial deletions with a conserved segment of 2103 Kb in between
[d]Clones with several structural anomalies, not better defined, involving chromosomes 1, 2, 3, 5, 8, 10, 11 and 12
[e]Results of FISH on nuclei
[f]Calculated from a-CGH results
[g]Result of chromosome analysis

on nuclei with informative probes or from the results of a-CGH with the appropriate formula [17] or from chromosome analysis (in one patient).

In nine patients, no anomalies were present in the BM at the date of sampling for RNA study, according to the available results of chromosome analyses, FISH with probes informative for i (7)(q10) and del (20)(q), and a-CGH (UPN 2, 26, 45, 51, 60, 70, 80, 81, 91). In this paper, we designated these patients as SDS-NK (normal karyotype) patients.

In the context of expression studies, we extrapolated the EIF6 RNA levels from the array raw data, and they are shown in Fig. 1a. The mean and the standard error for the expression levels of the nine normal controls and the nine SDS-NK patients are reported in black and grey bars, respectively, whereas the other bars refer to single patient specimens. Figure 1b shows the $\log_2$ heatmap for EIF6 expression levels.

Whole transcriptome (WT) results were analysed by principal component analysis (PCA) from both SDS patients (with and without chromosome anomalies) and controls. The graph showing PCA for all the subjects under study is shown in Fig. 2. A trend indicating the stratification of patients in groups is appreciable. WT cluster analysis led to the dendrogram shown in Fig. 3.

We analysed some specific gene sets by PCA and cluster analysis (Additional file 1: Figures S1, S2, S3, S4, S5 and S6), chosen as relevant in haemopoiesis and leukaemogenesis:

1) Gene set 1: KEGG Haematopoietic Cell Lineage (map 04640): this pathway is composed of 88 genes, the major portion belonging to cytokines, growth factors and cell differentiation markers that drive the differentiation process of the haematopoietic cell lineage [18].
2) Gene set 2: KEGG Acute Myeloid Leukemia (map 05221): this pathway is composed of 60 genes belonging to oncogenes, protein kinases, tumour suppressor genes, translocation cancer genes and

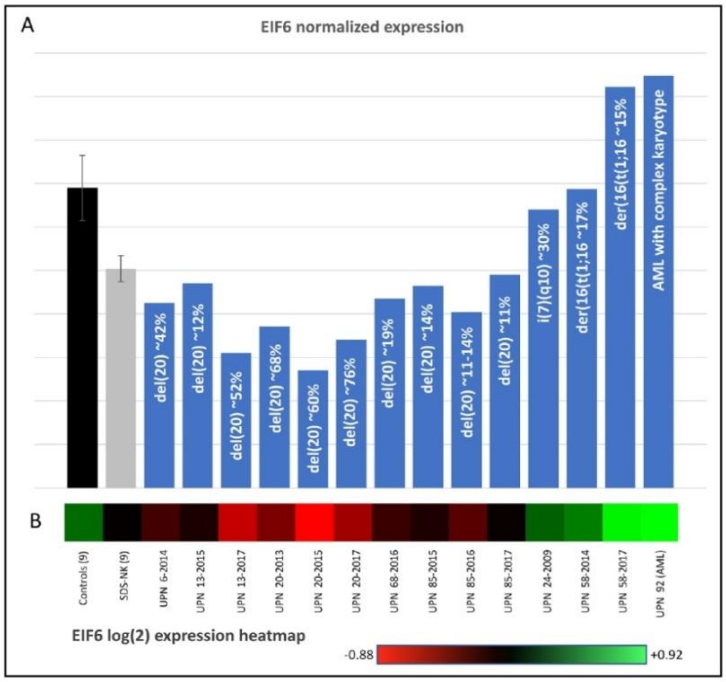

Fig. 1 EIF6 expression. **a** *EIF6* normalized expression extrapolated from array raw data. The expression values for the single probe A_23_P210939, included in the array used have been extrapolated by the imported $\log_2$ raw data with baseline normalization. Values of each specimen has been 2-power exponentially transformed in order to obtain the linear values. **b** The $\log_2$ heatmap for *EIF6* expression. The patients' samples are indicated at the bottom and their chromosome anomalies are inserted in the histogram bars, with the percentage of abnormal cells. The black and grey bars refer to the average value of the nine controls and the nine SDS-NK patients; the standard error is indicated

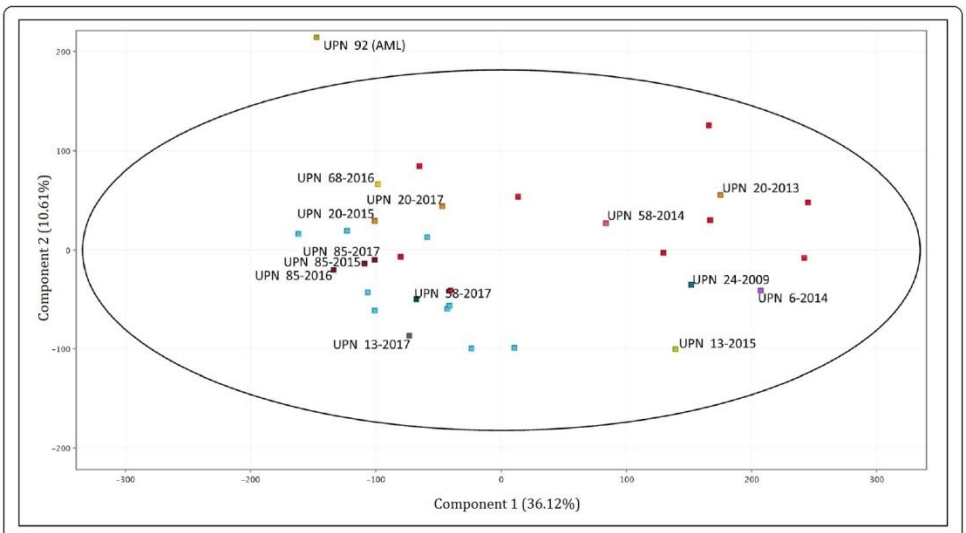

Fig. 2 Principal Component Analysis (PCA) plot for the whole transcriptome. Healthy controls are indicated by red squares. SDS-NK patients are indicated by light-blue squares. Patients with chromosomal anomalies are identified by their UPN number and the year of the sample near the related colored squares. Component 1 and 2 percentages of variance are indicated in the two axes. The black ellipse indicates the 95% confidence interval

transcription factors that might be deregulated in acute myeloid leukaemia patients [19].

3) Gene set 3: Gene Ontology Myeloid Leukocyte Differentiation (GO:0002573): this pathway is composed of 96 genes that drive a relatively unspecialized myeloid precursor cell to acquire the specialized features of any cell of the myeloid leukocyte lineage [20].

The analysis was performed with the same approach as WT for the three gene sets, and Table 2 summarizes a comparison among the results obtained in the patients with chromosome changes with those of the groups defined by PCA and cluster analyses of WT.

Discussion

The nine SDS-NK patients showed levels of EIF6 RNA slightly but significantly decreased in comparison to the nine healthy controls (Student's t test: $p = 0.02$). All patients carrying the del (20)(q) showed a more remarkable decrease compared to the healthy controls, with a trend related to the proportion of cells containing the deletion (Table 1, Fig. 1a). We postulate that low RNA levels lead to decreased amounts of EIF6 protein, even if we did not have enough material to prove it. The patient UPN 24, carrying i (7)(q10), exhibits normal EIF6 levels as expected, as does UPN 58 (with another different chromosome anomaly) (Fig. 1a). The patient with AML and a complex karyotype, UPN 92, exhibited increased levels of EIF6 (Fig. 1a); it is worth noting that numerous studies have demonstrated highly aberrant overexpression of EIF6 in human cancer [21].

In the WT study, the stratification of SDS patients shown by PCA offers some relevant conclusions. In particular (Fig. 2), the SDS-NK patients (light blue squares) group on the left, while the controls (red squares) are more dispersed, and most of them are far from the SDS-NK group. We recall that we worked on RNA extracted from whole marrow samples containing heterogeneous populations of cells; this may explain the lack of strictly homogeneous results in controls. The result, however, indicates that the WT expression pattern of these two groups is truly different. The difference from controls is in agreement with data already reported, but these reports were limited to leukaemia-related genes [14], apoptosis-related genes [10], ribosome biogenesis and RNA processing genes, and other specific genes relevant for SDS phenotype [11, 12, 15] without any relation to the presence of clonal chromosome anomalies.

The patients carrying the del (20)(q), which encompasses the *EIF6* gene in all cases, are indicated in Fig. 2 by squares of other colours, and they are distributed in the plot partially in agreement with the different percentage of cells of the abnormal clone.

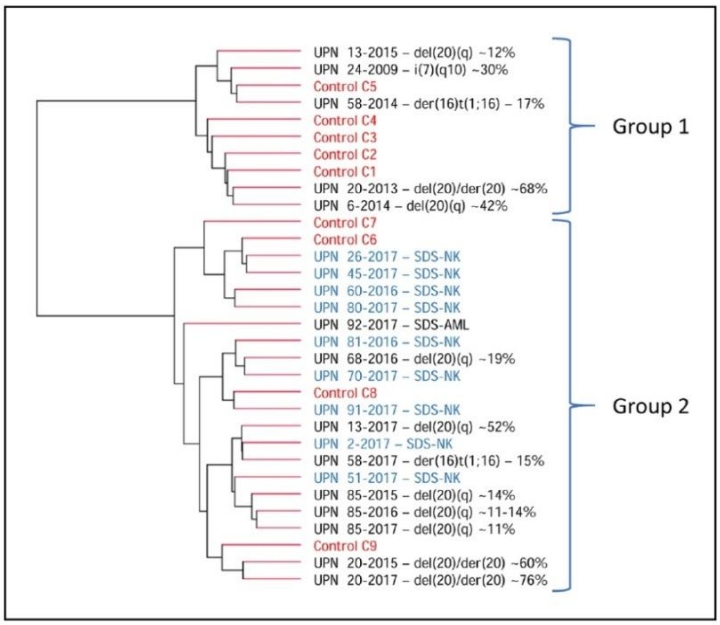

Fig. 3 Dendrogram of cluster analysis for the whole transcriptome. Two groups (1 and 2) may be identified. Healthy controls are in red and SDS-NK patients are indicated in light blue with their UPN number. Patients with chromosome anomalies are in black with their UPN number and sample (year), followed by the chromosome anomaly and the percentage of abnormal cells

Table 2 Transcription study of the selected gene sets relevant in haematopoiesis, leukaemogenesis and myeloid differentiation, identified as 1, 2, and 3 and described in the Results Section: comparison of the results obtained in patients with clonal anomalies (Table 1), grouped here as A and B. Group A includes most healthy controls and Group B all SDS-NK patients. Patient UPN 92, with AML and complex karyotype is not included in the Table, because her expression profile was different from all other subjects investigated and outside the groups identified

Sample[a]	Anomaly – %[b]	Gene Set 1		Gene Set 2		Gene set 3	
		Group		Group		Group	
		A	B	A	B	A	B
UPN 6–2014	del (20) – 44%	•		•		•	
UPN 13–2015	del (20) – 12%		•		•	•	
UPN 13–2017	del (20) – 52%		•		•		•
UPN 20–2013	del (20) – 68%	•		•		•	
UPN 20–2015	del (20) – 60%	•			•		•
UPN 20–2017	del (20) – 76%	•		•		•	
UPN 24–2009	i (7)(q10) – 30%	•		•		•	
UPN 58–2014	der(16)t(1;16) – 17%	•		•		•	
UPN 58–2017	der(16)t(1;16) – 15%		•		•		•
UPN 68–2016	del (20) – 19%	•			•		•
UPN 85–2015	del (20) – 14%		•		•		•
UPN 85–2016	del (20)		•		•		•
UPN 85–2017	del (20) – 11%		•		•		•

[a]See Table 1
[b]Clonal anomaly in short - % abnormal cells

Among these patients, the percentage of abnormal BM cells of UPN 68 and UPN 85 was rather low (Table 1), EIF6 expression was only slightly reduced (Fig. 1a), and the PCA plots these BM samples were near the SDS-NK group. Therefore, these two patients with a small number of cells with del (20)(q) show a WT expression pattern similar to SDS-NK patients.

In contrast, patients UPN 6 and UPN 20 (sample 2013), who carry a high proportion of cells with del (20)(q) in the BM (Table 1), with evident decreased levels of EIF6 transcript (Fig. 1a), are plotted in the PCA graph rather distantly from SDS-NK patients. The other two specimens of UPN 20 (sampled in 2015 and 2017, with similar del (20)(q) cell proportions and *EIF6* hypoexpression patterns) are plotted closer to the SDS-NK group. This patient also carried a subclone with a further rearrangement of the del (20)(q), with deletion of the short arm and portions of the chromosome duplicated and deleted [16]. The proportion of this subclone increased from 2013 to 2017, while neutropenia worsened: the difference in expression might be due to this subclone. We postulate that the loss of EIF6 protein was enough to give a transcription pattern similar to controls in 2013 but was less effective in 2015 and 2017. This could explain the different plots of the sample UPN 20–2013 from UPN 20–2015 and UPN 20–2017. The patient UPN 13 exhibited an unexpected pattern for the two specimens from 2013 and 2015. In particular, the UPN 13–2015 sample has a low number of cells with del (20)(q) (Table 1), and *EIF6* expression is only slightly reduced (Fig. 1a). It is plotted in the PCA far from the SDS-NK group. In contrast, specimen UPN 13–2013, with a high proportion of cells with del (20)(q) and a remarkably low level of *EIF6* transcript, is plotted closer to the SDS-NK group. In fact, patient UPN 13 showed two different extents of the deletion in these two different specimens (Table 1). This could explain the differences in the PCA plots.

In general, these data indicate that patients with a high proportion of cells containing del (20)(q) show a WT expression pattern similar to healthy controls in the absence of further changes that may modify the pattern. The positive prognostic role of del (20)(q) would be a consequence of this type of rescue mechanism [8, 9], although it would be limited to cases with a high proportion of abnormal cells [22].

Patient UPN 24, with the i (7)(q) present in ~ 30% of the cells (Table 1), is plotted by the PCA algorithm far from the SDS-NK group. In the isochromosome, the *SBDS* gene is present twice in the form of the mild mutation 258 + 2 T > C, and this fact leads to a different form of rescue mechanism in ribosome biogenesis, impaired by *SBDS* mutations, thanks to some amount of normal SBDS protein [23]. UPN 58, with specimens in 2014 and 2017, carries an unbalanced complex rearrangement that involves chromosomes 1 and 16 (Table 1). The two samples of this patient are plotted differently in the graph. We have no clear-cut explanation for this result, but in conditions different from SDS, gene effects of unbalanced chromosome anomalies may be detected and cause specific pathologic features [24]. The only patient that developed AML (UPN 92) has a complex karyotype (Table 1) and is plotted in the PCA graph far from all the other patients and outside the 95% confidence interval (Fig. 2).

The dendrogram shown in Fig. 3 resembles the PCA plots of Fig. 2. The interconnection lines identify two groups (1 and 2) with similar distribution to the PCA plot commented above.

The transcription study of the selected groups of genes relevant in haematopoiesis, leukaemogenesis and myeloid differentiation defined in the Results section gave results in PCA largely similar to WT: SDS-NK constitute a well-defined group in all gene sets, while most healthy controls do not constitute a real group and are more dispersed in the plot (Additional file 1: Figures S1, S3 and S5). Cluster analysis based on dendrogram diagrams and related heatmaps confirmed this difference, with particular evidence for gene sets 1 and 2 (Additional file 1: Figures S2, S4 and S6).

Regarding patients carrying clonal chromosome changes, Table 2 shows a comparison of their results with healthy donors and SDS-NK patients. Most patients carrying del (20)(q) at low percentages fall in the group of SDS-NK patients for all gene sets (group B in Table 2), which is expected because EIF6 RNA in these patients is close to normal levels and cannot lead to a rescue of the altered *SBDS* pathway. On the other hand, most of the patients with higher percentages of del (20)(q) fall closer to healthy controls (group A in Table 2), as expected by the rescue mechanism postulated when the level of EIF6 is reduced. Few exceptions are present, and the explanation would be as for WT. Additionally, the only patient with i (7)(q10) falls in the group of the healthy controls, as expected, by the other rescue mechanism described [23].

The following points about the three gene sets analysed are worth highlighting.

Gene set 1: An interesting subset of genes, including the oncogene *KIT*, *THPO* (Thrombopoietin), *EPO* (erythropoietin), *GP1BA* (Glycoprotein 1b Platelet Subunit Alpha), and some cytokines, are upregulated in controls and downregulated in SDS-NK patients (Additional file 1: Figure S2). Another group involving many cluster differentiation (CD) genes and other cytokines is upregulated in the SDS-NK group and downregulated in controls.

Gene set 2: The cluster analysis (Additional file 1: Figure S4) firmly indicates a group of genes, including oncogenes and transcription factors, that are upregulated in controls and downregulated in SDS-NK.
Gene set 3: The cluster analysis also showed that the gene *ANXA2* is extremely downregulated in the healthy controls, while it is expressed within the baseline level in the SDS-NK group (Additional file 1: Figure S6). *ANXA2* is frequently upregulated in many types of cancers [25]. A group of genes (*IL31RA*, *TNFSF11*, *TNFSF11A*, *KIT*, *CSF1*, *CSF2*, *CSF3*, *IL25*, *GPC3*, *FARP2*, *EFNA2*, *EPHA2*, *BMP4*, *CASP10*) is upregulated in healthy controls and, interestingly, in UPN 6, UPN 13–2015, UPN 20–2013, with del (20)(q), in UPN 24, with i (7)(q10), and in UPN 58–2014, with the der (16)(t(1;16). These genes are transcription factors, oncogenes, cytokines, signal transduction genes, growing factors and apoptotic regulators; they play an important role in many biological systems, including leukocyte differentiation, bone morphogenesis, and macrophage differentiation.

Conclusions

In summary, our transcription study shows the following:

- There is a difference between gene expression in BM of SDS patients and healthy subjects, both at the level of WT and that of selected gene sets relevant for BM functions;
- In SDS patients, the presence of clonal chromosome anomalies also makes the difference at the transcription level;
- The deletion del (20)(q), with the loss of EIF6 gene, present even in the smallest deletions, changes the transcription pattern of BM: a low proportion of abnormal cells led to a pattern similar to SDS patients without acquired chromosome anomalies, whereas a high proportion exhibit a pattern similar to healthy subjects; hence, the benign prognostic value of the del (20)(q) which has already been demonstrated in many patients [8];
- The single case of i (7)(q10) included in this study showed a benign transcription pattern, similar to healthy subjects, paralleling the already established positive prognostic role of this anomaly as well;
- Too little is known about other acquired clonal anomalies to reach any relevant conclusions for prognosis.

Methods

Patient selection and sample preparation

The materials for our study consisted of 23 BM samples from 17 patients with SDS, as in four cases the analysis was repeated at two different dates (two cases) or three (two other cases). The patients included three females and 14 males, with an age range of 2–44 years at the time of sampling for RNA analysis. All patients are part of the cohort of 97 Italian patients who have been followed for cytogenetics since 1999. All patients had biallelic mutations in the *SBDS* gene, including 14/17 cases with the two most frequent mutations. Some analyses were repeated at different dates in subsequent years, as the proportion of abnormal cells may vary considerably in time. A portion of the cytogenetic results has already been reported [16, 22, 26–28]. Table 1 gives the years of the cytogenetic analyses performed at the time of sampling for expression studies. All patients are identified by their UPN, as in our previous publications. We reported and discussed the haematological parameters of the patients with del (20)(q) [8], although the sampling date is often not the same as the present RNA study. Some additional haematological data of all the SDS patients reported here are provided in Additional file 2: Table S1.

Nine healthy subjects were used as controls, and their BM was drawn because they were donors for haematopoietic stem cell transplantation (HSCT).

Informed consent for this study was obtained according to the principles of the Declaration of Helsinki from the patients or the patients' parents.

Chromosome analyses were performed on BM with routine methods. FISH on BM nuclei was carried out by standard techniques with the following bac probes, informative for the deletion del (20)(q) detected in each patient: RP11-17F3 (UPN 6, 13, 20), CTD-2559C9 (UPN 13), XL Del(20q) probe (Metasystems, Altlussheim, Germany) (UPN 68), RP11-17F3 + RP11-29E13 (UPN 85).

The a-CGH was performed on DNA from BM samples with the 244 K genome-wide system (Agilent Technologies Inc., Santa Clara, CA, USA) according to the manufacturer's instructions, as already described [29]. All DNA was extracted from BM using a liquid-based Flexigene kit (Qiagen, Hilden, Germany) as recommended by Nacheva et al., 2017 [30].

For expression analysis of patients with SDS and controls, 2 ml of BM material was immediately pipetted into a PAXgene Bone Marrow RNA Tube (Qiagen, Hilden, Germany). The extraction was performed with the PAXgene Bone Marrow RNA Kit (Qiagen, Hilden, Germany). RNA integrity was assessed by Agilent's Bioanalyzer 2100 instrument (Agilent Technologies, Santa Clara, USA) according to the manufacturer's instructions. All the RNA samples used in this study exhibited an RNA Integrity Number (RIN) [31] above 8.0.

Whole transcriptome microarray and bioinformatical analysis

We used the Agilent Microarray System (Agilent Technologies, Santa Clara, USA) to perform microarray

expression profiling according to Agilent's One-Color Microarray-Based Gene Expression Analysis Low Input Quick Amp Labelling Protocol (Version 6.9.1) with Agilent's Whole Transcriptome (WT) Oligo Human Microarray slides 8 × 60 K format (G4851A, AMADID #028004).

Data analysis was performed using Agilent GeneSpring 14.9.1 software. Data from each sample were imported into the software with the following parameters: Threshold: 1, Logbase: 2, Normalization: Shift to 75.0 percentile, Baseline Transformation: median of all samples.

Clustering analysis was performed by hierarchical analysis on normalized intensity values with Euclidean Distance Metrics and Ward's linkage rules both on all genes as well as on selected gene sets. PCA was performed by the internal software plugin both with all genes as well as on selected gene sets.

Supplementary information

Supplementary information accompanies this paper at https://doi.org/10.1186/s13039-019-0466-9.

Additional file 1: Figures S1, S2, S3, S4, S5 and S6. PCA and cluster analysis, with heatmaps and dendrograms, of the three gene sets chosen as relevant in haemopoiesis and leukaemogenesis and defined in the Results section.

Additional file 2: Table S1. Blood count and bone marrow cellularity of all the SDS patients here reported at the date of sampling for RNA expression study.

Abbreviations

a-CGH: Array-based comparative genomic hybridization; AML: Acute myeloid leukaemia; BM: Bone marrow; DNA: Deoxyribonucleic acid; FISH: Fluorescent in situ hybridization; HSCT: Haematopoietic stem cell transplantation; MDS: Myelodysplastic syndrome; PCA: Principal component analysis; RIN: RNA integrity number; RNA: Ribonucleic acid; SDS: Shwachman Diamond syndrome; SDS-NK: SDS with normal karyotype; UPN: Unique patient number; WT: Whole transcriptome

Acknowledgements

The support of Associazione Italiana Sindrome di Shwachman (AISS) is gratefully acknowledged. The research leading to the microarray data resulted also from access to the Nanobiotechnology Laboratory under the Framework for open access to the Joint Research Centre Research Infrastructures of the European Commission. The authors thank Pascal Colpo. Abdul Waheed Khan is a PhD student enrolled in the Life Sciences and Biotechnology program of the XXXIII cycle.

Authors' contributions

AWK, AM, AF, GM, AB, MF, GP, FA, RV performed the research and analyzed the data. RMP, EB, RM, AP, SC, MC, MZ, FL followed the patients and contributed with all clinical data. RV, CD, EM, FP designed the research, analyzed the data and wrote the paper. All authors read and approved the final manuscript.

Funding

This work was supported by grants from the Associazione Italiana Sindrome di Shwachman (AISS). This research was supported by a Grant from the Italian Ministry of Education, University and Research (MIUR) to the Department of Molecular Medicine of the University of Pavia under the initiative "Dipartimenti di Eccellenza (2018–2022)".

Availability of data and materials

The data used and analyzed in the current study are available from the corresponding author on reasonable request.

Ethics approval and consent to participate

Informed consent to this study was obtained according to the principles of the Declaration of Helsinki from the patients, the patients' parents, and from healthy controls.

Consent for publication

Informed consent for publication was obtained from the patients, the patients' parents, and from healthy controls.

Competing interests

The authors declare that they have no competing interests.

Author details

[1]Genetica Umana e Medica, Dipartimento di Medicina e Chirurgia, Università dell'Insubria, Via J. H. Dunant, 5, 21100 Varese, Italy. [2]Genetica Medica, Fondazione IRCCS Policlinico S. Matteo and Università di Pavia, Pavia, Italy. [3]UOS Milano IRGB, Consiglio Nazionale delle Ricerche, Milano, Italy. [4]European Commission, Joint Research Centre (JRC), Ispra, Italy. [5]Haematopathology Division, European Institute of Oncology, Milano, Italy. [6]Department of Biotechnology and Life Sciences, Università dell'Insubria, Varese, Italy. [7]Department of Pediatric Hematology and Oncology, IRCCS Ospedale Pediatrico Bambino Gesù, Università di Roma Sapienza, Roma, Italy. [8]Pediatric Hematology / Oncology, Fondazione IRCCS Policlinico S. Matteo, Pavia, Italy. [9]SC Oncoematologia Pediatrica, Ospedale Pediatrico Microcitemico "Antonio Cao", Azienda Ospedaliera Brotzu, Cagliari, Italy. [10]Pediatric Hematology Oncology, Ospedale Donna Bambino, Azienda Ospedaliera Universitaria Integrata, Verona, Italy. [11]Cystic Fibrosis Center, Azienda Ospedaliera Universitaria Integrata di Verona, Verona, Italy.

Received: 24 October 2019 Accepted: 13 December 2019
Published online: 02 January 2020

References

1. Warren AJ. Molecular basis of the human ribosomopathy Shwachman-diamond syndrome. Adv Biol Regul. 2018;67:109–27.
2. Dhanraj S, Matveev A, Li H, et al. Biallelic mutations in DNAJC21 cause Shwachman-diamond syndrome. Blood. 2017;129:1557–62.
3. D'Amours G, Lopes F, Gauthier J, et al. Refining the phenotype associated with biallelic DNAJC21 mutations. Clin Genet. 2018;94:252–8.
4. Stepensky P, Chacón-Flores M, Kim KH, et al. Mutations in EFL1, an SBDS partner, are associated with infantile pancytopenia, exocrine pancreatic insufficiency and skeletal anomalies in a Shwachman-diamond like syndrome. J Med Genet. 2017;54:558–66.
5. Carapito R, Konantz M, Paillard C, et al. Mutations in signal recognition particle SRP54 cause syndromic neutropenia with Shwachman-diamond-like features. J Clin Invest. 2017;127:4090–103.
6. Myers KC, Davies SM, Shimamura A. Clinical and molecular pathophysiology of Shwachman-diamond syndrome: an update. Hematol Oncol Clin North Am. 2013;27:117–28.
7. Pressato B, Valli R, Marletta C, et al. Deletion of chromosome 20 in bone marrow of patients with Shwachman-diamond syndrome, loss of the EIF6 gene and benign prognosis. Br J Haematol. 2012;157:503–5.
8. Valli R, Minelli A, Galbiati M, et al. Shwachman-diamond syndrome with clonal interstitial deletion of the long arm of chromosome 20 in bone marrow: haematological features, prognosis and genomic instability. Br J Haematol. 2019;184:974–81.
9. Revy P, Kannengiesser C, Fischer A. Somatic genetic rescue in Mendelian haematopoietic diseases. Nat Rev Genet. 2019;20:582–98.
10. Rujkijyanont P, Watanabe K, Ambekar C, et al. SBDS-deficient cells undergo accelerated apoptosis through the Fas-pathway. Haematologica. 2008;93:363–71.
11. Nihrane A, Sezgin G, Dsilva S, et al. Depletion of the Shwachman-diamond syndrome gene product, SBDS, leads to growth inhibition and increased expression of OPG and VEGF-A. Blood Cells Mol Dis. 2009;42:85–91.
12. In K, Zaini MA, Müller C, et al. Shwachman-Bodian-diamond syndrome (SBDS) protein deficiency impairs translation re-initiation from C/EBPα and C/EBPβ mRNAs. Nucleic Acids Res. 2016;44:4134–46.

13. Frattini A, Fabbri M, Valli R, et al. High variability of genomic instability and gene expression profiling in different HeLa clones. Sci Rep. 2015;5:15377. https://doi.org/10.1038/srep15377.
14. Rujkijyanont P, Beyene J, Wei K, et al. Leukaemia-related gene expression in bone marrow cells from patients with the preleukaemic disorder Shwachman-diamond syndrome. Br J Haematol. 2007;137:537–44.
15. Rujkijyanont P, Adams SL, Beyene J, et al. Bone marrow cells from patients with Shwachman-diamond syndrome abnormally express genes involved in ribosome biogenesis and RNA processing. Br J Haematol. 2009;145:806–15.
16. Valli R, De Paoli E, Nacci L, et al. Novel recurrent chromosome anomalies in Shwachman-diamond syndrome. Pediatr Blood Cancer. 2017;64:e26454.
17. Valli R, Maserati E, Marletta C, et al. Evaluating chromosomal mosaicism by array comparative genomic hybridization in haematological malignancies: the proposal of a formula. Cancer Gene Ther. 2011;204:216–8.
18. Kyoto Encyclopedia of Genes and Genomes (KEGG): map 04640 Hematopoietic Cell lineage http://software.broadinstitute.org/gsea/msigdb/gene_families.jsp?geneSetName=KEGG_HEMATOPOIETIC_CELL_LINEAGE Accessed on 16 July 2019.
19. Kyoto Encyclopedia of Genes and Genomes (KEGG): map 05221 Acute Myeloid Leukemia http://software.broadinstitute.org/gsea/msigdb/cards/KEGG_ACUTE_MYELOID_LEUKEMIA.html Accessed on 16 July 2019.
20. The Gene Ontology Resource Gene set 3: M10998 - GO Myeloid Leukocyte Differentiation http://software.broadinstitute.org/gsea/msigdb/cards/GO_MYELOID_LEUKOCYTE_DIFFERENTIATION.htm Accessed on 16 July 2019.
21. Zhu W, Li GX, Chen HL, et al. The role of eukaryotic translation initiation factor 6 in tumors (review). Oncol Lett. 2017;14:3–9.
22. Pressato B, Valli R, Marletta C, et al. Cytogenetic monitoring in Shwachman-diamond syndrome: a note on clonal progression and a practical warning. J Pediatr Hematol Oncol. 2015;37:307–10.
23. Valli R, Frattini A, Minelli A. Shwachman-diamond syndrome: diagnosis, pathogenesis and prognosis. Expert Opin Orphan Drugs. 2017;5:753–67.
24. Noris P, Valli R, Pecci A, et al. Clonal chromosome anomalies affecting FLI1 mimic inherited thrombocytopenia of the Paris-trousseau type. Eur J Haematol. 2012;89:345–9.
25. Wang CY, Lin CF. Annexin A2: its molecular regulation and cellular expression in cancer development. Dis Markers. 2014:308976, e-pub ahead of print 23 January 2014. https://doi.org/10.1155/2014/308976.
26. Maserati E, Minelli A, Pressato B, et al. Shwachman syndrome as mutator phenotype responsible for myeloid dysplasia/neoplasia through karyotype instability and chromosome 7 and 20 anomalies. Genes Chromosom Cancer. 2006;45:375–82.
27. Maserati E, Pressato B, Valli R, et al. The route to development of myelodysplastic sindrome/acute myeloid leukaemia in Shwachman-diamond syndrome: the role of ageing, karyotype instability, and acquired chromosome anomalies. Br J Haematol. 2009;145:190–7.
28. Valli R, Pressato B, Marletta C, et al. Different loss of material in recurrent chromosome 20 interstitial deletions in Shwachman-diamond syndrome and in myeloid neoplasms. Mol Cytogenet. 2013;6:56.
29. Valli R, De Bernardi F, Frattini A, et al. Comparative genomic hybridization on microarray (a-CGH) in olfactory neuroblastoma: analysis of ten cases and review of the literature. Genes Chromosom Cancer. 2015;54:771–5.
30. Nacheva E, Mokretar K, Soenmez A, et al. DNA isolation protocol effects on nuclear DNA analysis by microarrays, droplet digital PCR, and whole genome sequencing, and on mitochondrial DNA copy number estimation. PLoS One. 2017;12:e0180467.
31. Schroeder A, Mueller O, Stocker S, et al. The RIN: an RNA integrity number for assigning integrity values to RNA measurements. BMC Mol Biol. 2006;7:3.

Publisher's Note

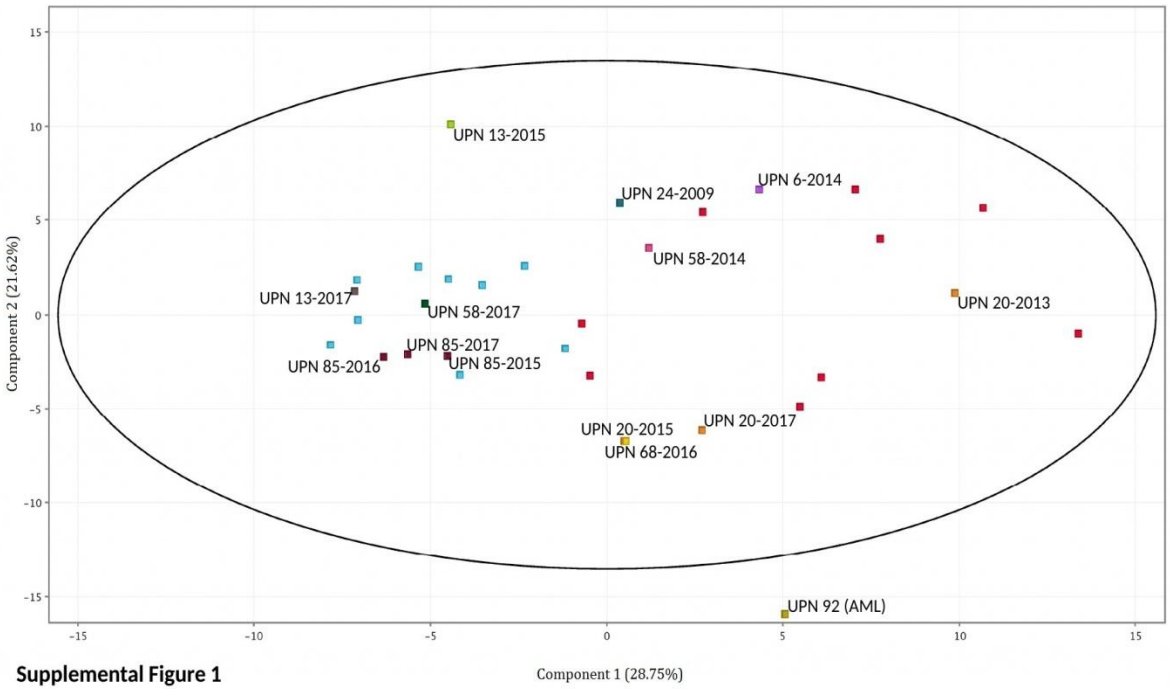

Supplemental Figure 1

Supplemental Fig. 1 Principal Component Analysis (PCA) plot for the Gene set 1 (KEGG Hematopoietic cell lineage). Healthy controls, SDS-NK patients, and patients with chromosome anomalies are identified as in Fig. 2 and in the text. Component 1 and 2 are indicated in the plot. The 95% confidence interval is shown by a black ellipse.

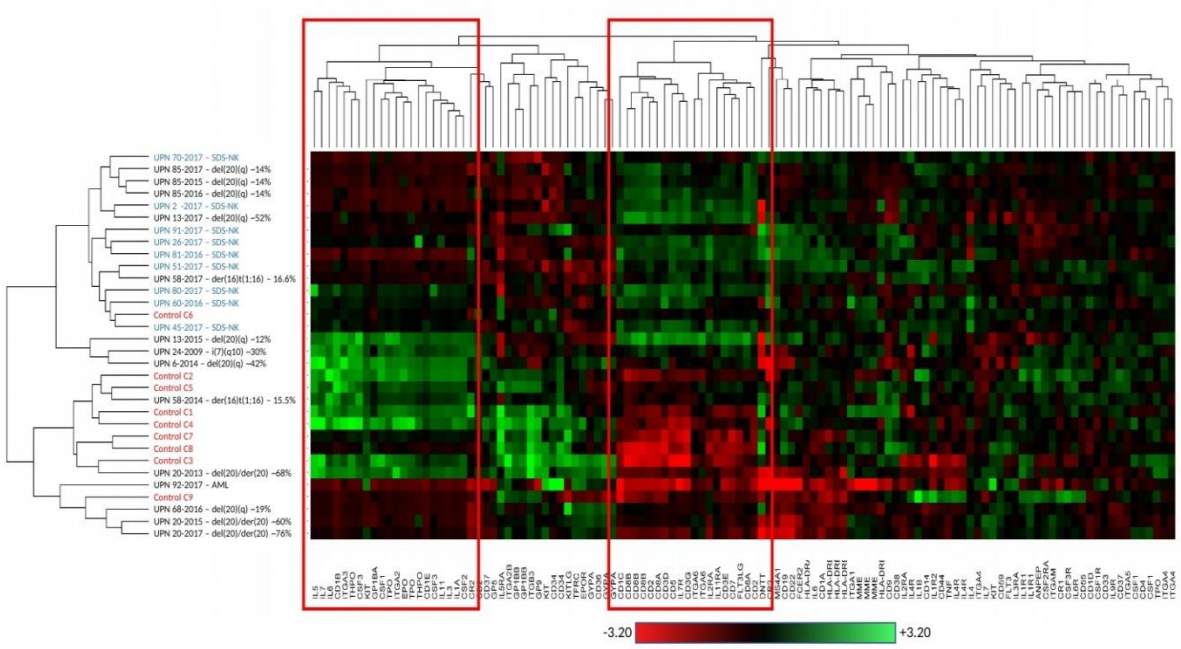

Supplemental Figure 2: KEGG Hematopoietic Cell Lineage

Supplemental Fig. 2 Heatmap and dendrogram of cluster analysis on both the axes for the Gene set 1 (KEGG Hematopoietic Cell Lineage). Healthy controls, SDS-NK and patients with chromosome anomalies are indicated near the dendrogram lines, with evidence of the sample (year), and the karyotype, as in Fig. 3 in the text. Two red boxes put in evidence genes with relevant differences of expression, related to the subgroups of controls and SDS-NK. Gene names and $\log_2$ color bar are under the heatmap.

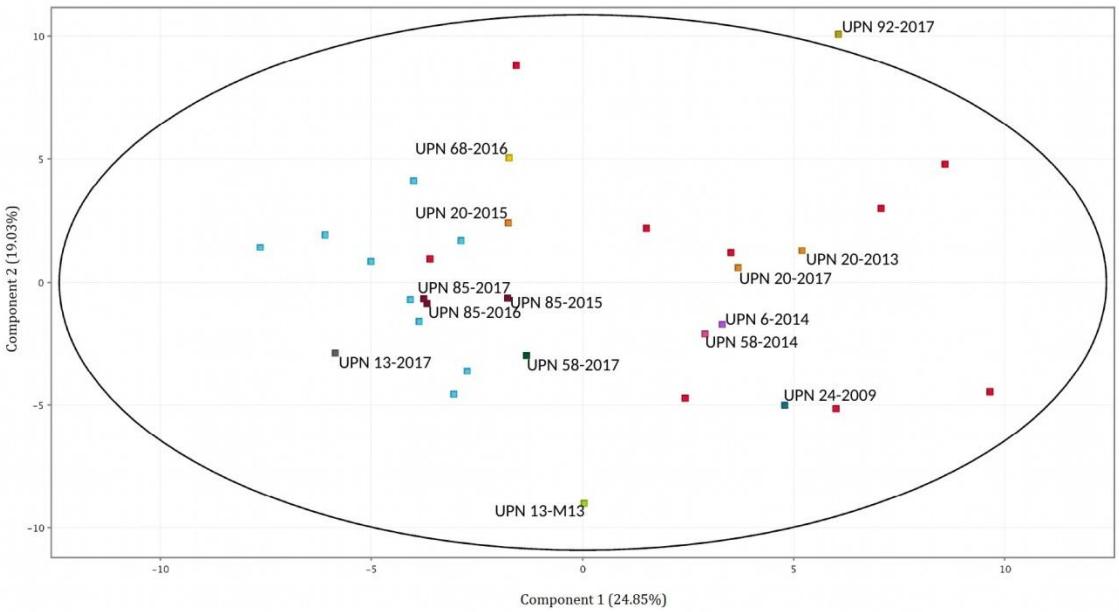

Supplemental Figure 3: KEGG Acute Myeloid Leukemia

Supplemental Fig. 3 Principal Component Analysis (PCA) plot for the Gene set 2 (KEGG Acute myeloid leukaemia). Healthy controls, SDS-NK patients, and patients with chromosome anomalies are identified as in Fig. 2 and in the text. Component 1 and 2 are indicated in the plot. The 95% confidence interval is shown by a black ellipse.

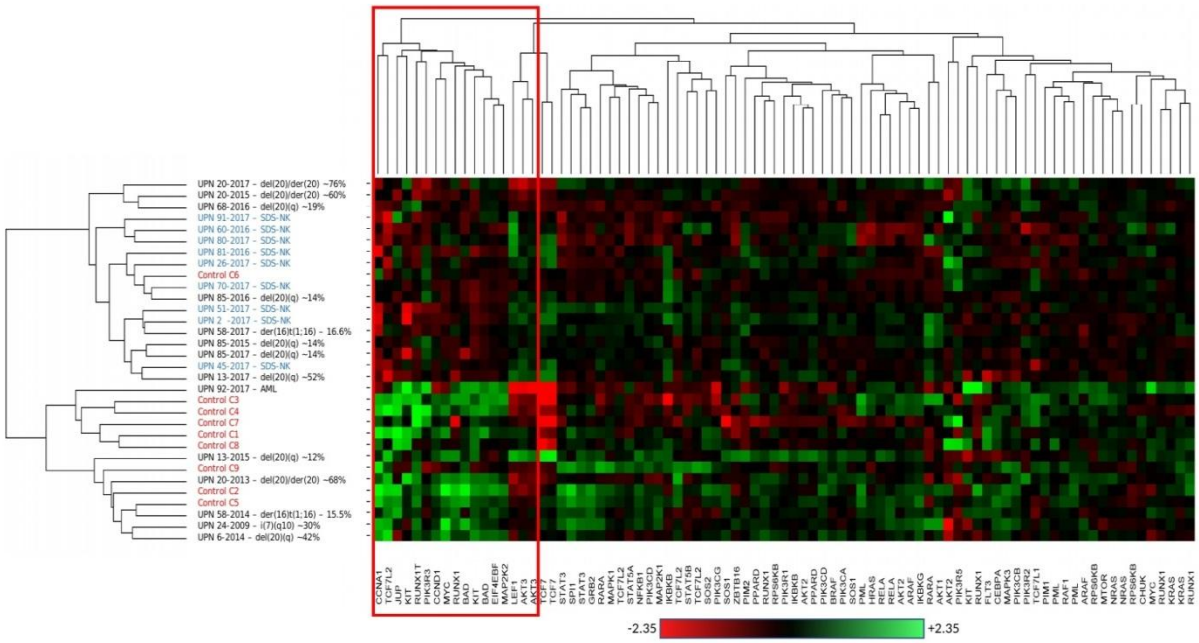

Supplemental Figure 4: KEGG Acute Myeloid Leukemia

Supplemental Fig. 4 Heatmap and dendrogram of cluster analysis on both the axes for the Gene set 2 (KEGG Acute myeloid leukaemia). Healthy controls, SDS-NK and patients with chromosome anomalies are indicated near the dendrogram lines, with evidence of the sample (year), and the karyotype, as in Fig. 3 in the text. A red box put in evidence genes particularly up/down-regulated, with difference in the groups of controls and SDS-NK. Gene names and $\log_2$ color bar are under the heatmap.

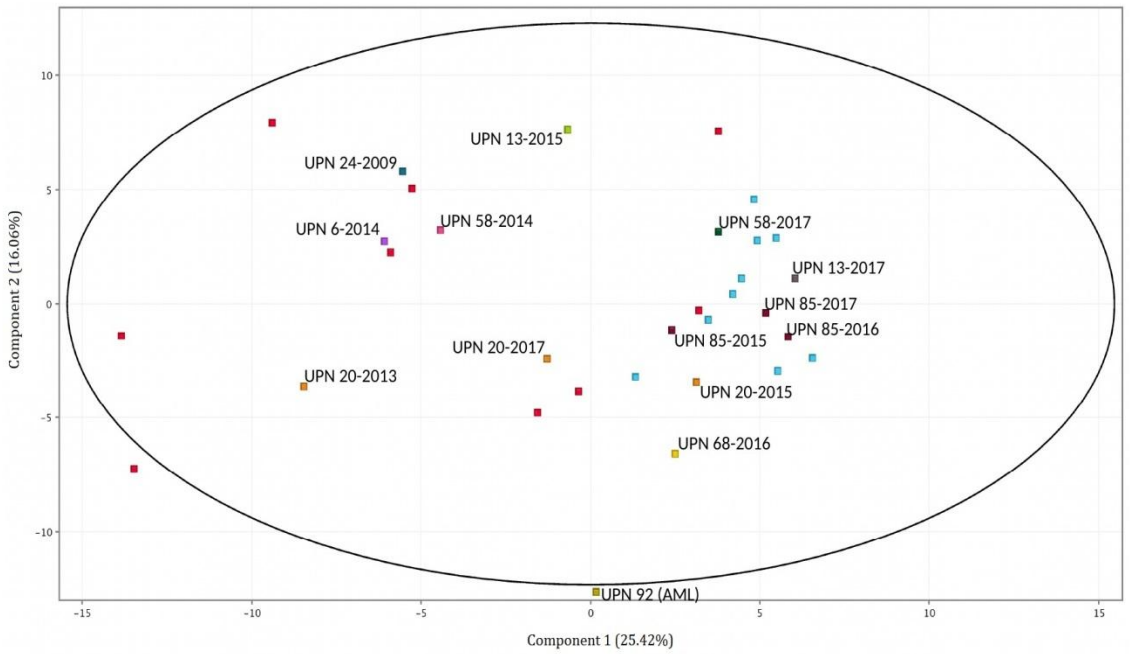

Supplemental Figure 5: Gene Onthology Myeloid Leukocyte Differentiation

Supplemental Fig. 5 Principal Component Analysis (PCA) plot for the Gene set 3 (Gene Ontology Myeloid Leukocyte Differentiation). Healthy controls, SDS-NK patients, and patients with chromosome anomalies are identified as in Fig. 2 and in the text. Component 1 and 2 are indicated in the plot. The 95% confidence interval is shown by a black ellipse.

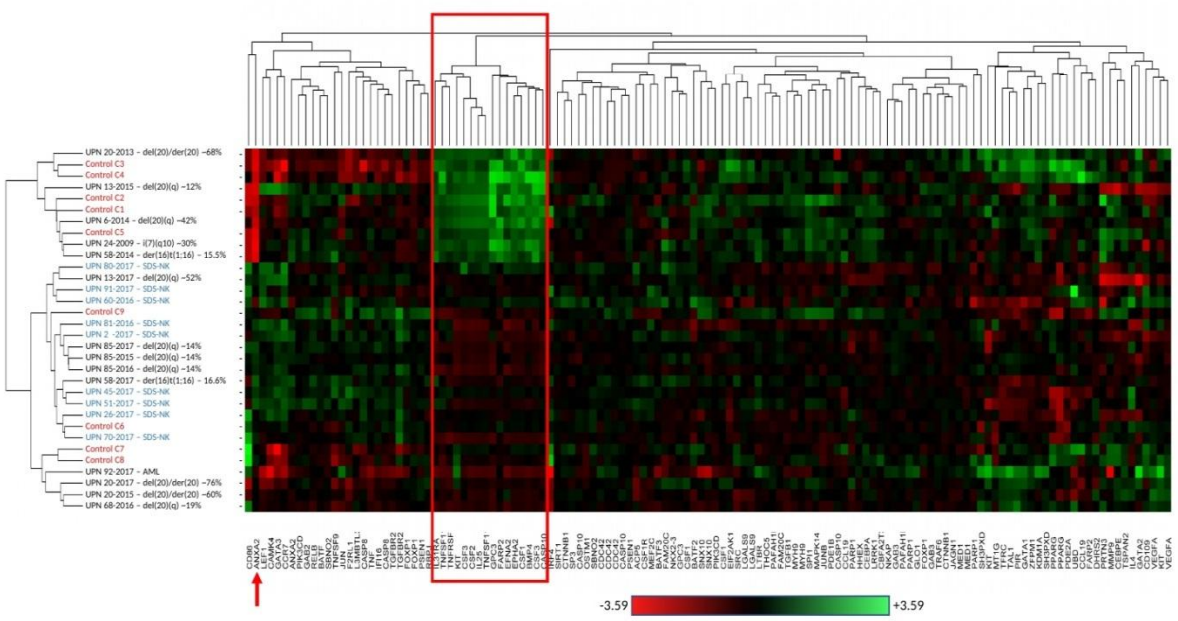

Supplemental Figure 6: Gene Onthology Myeloid Leukocyte Differentiation

Supplemental Fig. 6 Heatmap and dendrogram of cluster analysis on both the axes for the Gene set 3 (Gene Ontology Myeloid Leukocyte Differentiation). Healthy controls, SDS-NK and patients with chromosome anomalies are indicated near the dendrogram lines, with evidence of the sample (year), and the karyotype, as in Fig. 3 in the text. A red arrow and a red box put in evidence genes particularly up/down-regulated, with difference in the groups of controls and SDS-NK. Gene names and $\log_2$ color bar are under the heatmap.

Table S1: Neutrophil count (x10^3/µl), haemoglobin (Hb) concentration (g/100 ml) and platelet count (x10^3/µl) for the SDS patients here reported. Chromosome clonal anomaly and percentage of abnormal cells are recalled. BM cellularity evaluation is also indicated.

UPN	Sample	Cytogenetics	Neutrophils	Hb	Platelet	BM cellularity
UPN6	2014	del(20)(q11.21q13.13) ~44%	2,39	13,7	57	almost normal
UPN13	2015	del(20)(q11.21q13.32) ~12%	0,63	11	65	mild hypoplasia
UPN13	2017	del(20)(q11.21q13.13) ~52%	1,13	12,5	80	mild hypoplasia
UPN20	2013	del(20)(q11.21q13.32) ~68%	0,5	14,8	91	almost normal
UPN20	2015	del(20)(q11.21q13.32) ~60%	0,3	14,7	73	mild hypoplasia
UPN20	2017	del(20)(q11.21q13.32) ~76%	0,5	14,6	81	mild hypoplasia
UPN58	2014	der(16)t(1;16)(q21;q23) ~17%	0,33	11	134	mild hypoplasia
UPN58	2017	der(16)t(1;16)(q21;q23) ~15%	0,76	10,1	197	mild hypoplasia
UPN68	2016	del(20)(q11.21q13.12) del(20)(q13.12q13.13) ~19%	2,31	17,4	130	mild hypoplasia
UPN85	2015	del(20)(q11.21q11.23) ~14%	0,9	16,5	104	normal
UPN85	2016	del(20)(q11.21q11.23)	0,9	15,9	107	almost normal
UPN85	2017	del(20)(q11.21q11.23) ~11%	2	15,1	96	almost normal
UPN24	2009	i(7)(q10) ~30%	1,9	11,4	108	almost normal
UPN92	2017	complex karyotype[a]	0,54	10,8	12	almost normal[a]
UPN2	2017	normal karyotype	0,7	14,2	113	severe hypoplasia
UPN26	2017	normal karyotype	0,5	13	97	mild hypoplasia
UPN45	2017	normal karyotype	1,08	12	215	severe hypoplasia
PN51	2017	normal karyotype	3,24	12,8	195	almost normal
UPN60	2016	normal karyotype	1,45	11,8	101	normal
UPN70	2017	normal karyotype	1,59	15,4	111	severe hypoplasia
UPN80	2017	normal karyotype	0,32	10,8	174	mild hypoplasia
UPN81	2016	normal karyotype	0,4	11,9	189	not available
UPN91	2017	normal karyotype	1,09	13	193	normal

[a] Patient with Acute Myeloid Leukaemia (AML): data after chemotherapy.

RESULTS (SECTION 4)

Specific contribution

"*Abdul Waheed Khan contributed in experimental work such as expression arrays and immunofluorescence experiments, data analysis and manuscript proofreading"*

- Manuscript Draft -

Functional impairment of osteoblasts derived from patients affected by Shwachman-Diamond Syndrome: a novel role of SBDS

Isabella Villa[1], Simona Bolamperti[1], Roberto Valli[2], Marco Cipolli[3], Rita Maria Pinto[4], Elena Bergami[5], Maria Rita Frau[6], Simone Cesaro[7], Michela Signo[1], Valentino Bezzerri[8], Giovanni Porta[2], Abdul Waheed Khan[2§], Alessandro Rubinacci[1], Annalisa Frattini[2,9]

[1] Bone Metabolism Unit, IRCCS Ospedale San Raffaele, Via Olgettina, 60, 20132 Milano, Italy.
[2] Department of Medicine and Surgery (DMC), Universita' degli Studi dell'Insubria, Via J.H. Dunant, 5, 21100 Varese, Italy.
[3] Cystic Fibrosis Center, Azienda Ospedaliera Universitaria Integrata di Verona, Piazzale Aristide Stefani, 1, 37126 Verona, Italy.
[4] Department of Onco-Hematology, Ospedale Bambino Gesù IRCCS, Piazza S.Onofrio, 4, 00165 Roma, Italy.
[5] Pediatric Onco-Hematology, IRCCS Policlinico San Matteo, Viale Camillo Golgi, 19, 27100 Pavia, Italy.
[6] Pediatrics and Intensive Neonatal Therapy, Ospedale San Francesco, Via Salvatore Mannironi, 08100 Nuoro, Italy.
[7] Pediatric Hematology Oncology, Ospedale Donna Bambino, Azienda Ospedaliera Universitaria Integrata, Piazzale Aristide Stefani, 1, 37126 Verona, Italy.
8 Cystic Fibrosis Center, Azienda Ospedaliero Universitaria Ospedali Riuniti di Ancona, Via Conca, 71, 60126 Ancona, Italy.
[9] Institute for Genetic and Biomedical Research (IRGB), UOS Milano CNR, Via Fantoli, 15/16, 20138 Milano, Italy.
[§] PhD student enrolled in the Life Sciences and Biotechnology program of the XXXIII cycle

Corresponding author: Annalisa Frattini, Institute for Genetic and Biomedical Research (IRGB), UOS Milano CNR, Via Fantoli 15/16, 20090 Milano, Italy. tel: +39 0332 217113 e mail: annalisa.frattini@irgb.cnr.it

ABSTRACT

Shwachman-Diamond syndrome (SDS) is a rare autosomal recessive multi-system disorder characterized by bone marrow failure, exocrine pancreatic insufficiency and skeletal abnormalities, principally caused by loss-of-function mutations in the SBDS gene, a factor mainly involved in ribosome biogenesis. By analyzing osteoblasts derived from SDS patients (SDS-OBs), we showed that SDS-OBs displayed reduced SBDS gene and undetectable SBDS protein expression compared to osteoblasts from healthy subjects (H-OBs). Whole transcriptome analysis showed significant differences in the gene expression of SDS-OBs versus H-OB. In SDS-OBs the expression of the main genes responsible of osteoblastogenesis were lower except for OSX. Western blot showed a similar trend of the relevant proteins. In addition, SDS-OBs showed higher protein levels of p53, an inhibitor of collagen production and, when cultured in osteogenic medium, displayed lower mineralization capacity compared to H-OBs. In conclusion, this study demonstrates that SBDS play an important role in osteoblast function.

1. INTRODUCTION

Shwachman-Diamond syndrome (SDS1, OMIM #260400) is a rare autosomal recessive monogenic inherited multisystemic disorder mainly characterized by exocrine pancreatic dysfunction, bone marrow failure, and predisposition toward myelodysplasia syndrome (MDS) or acute myeloid leukemia (AML) (Shwachman et al, 1964, Bodian et al., 1964). The estimated incidence of SDS is 1/75,000. However, it is difficult to determine the real frequency of SDS in the general population due to its high phenotypic variability (Lindsley et al., 2017). Approximately 90% of patients affected by SDS carry biallelic mutations in the Shwachman-Bodian-Diamond Syndrome (*SBDS*) gene, which is located on chromosome 7q11.21 (Liu et al., 2018). The most frequent biallelic inactivating mutations in the *SBDS* gene are the 183-184TA>CT that introduces a premature in frame termination codon, resulting in the amino-acid change K62X, and the 258+2T→C that affects the donor splice site of intron 2. The latter mutation promotes the use of an upstream cryptic donor splice site at position 251_252, that generates a transcript with an 8 bp deletion resulting in a frameshift and in a premature termination codon (C84fsX3) (Boocock et al., 2003; Austin et al., 2005). No homozygotes for the null allele [i.e. c.183_184TA>CT] were reported in humans, suggesting that the complete loss of functional SBDS protein is incompatible with life. This finding is in agreement with other evidence obtained in Dictyostelium discoideum (Wong et al., 2011), in zebrafish (Provost et al., 2012) and in mice, in which the complete loss of *Sbds* results in early embryonic lethality (Zhang et al., 2006). Therefore, this implies that SDS patients should express at least one hypomorphic *SBDS* allele, as shown by the detection, although at very low level, of full-length SBDS protein in their cells (Austin at al., 2005; Wong et al., 2011).
In addition to the reported role of the SBDS protein in the spindle apparatus stability and chromosome segregation (Austin et al. 2008; Orelio et al., 2009), in DNA replication and repair (Morini et al., 2015), telomere protection (Liu et al., 2018) and in endoplasmic reticulum stress, SBDS plays an essential role in the final step of ribosomal maturation (Burwick et al, 2012). SBDS protein through the coupling with EFL1 (GTPase Elongation Factor-like 1), promotes the release of eIF6 (Eucaryotic Initiation Factor 6) from the pre-60S ribosomal subunit to generate the mature 80S functional ribosome (Finch et al., 2011; Weis et al., 2015). Association of the large 60S ribosomal subunit to the small 40S subunit is sterically blocked by eIF6. The release of eIF6 allows the joining of the 60S and 40S subunits and the formation of the

translationally active 80S ribosome (Warren, 2018; Luviano et al., 2019). In addition, SBDS plays a role in the conformational maturation of the ribosomal P-site (Weis et al., 2015).
A variety of skeletal abnormalities, evolving over time, are commonly reported in patients with SDS and are related to abnormal development of the growth plates, delay of secondary ossification centers resulting in metaphyseal dysostosis, in particular at femoral head, shortened ribs with flared anterior ends, and costochondral thickening (Mäkitie et al., 2004; Burroughs er al., 2009). The skeletal dysplasia is highly variable, even in patients with identical genotypes, and its severity and location vary with age (Toiviainen-Salo et al., 2007). Remarkably, the bone of the majority of the SDS affected individuals, beside its dysplastic morphology, shows the features of a low turnover osteoporosis with increased risk of fragility fracture: a tragic outcome in individuals already affected by a severe deterioration in the quality of life. The reduction in bone mass is present at different skeletal sites including ribs, femurs, knees, heads of humerus, wrists, ankles, and vertebrae (Mäkitie et al., 2004; Aggett et al., 1980; Ginzberg et al., 1999). Reduced trabecular bone volume (BV/TV), low numbers of osteoblasts (OB.S/BSs) and osteoclasts (OCs/BS), and reduced amount of osteoid (OS/BS) are also reported in the histomorphometric analysis of the few bone biopsies obtained (Toiviainen-Salo et al., 2007). In particular, the observed low values of BV/TV, OB.S/BSs, OS/BS, and OCs/BS consistently indicated a focal bone remodeling unbalance, primarily related to the inefficiency of the bone formation phase. Osteoblasts are characterized by high protein secretion, particularly structural proteins, such as collagen, that are critical for bone mechanical competence (Zimmermann et al., 2019). It is therefore likely, that the altered SBDS protein levels, which affects global protein translation, might induce defective translation of critical proteins in osteoblasts that are involved in acquisition and maintenance of bone mass and quality during skeletal development (Trainor & Merrill, 2014). Considering the bone feature defects observed in SDS, we designed the present study to characterize the role of *SBDS* in osteoblasts functionality. For this purpose, we cultured osteoblasts derived from bone of SDS patients (SDS-OBS) and examined their gene expression profile and their ability to mineralize compared to osteoblast from healthy (H-OBs) age- and sex-matched subjects. The availability of osteoblasts from a monogenic disorder offers the unique opportunity to assess the effects of a single gene mutation on the physiology of bone metabolism, and enables the identification of novel molecular mechanisms, as it occurred for other monogenic disorders (Mäkitie et al., 2019). At present, this is the first study to evaluate the functions of osteoblasts derived from SDS patients.

2 | MATERIALS AND METHODS

2.1 | Cell culture: Human samples were obtained and analyzed in accordance with the declaration of Helsinki, after written consent. All protocols were approved by the Azienda Ospedaliera Universitaria Integrata (Verona, Italy), approval No. 658 CESC, and Azienda Ospedaliero Universitaria Ospedali Riuniti (Ancona, Italy), approval No. CERM 2018-82.
Primary human osteoblast cultures were established by means of a modified version of the Gehron-Robey and Termine (1985) procedure from remnants of bone marrow biopsies for SDS patients or from waste material during orthopedic surgery or bone marrow biopsies for healthy controls. The trabecular bone was cut into small pieces and incubated with rotation at 37 C for 30min with Joklik's modified MEM (Sigma-Aldrch, M0518) serum-free medium containing 0.5mg/ml type IV collagenase (Sigma-Aldrich, C1889). The pieces from each sample were then placed in 25cm2 flasks and cultured in Iscove's modified medium (Sigma-Aldrich, I3390) containing 10% FBS (Euroclone, ECS0180L), penicillin, streptomycin, amphotericin B (Sigma-Aldrich, A5955, 1:100) until confluence; the culture medium was changed every 2–3days. Cells were used at the second passage to reduce the possibility of phenotype changes. To induce mineralization, confluent osteoblasts were cultured for 28 days in osteogenic medium containing 10-7M dexamethasone (Sigma-Aldrich, D8893), 50ng/ml ascorbic acid (Sigma-Aldrich, A8960) and 5mM β-glicerophosphate (Sigma-Aldrich, G9422). Osteogenic medium was changed three times/week.
Lymphoblastoid cell lines (LCLs) were obtained by infecting peripheral blood lymphocytes (PBL) with Epstein Barr Virus (EBV).

2.2 | Alizarin Red staining: Osteoblasts fixed in ethanol 75% were stained for 10 minutes with Alizarin Red solution and then thoroughly washed with deionized water. The staining was quantified by measuring the absorbance with the plate reader Infinite 200 (Tecan Group Ltd., Männedorf, CH).

2.3 | Immunofluorescence staining: Cells were fixed in 1% formaldehyde in PBS and immunostained with a rabbit anti-SBDS antibody (1:50, Abcam plc, Cambridge, UK, Cat# ab128946, RRID:AB_11001034) for 3h, followed by an incubation with a 488-Alexa Fluor conjugated anti rabbit secondary antibody (1:500, Thermo Fisher Scientific Inc., Waltham, MA USA, Cat# A-11034, RRID:AB_2576217). DAPI (1μg/ml, Thermo Fisher Scientific Inc., Waltham, MA USA, Cat# D1306, RRID:AB_2629482, 1μg/ml) was used for nuclear labeling. 555-Alexa Fluor conjugated phalloidin (1:40, Thermo Fisher Scientific Inc., Waltham, MA USA, Cat#A34055,) was used for actin labeling. Cover slips were mounted with FluoromountG (Southern Biotech, Birmingham, AL, USA, Cat#0100-01). Images were acquired using the Leica DM5000B, 100X objective.

2.4 | Reverse transcription, RT-qPCR: RNA was extracted from second passage confluent osteoblast culture using RNeasy Plus kit (Qiagen Germantown, MD, USA, Cat#74134). RNA was quantified using ND-1000 UV-Vis spectrophotometer (Thermo Scientific, Wilmington, DE, USA), and the integrity of the RNA was assessed with Agilent 2100 Bioanalyzer (Agilent Technologies Inc., Lexington, MA, USA) according to

the manufacturer's instructions. All the RNA samples used in this study exhibited a 260/280 ratio above 1.9 and an RNA Integrity Number (RIN) above 9.0. Five hundred ng of total RNA were reverse transcribed to cDNA using oligo(dT) and random primers and RNase H+ and MMLV reverse transcriptase (Bio-Rad, Hercules, CA, USA iScript Reverse Transcription kit, Cat#1708890). The relative expression of ribosomes biogenesis related genes (*SBDS*, *ELF1*, *eIF6*), of osteogenesis related genes (*RUNX2*), osterix (*OSX*), osteopontin (*OPN*), bone-sialo protein (*BSP*), osteocalcin (*BGP*), alkaline phosphatase (*ALP*) collagen type I (*COL1A*), and of tumor protein p53 (*TP53*) mRNA was evaluated.

cDNAs were subjected to RT-qPCR reactions using the following specific primer:

*SBDS*_FW: AGATAGAACGTGCTCACATGAGGC
*SBDS*_REV: GGTGTCATTCAAATTTCTCATGTC
*EFL1*_FW: CCGCTGTTCGCATTTGTGATG
*EFL1*_REV: AAACCGGACGGATGTTTTCAA
*eIF6*_FW: CCGACCAGGTGCTAGTAGGAA
e*EIF6*_REV: CAGAAGGCACACCAGTCATTC
β-*ACT*_FW: CATGTACGTTGCTATCCAGGC
β-*ACT*_REV: CTCCTTAATGTCACGCACGAT.

or primer-probe sets validated and purchased as "Assay-on-Demand" (Thermo Fisher Scientific Inc., Waltham, MA USA) in singleplex PCR mix. RT-qPCR reaction was performed in an ABI PRISM® 7900 Sequence Detection System (Thermo Fisher Scientific Inc., Waltham, MA, USA). Each gene expression was first normalized with *β-actin* content and the relative quantification was calculated with the $2^{-\Delta Ct}$ method. Three replicates were performed for each experimental point and experiments were repeated with cells obtained from different donors.

To analyze the alternative *SBDS* transcript, RNA was extracted, from lymphoblastoid cell lines and osteoblasts cell lines of a healthy control, of a SDS patient (UPN24) carrying the mutation 258+2T>C in heterozygous state and of a SDS patient (UPN51, homozygous for the mutation 258+2T>C). PCR reactions was performed using the specific primer: *SBDS*_FW GGAACAGATGACCAAACTGAAATC; *SBDS*_REV TCAATAAGGATCACGGTGTATGG at the following condition: 94°C for 30sec, 94°C for 10 sec, 62°C for 15 sec, 72°C for 20sec for 35 cycles and a final step of 72°C for 7min 30sec. For the PCR reaction 25ng of WT LCLs and hOBs cDNA, 50ng of UPN24 LCLs and hOBs cDNA and 250ng of UPN51 LCLs and hOBs cDNA were used. The RT-PCR products were run on agarose gel at 5% using the *GellyPhor* ULTRA agarose (Euroclone, Milano, Italy, Cat#EMR915100,)

2.5 | One-Color Expression Arrays: We performed microarray expression profiling according to Agilent's One-Color Microarray-Based Gene Expression Analysis Low Input Quick Amp Labeling Protocol (Version 6.9.1) using Low Input Quick Amp Labeling Kit, One-ColorAgilent (Cat#5190-230) and Agilent Whole Transcriptome (WT) Oligo Human Microarray slides 8 x 60K format (G4851A, AMADID #028004, Agilent Technologies, Santa Clara, USA). Data analysis was performed using Agilent GeneSpring 14.9.1 software. Data from each sample was imported into the software with the following parameters: Threshold: 1, Logbase: 2, Normalization: Shift to 75.0 percentile, Baseline Transformation: median of all samples. Clustering analysis was performed by hierarchical analysis on normalized intensity values with Euclidean Distance Metrics and Ward's linkage rules both on all genes as well as on selected gene sets. Principal Component Analysis (PCA) was performed by the internal software plugin both with all genes as well as on selected gene sets.

2.6 | Western Blot analysis: After removing the medium, adherent cells were gently scraped in 75µl modified RIPA buffer (EDTA 10mM) with protease and phosphatase-inhibitor cocktail (1:50 Sigma-Aldrich, P8340 and 1:100 Sigma-Aldrich, P5726). The lysates were centrifuged at 12,000 rpm for 10 min at 4°C, supernatants were collected, and the total protein concentration was determined by BCA assay (Pierce, Rockford, IL, USA). Thirty µg of total protein extract were mixed with the appropriate volume of denaturating Laemmli's sample loading buffer, heated at 100°C for 5 min, and loaded onto 4-15% Tris-Gly precast polyacrylamide gels (Bio-Rad, Hercules, CA, USA). Western blots were performed using specific antibodies against human SBDS (1:300, Santa Cruz Biotechnology Inc., Heidelberg, Germany, Cat# sc-271350, RRID:AB_10611192), p53 (1:300, Santa Cruz Biotechnology Inc., Heidelberg, Germany, Cat# sc-126, RRID:AB_628082,), β-actin (1:2000, Santa Cruz Biotechnology Inc., Heidelberg, Germany, Cat#sc-1616), ALP (1:500, Santa Cruz Biotechnology Inc., Heidelberg, Germany, Cat# sc-166261), BSP (1:1000, Immunological Sciences, Rome, Italy, Cat# AB-81521) and OSX (1:1000, Immunological Sciences, Rome, Italy, Cat# AB-J2773). Antibodies were diluted in 5% milk or BSA Tris buffered saline with 0.1% Tween20 (Sigma-Aldrich, P9416). After washing, membranes were treated with specific horseradish peroxidase-conjugated secondary antibodies (1:2000; Rockland Immunochemicals Inc., Limerick, PA, USA, anti-mouse Cat# 610-4320, anti-goat Cat# 805-7302; Jackson ImmunoResearch Laboratories, Baltimore, USA, anti-rabbit Cat# 111-035-003). Bound peroxidase activity was revealed using the enhanced chemiluminescence substrate (Pierce, Rockford, IL, USA). The signal was acquired with the UVITEC MiniHD9 (Cambridge, UK) and quantified by means of the manufacturer's Nine Alliance software vs. 17.01. β-actin was used as loading controls.

2.7 | Statistical Analysis: Statistical analysis was performed with Prism vs 5.04, (GraphPad Software, San Diego, CA, USA). Statistically significant differences were determined using the nonparametric ANOVA test (Kruskal-Wallis test) followed by multiple-comparison test (Dunn's post test) or by the Mann-Whitney test. Up and down regulated genes in the array results have been extrapolated by applying moderated t-test followed by Benjamini-Hochberg p-value correction with a threshold of p=0.05 and fold change cut-off > 2.0 to the SDS patients-derived osteoblasts vs healthy subjects derived osteoblasts.

3| RESULTS

In Table 1 are indicated the clinical features and the genetic characteristics of the SDS patients from whom we established the primary osteoblast culture (SDS-OBs).

3.1 | Amount and cellular localization of SBDS in osteoblasts derived from SDS patients

First, we evaluated SBDS protein amount in osteoblasts derived from these patients (SDS-OBs) compared to osteoblasts from healthy subjects (H-OBs). SBDS protein analyzed by western blot was almost undetectable in SDS-OBs (Figure 1a).
Immunofluorescent staining for SBDS with an antibody specific for the C-terminus of the protein, which is deleted in the protein derived from the mutated *SBDS* gene, revealed the presence of some residual full length SBDS and a different distribution of the protein in SDS -OBs compared to H-OBs (Figure 1b). In SDS-OBs the staining was confined to the nucleus whereas in H-OBs, SBDS fluorescence was detected mainly in the cytoplasm (Figure 1b).
The identification of residual full length SBDS protein led us to investigate the presence of residual *SBDS* wild type transcript. Total RNA was extracted from lymphoblastoid cell lines and osteoblast cultures of a healthy control (H), of UPN24, who carries the mutation c.258+2T>C in heterozygous state, and of UPN51 who carries the mutation in homozygous state (Table 1). As expected, in healthy control PCR analysis showed a single band of 176 base pairs, which corresponds to the full length *SBDS* transcript. UPN24 (het) displayed the band of 176 base pairs and a second band of 168 base pairs which corresponds to the truncated transcript of *SBDS*. UPN51 (homo) had the same bands as UPN24, with the full transcript band being less intense than the truncated (Figure 2a). Noteworthy to detect any visible band in the patients derived cells it was necessary an amount of cDNAs 2 times higher for patient UPN24, and 10 times higher for patient UPN 51, than control. The presence of low levels of normal *SBDS* transcript (verified by sequencing) suggests that the mutation 258+2T>C causes the conversion of the nucleotide T>C, creating a new non canonical GC 5' splice site that allows the transcription of the correct form of *SBDS* mRNA (Figure S1) (Abramowicz & Gos , 2018).
We then evaluated total *SBDS* transcript and found that was significantly ($P<0.001$) lower in SDS-OBs compared to H-OBs. *ELF1* and *eIF6* were not significantly modified (Figure 2b).

3.2 | Osteogenesis-related gene and protein expression are reduced in SDS-OBs

Microarray analysis showed significant differences in the whole transcriptome between SDS-OBs and H-OBs (Figure 3a). By applying a suitable statistical test (see methods section), 2373 regulated genes with a fold change >2 was evidenced. In particular, 2330 genes resulted down-regulated in SDS-OB only 43 resulted up -regulated. (Figure 3b). Genes involved in the ossification process (GO:0001503) reported remarkable changes in expression, with 80 down-regulated genes and 49 up-regulated genes (Table S1).
Quantitative PCR (RT-qPCR) of the main osteogenesis -related genes showed in SDS-OBs a lower expression of Runt-Related Transcription Factor 2 (*Runx2*; $P<0.05$), osteopontin (*OPN*; $P<0.01$), bone sialo-protein (*BSP;* $P<0.05$), osteocalcin (*BGP*; $P<0.05$) alkaline phosphatase (*ALP;* $P<0.05$)and collagen type I (*COL1A*; $P<0.05$) compared to H-OBs. Osterix (*OSX*) levels were unchanged (Figure 3c).
Protein levels of OSX, BSP, ALP and collagen type I were analyzed by Western blot (Figure 4a). ALP, BSP and collagen type I protein levels were significantly ($P<0.05$) lower in SDS-OBs respect to H-OBs. OSX protein levels showed no difference between the two groups (Figure 4b).

3.3 | p53 protein expression is higher in SDS-OBs

Since previous studies have shown that bone marrow from SDS patients express higher levels of p53 than healthy subjects (Elghetany & Alter, 2002) and that p53 exerts an inhibitory action on osteogenesis (Wang et al., 2006), we evaluated p53 protein amount in SDS-OBs by Western blot (Figure 5a). Our results showed that p53 content in SDS-OBs was significantly higher ($P<0.05$) compared to H-OBs (Figure 5b).

3.4 | Mineralization in SDS-OBs is impaired

On the basis of the data showing a reduced gene and protein expression of factors related to osteoblast activity, we evaluated the capacity of SDS-OBs to mineralize when grown in an osteogenic medium (OMEM). Alizarin red staining performed after 28 days of culture in OMEM showed a reduced mineralization capacity of SDS-OBs compared to H-OBs and the difference was statistically significant ($P<0.05$; Figure 6a,b).

4 | DISCUSSION

The present study showed that low levels of SBDS protein compromise the physiological transcription of osteogenesis-related genes in osteoblasts and negatively affects osteoblast mineralization capacity in SDS patients, thus supporting the hypothesis that low SBDS level affects the osteogenic process, likely contributing to the altered bone phenotypic traits of SDS.
Besides low amount of SBDS protein, SDS-OBs displayed a lower level of *SBDS* mRNA, compared to H-OBs, but unaltered gene expression of *ELF1* and *eIF6*, the other components of ribosomes assembly. The reduced levels of *SBDS* mRNA could be due to the activation of the nonsense-mediated mRNA decay (NMD) process. In order to protect the cell from the accumulation of C-terminal truncated proteins with potential deleterious functions, the NMD machinery selectively recognizes and degrades mRNAs whose open reading frame is truncated by the presence of a premature stop-codon (p.K62X and p.84Cfs3), causing reduced amounts of mRNAs available to be detected (Frischmeyer & Dietz, 1999).
Considering that a possible diverse localization of SBDS might impact its activity (Austin et al., 2005), we evaluated SBDS intracellular localization and found that residual SBDS protein in SDS-OBs was mainly localized in the nucleus at difference with hOBs

derived from healthy controls, where it was distributed in the nucleus and in the cytoplasm. This altered intracellular localization of SBDS in the SDS-OBs, suggests that the different mobility capacity of SBDS protein might be related to an altered structure or function. Interestingly, Orelio et al. showed that deletion of the SBDS C-terminus, similarly to what occurs in SDS patients, results in a prominent nuclear localization of SBDS, thus indicating that C-terminus plays a dominant role in cytoplasmic localization (Orelio et al., 2011). However, the antibody used in this study, being raised against the C-terminus of SBDS, should stain the intact SBDS protein, thus detecting the presence of the wild type form of SBDS. Nevertheless, the presence of a wild type SBDS in SDS-OBs is plausible as the full length SBDS in SDS-OBs derives from a new-forming non canonical GC 5'splice site during the transcription of the allele carrying the splicing mutation (258+2T>C), that allows the formation of a residual wild type *SBDS* transcript. However, it is not known yet if the generated protein retains the full functionality as the wild type.

SDS is an inherited bone marrow failure syndrome (Kennedy & Shimamura, 2019) characterized by peripheral cytopenia. About 10% of SDS patients develop myelodysplastic syndrome (MDS) and/or acute leukemia (AML) (Dror, 2005; Warren, 2018; Bezzerri & Cipolli, 2019). It has been reported that the bone marrow of SDS-patients bears frequent clonal chromosome anomalies, such as the isochromosome of the long arm of chromosome 7, i(7)(q10), and the interstitial deletion of the long arm of chromosome 20, del(20)(q). The i(7)(q10) generates a duplication of the hypomorphic *SBDS* allele, which is predicted to increase wild type SBDS protein amount, while the del (20)(q), leads to the deletion of a DNA region containing *eIF6* gene, resulting in *eIF6* haploinsufficiency. Both the i(7)(q10) and the del(20) (q), may results in a more efficient ribosomogenesis, reduced cellular stress and lower risk of developing MDS and/or AML (Valli et al., 2019). Interestingly, in SDS-OBs we did not find neither reduction of eIF6 expression nor chromosomal anomalies (data not shown).

SDS patients showed a different whole transcriptome profile of osteoblasts compared to healthy subjects, with the 98% of genes being downregulated. Accordingly, the main genes related to osteogenesis were all significantly reduced in SDS-OBs. *Runx2* which is a transcription factor essential for osteoblast differentiation and is required for the commitment of precursor cells to the osteoblast lineage was significantly lower in SDS-OBs. It induces the differentiation of multipotent mesenchymal cells into osteoblasts, and, during the early stages of osteoblast differentiation, activates the transcription of non-collagenous matrix protein genes (Komori, 2019). Since the non-collagenous matrix proteins contribute to the correct development of the skeleton, the acquisition and maintenance of bone strength, it is likely that *Runx2* down-regulation could affect bone quality in SDS patients.

Consistent with *Runx2* reduction, also the gene expression of *BGP* and *OPN* were reduced in SDS-OBs compared with healthy controls. The reduced expression of *BGP* could contribute to the mineralization defect observed in SDS-OBs since BGP is a critical factor that enhances calcium binding, it is highly expressed at the onset of mineralization, and it is synthesized concomitantly with hydroxyapatite deposition during skeletal growth (Lian et al., 1982). The interpretation of the reduced expression level of *OPN* is more ambiguous. OPN is a potent inhibitor of hydroxyapatite formation (Holm et al., 2014) and its reduced expression could represent an attempt to balance the mineralization defect here observed in the SDS-OBs *in vitro* and by Toiviainen-Salo and colleagues (2007) *in vivo*. *OPN* is also a promoter of osteoclastogenesis and osteoclast activity (Singh et al., 2018) thus its reduced expression could contribute to the low bone turnover phenotype observed in SDS patients and it is consistent with the low number of osteoclasts observed in SDS bone biopsies (Toiviainen-Salo et al., 2007).

Beside the reduced expression of *Runx2*, *BGP* and *OPN*, the gene and protein expression of BSP, ALP and collagen type I were also reduced in SDS-OBs. BSP expression is tightly associated to the mineralization process, it marks a late stage of osteoblastic differentiation and early stage of mineralization. Like the major glycoproteins of bone matrix, BSP contains the tripeptide sequence, Arg-Gly-Asp (RGD) that mediates the interaction between the matrix and the integrins of bone cells. Moreover, BSP has a high capacity of binding calcium ions and is a determining factor in promoting the nucleation of hydroxyapatite crystals in a variety of in vitro assays (Ganss et al., 1999). *BSP* knockout mouse model is associated to defects in bone mineralization and formation (Bouleftour et al., 2014). Due to its involvement in the regulation of matrix mineralization and in the early stage of osteogenesis, a low expression of *BSP* could be responsible, at least in part, of the impaired mineralization observed in SDS-OBs.

Alkaline phosphatase is an ubiquitous membrane-bound glycoprotein that plays an important role in matrix mineralization. It catalyzes the hydrolysis of phosphate monoesters at basic pH values. By favouring the ratio between inorganic phosphate, (*Pi*), which fosters mineralization and inorganic pyrophosphate (*ePPi*), which instead inhibits this process, ALP exerts a primary role in the regulation of the mineralization. The reduced expression of *ALP* might conversely favour the Pi/PPi ratio thus leading towards impaired mineralization (Osathanon et al., 2009).

Collagen type I constitutes the matrix scaffold, that will be mineralized in a following step. Therefore, the lower collagen amount produced by SDS-OBs could contribute to a lower matrix deposition. As collagen confers mechanical stiffness and strength to bone, the lower amount of collagen produced by SDS-OBs could lead to enhanced fracture risk in SDS patients and is in agreement with the lower amount of osteoid observed in bone biopsies of these patients (Toiviainen-Salo et al., 2007). The lower collagen type I observed in SDS-OBs was associated with higher amount of the tumor suppressor protein p53. p53 is known to increase after DNA damage (Brady & D'Attardi, 2010) and/or upon ribosomal biogenesis impairment (Vousden & Privers, 2009), as it occurs in SDS (Warren, 2018). Previous study has shown that p53 has an inhibitory action on

osteogenesis (Elghetany & Alter 2002). In particular, it inhibits OSX transcriptional and osteogenic activity by repressing its interaction with DNA and its transcriptional partner. This interaction results in a p53-mediated repression of OSX transcriptional activity leading to a downregulation of the osteogenic program (Artigas et al. 2017). It is therefore likely that the lower expression of collagen type I in SDS-OBs could be induced by p53 that, by interacting with OSX, reduces OSX-*COL1A* promoter interaction and relevant *COL1A* transcription. This mechanism of action of p53 is in accordance with our results, showing that OSX levels were not different between SDS-OBs and H-OBs albeit the reduction of BSP and collagen type I production. Furthermore, it has been published that the lack of p53 in *Trp53*-deficient bone marrow-derived MSCs results in a higher capacity to differentiate towards the osteoblastic fate (He et al., 2015). It can be speculated that the high level of p53, observed in the present study could contribute to the impaired osteoblast maturation. Similar high p53 levels were also previously observed in bone marrow from SDS subjects (Elghetany & Alter, 2002). The authors hypothesized that p53 protein overexpression could represent an early indicator of significant DNA genetic alteration, that in the bone marrow environment could play a crucial step in the process of leukemogenesis (Elghetany & Alter, 2002).

The lack of KO mice models that recapitulate SDS complex phenotype limits their use in the investigation of this syndrome and reduces the possibility of a clear understanding of the pathophysiology of SDS. It remains a conundrum how the impairment of ribosome biogenesis, which is a process that occurs in every tissue, could induce cell and tissue specific alterations. The identification of cell types showing specific dysfunctions is therefore relevant for unraveling the molecular mechanisms underlying the function of SBDS.

In conclusion this study demonstrated that the lack of SBDS in osteoblasts is associated to a reduced expression of the main genes involved in the differentiation and maturation of osteoblasts and to a reduced mineralization capacity that is consistent with the low bone mass phenotype observed in SDS patients, thus suggesting that SBDS plays an important role in osteoblast differentiation and function.

CONFLIT OF INTERESTS

The authors declare that there are no conflicts of interests.

AUTHORS' CONTRIBUTIONS

I.V. and A.F. designed the study, established primary culture, analyzed the data, drafted and revised the paper; S.B. performed WB, immunofluorescence staining and interpreted the data; M.S. performed Real Time PCR and WB; R.V. and A.W.K. performed arrays; M.C., R.M.P., E.B., M.R.F., S.C. provided the biological samples; V.B., .G.P. and A.R. revised the paper.

DATA AVAILABILITY

Microarray data are available at https://www.ebi.ac.uk/arrayexpress/; accession number: E-MTAB-9397.

REFERENCES

Abramowicz, A., & Gos, M. (2018). Splicing mutations in human genetic disorders: examples, detection, and confirmation. *Journal of Applied Genetics*, 59(3), 253-268. https://doi:10.1007/s13353-018-0444-7.

Aggett, P. J., Cavanagh, N. P., Matthew, D. J., Pincott, J. R., Sutcliffe, J., & Harries, J. T (1980). Shwachman's syndrome. A review of 21 cases. *Archives of Disease in Childhood,* 55 (5), 331-347. https://doi:10.1136/adc.55.5.331.

Artigas, N., Gámez, B., Cubillos-Rojas, M., Sánchez-de Diego, C., Valer, J. A., Pons, G., … Ventura, F. (2017). p53 inhibits SP7/Osterix activity in the transcriptional program of osteoblast differentiation. *Cell Death and Differentiation*, 24(12), 2022-2031. https://doi:10.1038/cdd.2017.113.

Austin, K. M., Gupta, M. L. Jr, Coats, S. A., Tulpule, A., Mostoslavsky, G., Balazs, A. B., … Shimamura, A. (2008). Mitotic spindle destabilization and genomic instability in Shwachman-Diamond syndrome. *The Journal of Clinical Investigation*, 118, 1511-1518. https://doi:10.1172/JCI33764.

Austin, K. M., Leary. R. J. & Shimamura, A. (2005). The Shwachman-Diamond SBDS protein localizes to the nucleolus. *Blood*, 106(4),1253-1258. https://doi:10.1182/blood-2005-02-0807

Bezzerri, V., & Cipolli, M. (2019). Shwachman-Diamond syndrome: molecular mechanisms and current perspectives. Molecular Diagnosis&Therapy, 23(2), 281-290. https://doi:10.1007/s40291-018-0368-2.

Bodian, M., Sheldon, W., & Lightwood, R. (1964). Congenital hypoplasia of the exocrine pancreas. *Acta Paediatrica*, 5, 282–293. https://doi:10.1111/j.1651-2227.1964.tb07237.x.

Boocock, G. R., Morrison, J. A., Popovic, M., Richards, N., Ellis, L., Durie P. R., & Rommens, J. M. (2003). Mutations in SBDS are associated with Shwachman-Diamond syndrome. *Nature Genetics*, 33(1), 97–101. https://doi:10.1038/ng1062.

Bouleftour, W., Boudiffa, M., Wade-Gueye, N. M., Bouët, G., Cardelli, M., Laroche, N., … Malaval, L. (2014). Skeletal development of mice lacking bone sialoprotein (BSP) impairment of long bone growth and progressive establishment of high trabecular bone mass. *PLoS One*, 9(5), e95144. https://doi:10.1371/journal.pone.0095144.

Brady, C. A., & D'Attardi, L. (2010). p53 at a glance. *Journal of Cell Science*, 123(Pt 15),2527-2532. https://doi:10.1242/jcs.064501.

Burroughs, L., Woolfrey, A., & Shimamura, A. (2009). Shwachman-Diamond syndrome: a review of the clinical presentation, molecular pathogenesis, diagnosis, and treatment. *Hematology/Oncology Clinics of North America*, 23(2), 233-248. https://doi:10.1016/j.hoc.2009.01.007.

Burwick, N., Coats, S. A., Nakamura, T., & Shimamura, A. (2012). Impaired ribosomal subunit association in Shwachman-Diamond syndrome. *Blood*, 120(26), 5143-5152. https://doi:10.1182/blood-2012-04-420166.

Dror, Y. (2005). Shwachman-Diamond syndrome. *Pediatric Blood&Cancer*, 45(7), 892-901. https://doi:10.1002/pbc.20478.

Elghetany, M. T., & Alter, B. P. (2002). p53 protein overexpression in bone marrow biopsies of patients with Shwachman-Diamond syndrome has a prevalence similar to that of patients with refractory anemia. *Archives of Pathology & Laboratory Medicine*, 126(49, 452-455. https://doi:10.1043/0003-9985(2002)126<0452:PPOIBM>2.0.CO;2.

Finch, A. J., Hilcenko, C., Basse, N., Drynan, L. F., Goyenechea, B., Menne, T. F., … Warren, A. J. (2011). Uncoupling of GTP hydrolysis from eIF6 release on the

ribosome causes Shwachman-Diamond syndrome. *Genes & Development*, 25(9), 917–29. https://doi:10.1101/gad.623011.

Frischmeyer, P. A., & Dietz, H. C. (1999). Nonsense-mediated mRNA decay in health and disease. *Human Molecular Genetics*, 8(10), 1893-900. https://doi:10.1093/hmg/8.10.1893.

Ganss, B., Kim, R. H., & Sodek, J. (1999). Bone sialoprotein. *Critical Reviews in Oral Biology and Medicine*, 10(1), 79-98. https://doi:10.1177/10454411990100010401.

Gehron-Robey, P., & Termine, J.D. (1985). Human bone cells in vitro. *Calcified Tissue International*, 37(5), 453–460. https://doi:10.1007/BF02557826.

Ginzberg, H., Shin, J., Ellis, L., Morrison, J., Ip, W., Dror, Y., … Durie, P. R. (1999). Shwachman syndrome: phenotypic manifestations of sibling sets and isolated cases in a large patient cohort are similar. The *Journal of Pediatrics*, 135(1), 81-88. https://doi:10.1016/s0022-3476(99)70332-x.

He, Y., de Castro, L. F., Shin, M. H., Dubois, W., Yang H. H., Jiang S., … Huang, J. (2015). *Stem Cells*, 33(4), 1304-1319. https://doi:10.1002/stem.1925.

Holm, E., Gleberzon, J. S., Liao, Y., Sørensen, E. S., Beier, F., Hunter, G. K., & Goldberg, H. A. (2014). Osteopontin mediates mineralization and not osteogenic cell development in vitro. *The Biochemical Journal*, 464(3), 355-364. https://doi:10.1042/BJ20140702.

Kennedy, A. L., & Shimamura, A. (2019). Genetic predisposition to MDS: clinical features and clonal evolution. *Blood*, 133(10), 1071-1085. https://doi:10.1182/blood-2018-10-844662.

Komori, T. (2010). Regulation of osteoblast differentiation by RUNX2. *Advances in Experimental Medicine and Biology*, 658,43-49. https://doi:10.1007/978-1-4419-1050-9_5.

Lian, J. B., Roufosse, A. H., Reit, B., & Glimcher, M. J. (1982). Concentrations of osteocalcin and phosphoprotein as a function of mineral content and age in cortical bone. *Calcified Tissue International*, 34 Suppl 2: S82-77.

Lindsley, R. C., Saber, W., Mar, B. G., Redd, R., Wang, T., Haagenson, M. D., … Ebert, B. L. (2017). Prognostic mutations in myelodysplastic syndrome after stem-cell transplantation. *New England Journal of Medicine*, 376(6),536–547. https://doi:10.1056/NEJMoa1611604.

Liu, Y., Liu, F., Cao, Y., Xu, H., Wu, Y., Wu, S., … Ma, W. (2018). Shwachman-Diamond syndrome protein SBDS maintains human telomeres by regulating telomerase recruitment. *Cell Reports,* 22(7),1849-1860. https://doi:10.1016/j.celrep.2018.01.057.

Luviano, A., Cruz-Castañeda, R., Sánchez-Puig, N., & García-Hernández, E. (2019). Cooperative energetic effects elicited by the yeast Shwachman-Diamond syndrome protein (Sdo1) and guanine nucleotides modulate the complex conformational landscape of the elongation factor-like 1 (Efl1) GTPase. *Biophysical Chemistry*, 247,13-24. https://doi:10.1016/j.bpc.2019.02.003.

Mäkitie, O., Ellis, L., Durie, P. R., Morrison, J. A., Sochett, E. B., Rommens, J. M., & Cole, W. G. (2004). Skeletal phenotype in patients with Shwachman-Diamond syndrome and mutations in SBDS. *Clinical Genetics*, 65(2), 101-112. https://doi:10.1111/j.0009-9163.2004.00198.x.

Mäkitie, R. E., Costantini, A., Kämpe, A., Alm, J. J., & Mäkitie O. (2019). New insights into monogenic causes of osteoporosis. *Frontiers in Endocrinology (Lausanne)*, 10,70. https://doi:10.3389/fendo.2019.00070.

Morini, J., Babini, G., Mariotti, L., Baiocco, G., Nacci, L., Maccario, G., … Danesino, C. (2015). Radiosensitivity in lymphoblastoid cell lines derived from Shwachman-Diamond syndrome patients. *Radiation Protection Dosimetry*, 166(1-4), 95–100. https://doi:10.1093/rpd/ncv152.

Orelio, C., van der Sluis, R. M., Verkuijlen, P., Nethe, M., Hordijk, P. L., van den Berg, T. K., & Kuijpers, T. W. (2011). Altered intracellular localization and mobility of SBDS protein upon mutation in Shwachman-Diamond syndrome. *PLoS One*, 6(6), e20727. https://doi:10.1371/journal.pone.0020727.

Orelio, C., Verkuijlen, P., Geissler, J., van den Berg, T. K. & Kuijpers, T. W. (2009). SBDS expression and localization at the mitotic spindle in human myeloid progenitors. *PLoS One,* 4(9), e7084. https://doi:10.1371/journal.pone.0007084.

Osathanon, T., Giachelli, C. M. & Somerman, M. J. (2009). Immobilization of alkaline phosphatase on microporous nanofibrous fibrin scaffolds for bone tissue engineering. *Biomaterials*, 30(27), 4513-4521. https://doi:10.1016/j.biomaterials.2009.05.022.

Provost, E., Wehner, K. A., Zhong, X., Ashar, F., Nguyen E., Green R., … Leach, S. D. (2012). Ribosomal biogenesis genes play an essential and p53-independent role in zebrafish pancreas development. *Development,* 139(17), 3232-3241. https://doi:10.1242/dev.077107.

Shwachman, H., Diamond, L. K., Oski, F. A., & Khaw, K. T. (1964). The syndrome of pancreatic insufficiency and bone marrow dysfunction. *The Journal of Pediatrics*, 65, 645–663. https://doi:10.1016/s0022-3476(64)80150-5.

Singh, A., Gill, G., Kaur, H., Amhmed, M., & Jakhu, H. (2018). Role of osteopontin in bone remodeling and orthodontic tooth movement: a review. *Progress in Orthodontic*, 19(1),18. https://doi:10.1186/s40510-018-0216-2.

Toiviainen-Salo, S., Mäyränpää, M. K., Durie, P. R., Richards, N., Grynpas, M., Ellis, L., … Mäkitie, O. (2007). Shwachman-Diamond syndrome is associated with low-turnover osteoporosis. *Bone*, 41(6), 965-972. https://doi:10.1016/j.bone.2007.08.035.

Trainor, P. A., & Merrill, E. A. (2014). Ribosome biogenesis in skeletal development and the pathogenesis of skeletal disorders. *Biochimica et Biophysica Acta*, 1842(6), 769-778. https://doi:10.1016/j.bbadis.2013.11.010.

Valli, R., Minelli, A., Galbiati, M., D'Amico, G., Frattini, A., Montalbano, G., … Maserati, E. (2019). Shwachman-Diamond syndrome with clonal interstitial deletion of the long arm of chromosome 20 in bone marrow: haematological features, prognosis and genomic instability. *British Journal of Haematology*, 184(6), 974-981. https://doi:10.1111/bjh.15729

Vousden, K. H., & Prives, C. (2009). Blinded by the light: the growing complexity of p53. *Cell*, 137(3), 413-431. https://doi:10.1016/j.cell.2009.04.037.

Wang, X., Kua, H-Y., Hu, Y., Guo, K., Zeng, Q., Wu., Q., … Li, B. (2006). p53 functions as a negative regulator of osteoblastogenesis, osteoblast-dependent osteoclastogenesis, and bone remodeling. *The Journal of Cell Biology*, 172(1), 115–125. https://doi:10.1083/jcb.200507106.

Warren, A. J. (2018). Molecular basis of human ribosomopathy Shwachman-Diamond syndrome. *Advances in Biological Regulation*, 67,109-127. https://doi:10.1016/j.jbior.2017.09.002.

Weis, F., Giudice, E., Churcher, M., Jin, L., Hilcenko, C., Wong, C. C., … Warren, A. J. (2015). Mechanism of eIF6 release from the nascent 60S ribosomal subunit. *Nature Structural & Molecular Biology*, 22(11), 914–919. https://doi:10.1038/nsmb.3112.

Table 1 Clinical features and genetic characteristics of the patients with Shwachman-Diamond syndrome

ID	***SBDS*** **mutations (m=maternal; p=paternal; u=undetermined)**	**Age at diagnosis**	**Clinical features at diagnosis**			**Bone defects**	**Age at bone biopsy**
			Pancreatic insufficiency	**Anemia Neutropenia**	**Growth retardation**		
UPN2	c.356G>A; p.V57I (m) c.258+2T>C; p.C84fsX3 (p)	3y	x	no	x	no	18y
UPN20	183_184TA>CT; p.K62X (m) 258+2T>C; p.C84fsX3 (p)	9y	x	x	x	x	43y
UPN24	183_184TA >CT; p.K62X (m) 258 +2T>C; p.C84fsX3 (p)	11y	no	x	x	x	23
UPN45	258+2T>C; p.C84fsX3 (m) 183_184TA>CT; p.K62X (p)	2y	x	x	x	x	9y
UPN51	OMO c.258+2T>C; p.C84fsX3 (m;p)	3y	x	x	no	no	13y
UPN68	258+2T>C; p.C84fsX3 (m) 183_184TA>CT; p.K62X (p) 258+2T>C; p.C84fsX3 (de novo mutation)	10y	x	x	no	x	26y
UPN70	c.258+2T>C; p.C84fsX3 (u); c.92_93GC>AG; p.C31X (u)	1y	x	x	x	x	27y
UPN84	258+2T>C; p.C84fsX3 (m) 183_184TA>CT; p.K62X (p)	5y	x	x	x	x	14y
UPN85	183_184TA>CT; p.K62X (m) 258+2T>C; p.C84fsX3 (p)	19y	no	x	no	no	20y
UPN92	c.183_184TA>CT; p.K62X (u) c.258+2T>C, p.C84fsX3 (u)	14y	x	x	no	no	14y

(UPN: *Unique Patient Number*)

LEGENDS TO FIGURES

FIGURE 1 (a) Representative image of western blot analyses of SBDS protein expression in osteoblasts from healthy subjects (H) and SDS patients. (b) Representative image of immunofluorescence for SBDS in osteoblasts derived from a healthy subject (H2, b1-3) and a SDS patient (UPN92, b4-6) age and sex matched. Actin fibers red; SBDS green; nuclei blue. Magnification 100X.

FIGURE 2 (a) RT-PCR on RNA of lymphoblastoid cells (LCLs) and osteoblasts (OBs) derived from a healthy control (H), a patient (UPN24) who carriers the mutation c.258+2T>C in heterozygous state, and a patient (UPN51) carrying the mutation in homozygous state revealed the residual transcript of wt *SBDS* in both patients. To detect the residual wt amplicon, cDNA of both patients was used at a concentration 2 times (UPN24) and 10 times (UPN51) more than the healthy cDNA concentration**. C- :** negative control; **M:** marker 100bp. (b) Relative mRNA expression of *SBDS*, *eIF6* (eukaryotic initiation factor 6) and *EFL1* (GTPase elongation factor-like 1) in osteoblasts from SDS patients (SDS) and age and sex-matched healthy subjects (H), n=4. Mann Whitney test, * P<0.05 vs healthy.

FIGURE 3 (a) Heat map showing differentially expressed mRNAs of Gene Ontology ossification (GO:0001503) comparing 3 healthy individuals versus patients with SDS. Each row represents one mRNA, and each column represents a sample. Red, upregulation; green, downregulation. (b) Volcano plot of gene expression changes between SDS-derived osteoblasts vs healthy subjects derived osteoblasts. The x-axis displays the log2 fold change value and the y -axis corresponds to the negative logarithm to the base 10 of the t-test p-values. A total of 2373 genes were differentially expressed in SDS-derived osteoblasts vs healthy osteoblasts. The red dots represent upregulated genes (43 genes) and the blue dots represent downregulated genes (2330 genes). The gray dots correspond to genes with no significant difference. Analysis has been conducted with moderated t-test with Benjamini-Hochberg correction. Genes with corrected p-value <0.05 has been taken into account. (c) Relative mRNA expression of the main osteogenesis-related genes in osteoblasts of healthy subjects (H; n=8) and SDS patients (SDS; n=10). Runt-Related Transcription Factor 2 (*Runx2*), Osterix (*OSX*), osteopontin (*OPN*), bone sialo-protein (*BSP*), osteocalcin (*BGP*), alkaline phosphatase (*ALP*), collagen type I (*COL1A*); Mann Whitney test, * P<0.05; **P<0.01.

FIGURE 4 (a) Representative image of western blot analyses of collagen type I (Col1), alkaline phosphatase (ALP), bone sialo protein (BSP) and osterix (OSX) protein expression in osteoblasts from healthy subjects (H) and SDS patients and (b) relevant quantification (H; n=5; SDS; n=9). Mann Whitney test, * P<0.05.

FIGURE 5 (a) Representative image of western blot analyses of p53 protein expression in osteoblasts from age and sex matched healthy subjects and SDS patients (SDS) and (b) relevant quantification (n=9). Mann Whitney test, * P<0.05.

FIGURE 6 (a) Representative image of Alizarin Red staining of osteoblasts from a healthy subject (H1) and a SDS pa-

FIGURE 1

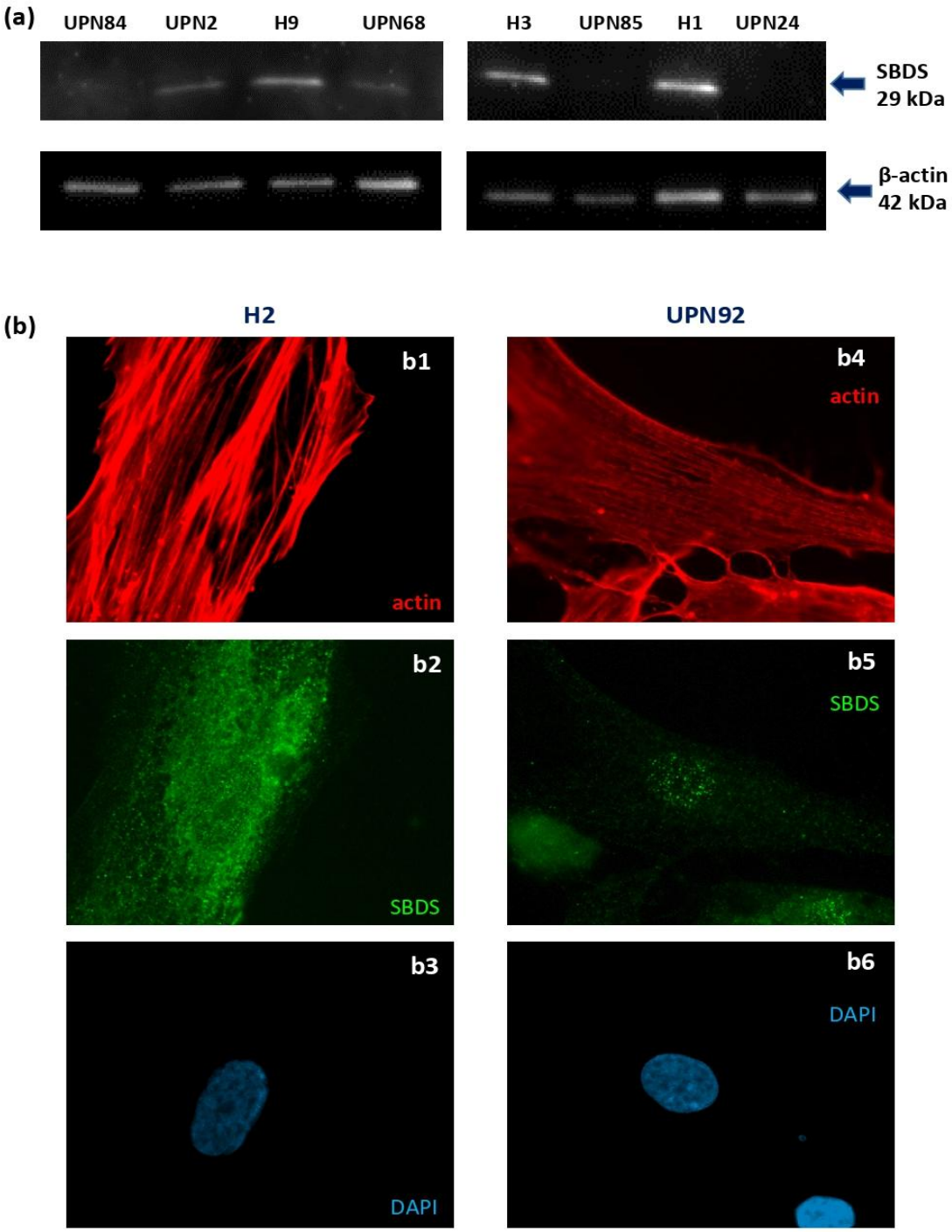
(a)
UPN84
UPN2
H9
UPN68
H3
UPN85
H1
UPN24
SBDS
29 kDa
β-actin
42 kDa
(b)
H2
UPN92
b1
actin
b4
actin
b2
SBDS
b5
SBDS
b3
DAPI
b6
DAPI

FIGURE 2

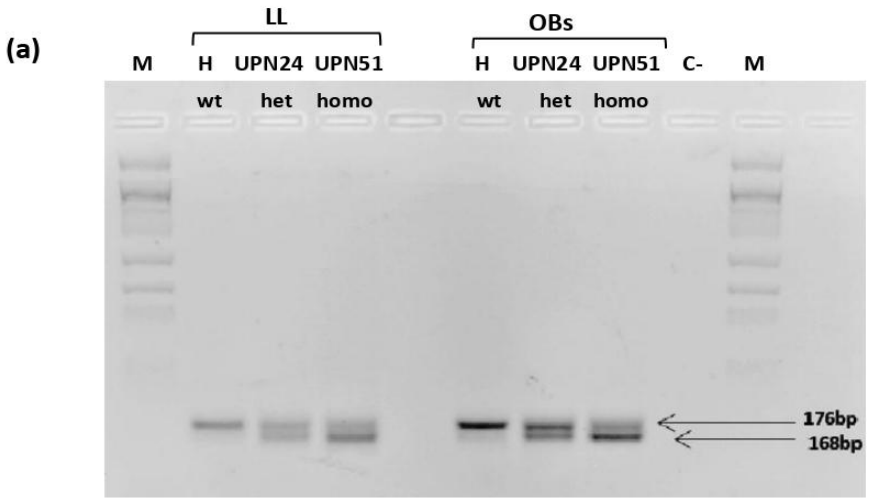
(a)
LL
OBs
M
H
UPN24
UPN51
H
UPN24
UPN51
C-
M
wt
het
homo
wt
het
homo
176bp
168bp

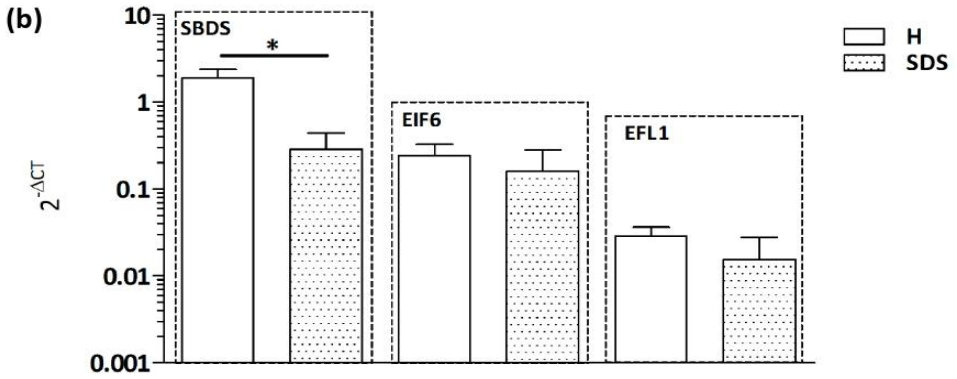
(b)
10
1
0.1
0.01
0.001
$2^{-\Delta CT}$
SBDS
*
EIF6
EFL1
H
SDS

FIGURE 3

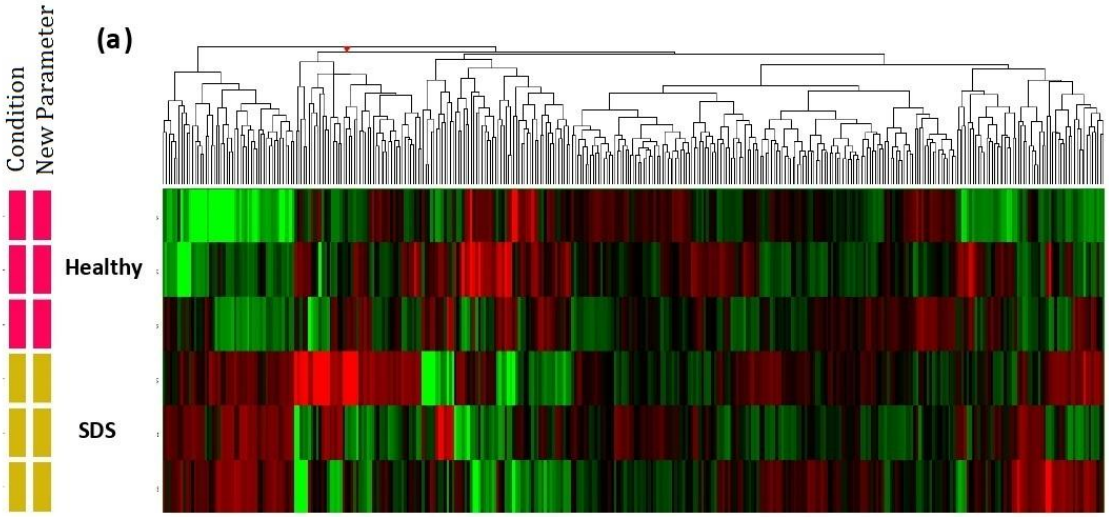
(a)
Condition
New Parameter
Healthy
SDS

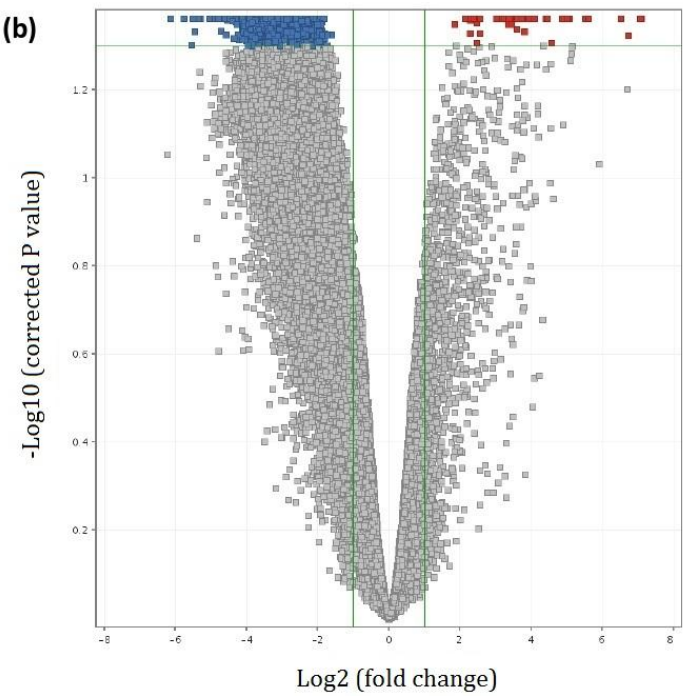
(b)
-Log10 (corrected P value)
Log2 (fold change)

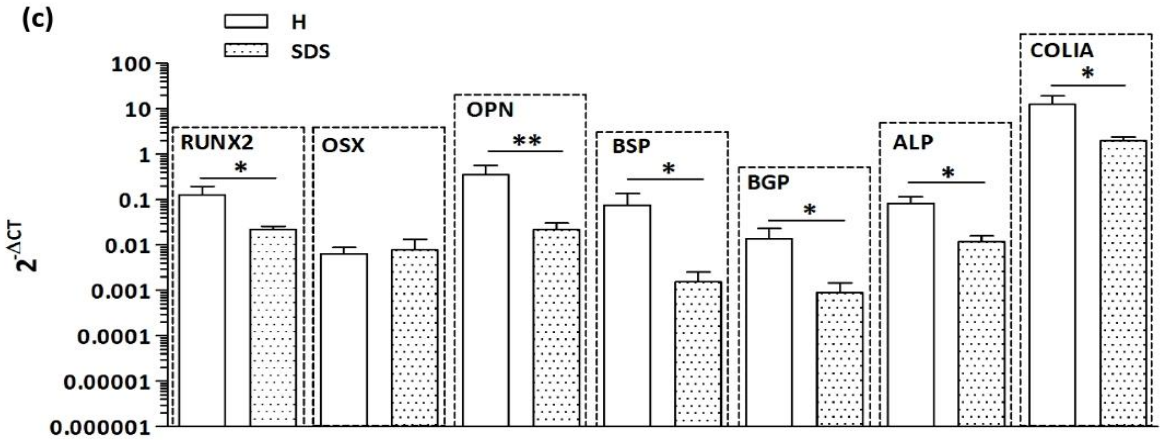
(c)
H
SDS
100
10
1
0.1
0.01
0.001
0.0001
0.00001
0.000001
$2^{-\Delta CT}$
RUNX2
*
OSX
OPN
**
BSP
*
BGP
*
ALP
*
COLIA
*

FIGURE 4

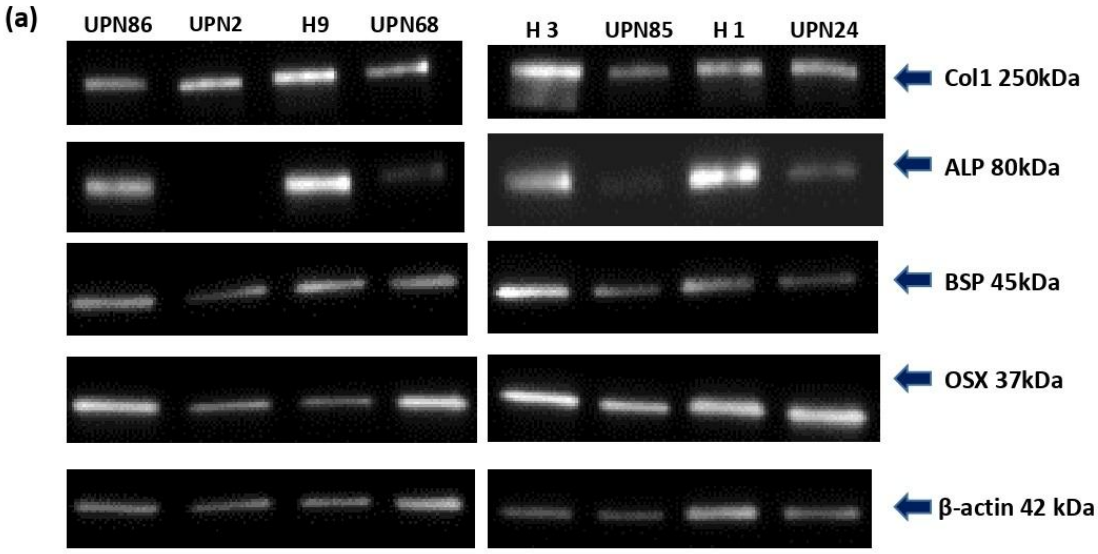
(a)
UPN86
UPN2
H9
UPN68
H 3
UPN85
H 1
UPN24
Col1 250kDa
ALP 80kDa
BSP 45kDa
OSX 37kDa
β-actin 42 kDa

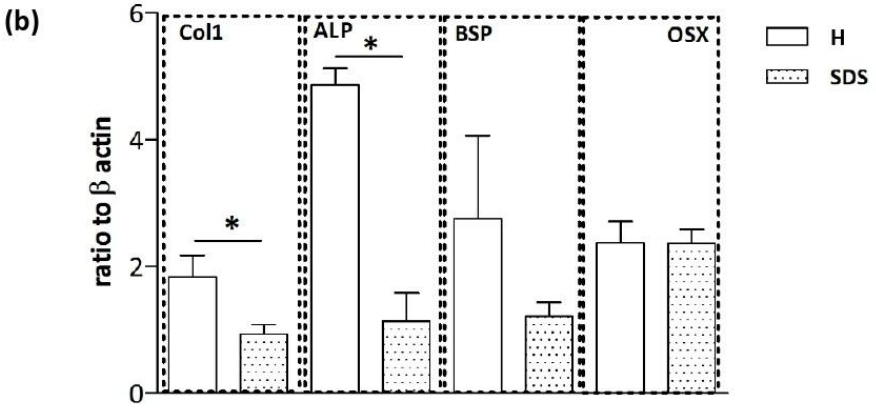
(b)
ratio to β actin
6
4
2
0
Col1
ALP
BSP
OSX
*
*
H
SDS

FIGURE 5

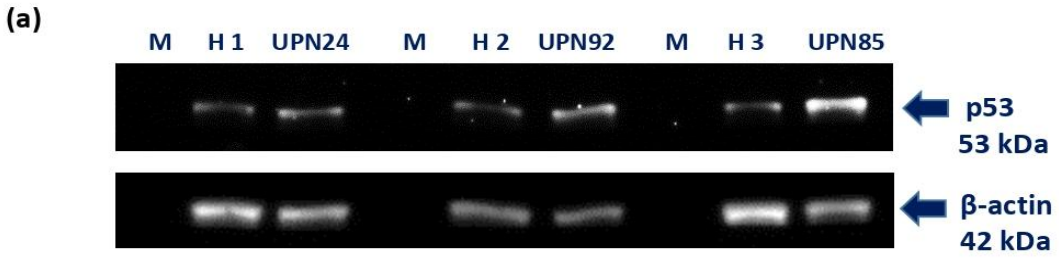
(a)
M
H 1
UPN24
M
H 2
UPN92
M
H 3
UPN85
p53
53 kDa
β-actin
42 kDa

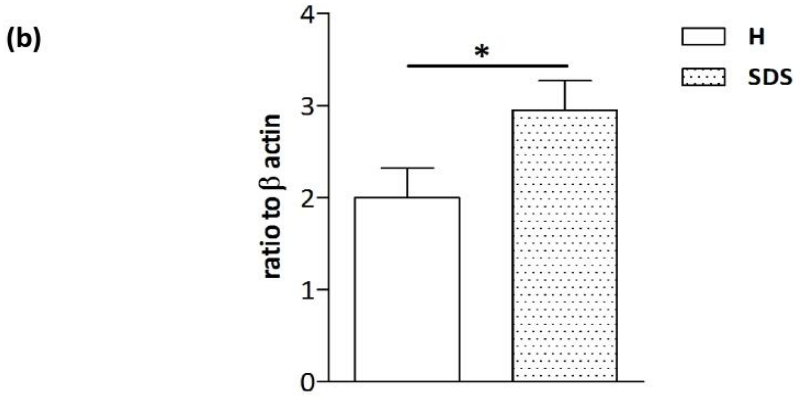
(b)
ratio to β actin
0
1
2
3
4
*
H
SDS

FIGURE 6

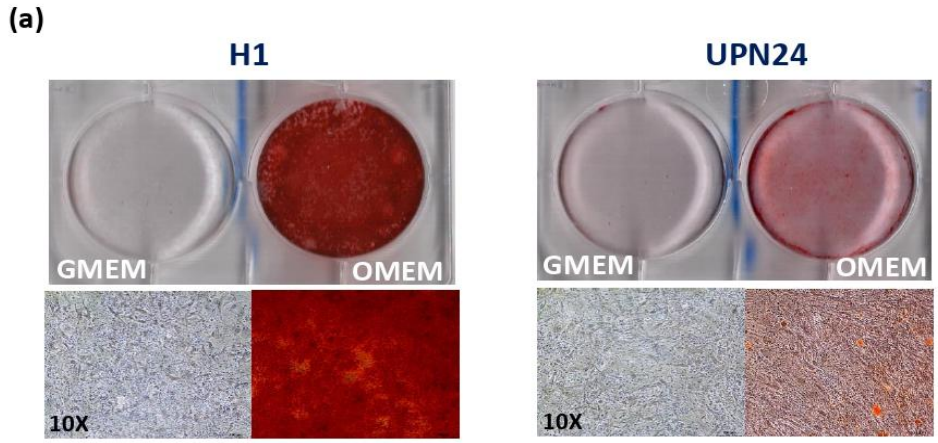
(a)
H1
UPN24
GMEM
OMEM
GMEM
OMEM
10X
10X

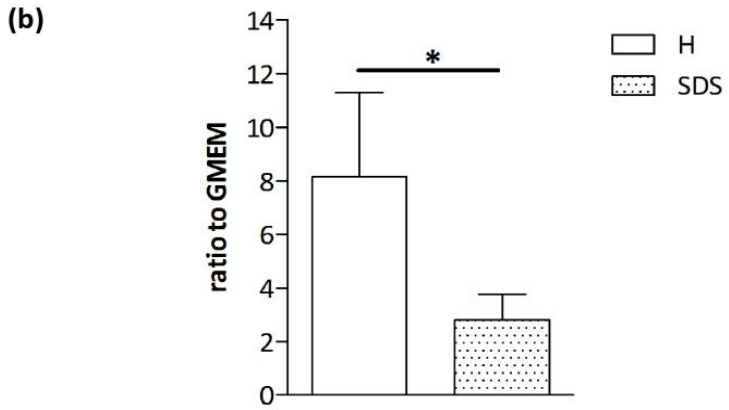
(b)
ratio to GMEM
14
12
10
8
6
4
2
0
*
H
SDS

Figure S1

(a)

```
>Human SBDS chromosome:GRCh37:7:66452064:66461188
     1 aattagcttggcgtggccgctcacacctgtagtcccagctacttgggaagctaacgctgg     60
    61 aagatcgctcgaacccaggaggtcgaagctgcagtggggccatgaccctgccactgcact    120
   121 ccagcctgggtgacagagtgagactgacttaaaaaaaaaactgtaaataaaaaagcaaca    180
   181 aaaaaatgaaaaaagaataaaacaaggatggcaaaatgttgatagcggggtgatgggtac    240
   241 atagaaggttcattacacttttttgtctacattttatgttaaaatatttctattataaaa    300
   301 gggtgagtaaataaaaatatttattataaaataattctattataaaaaatatttatatta    360
   361 taaagtgggtctggcccttgaattccgcggaacgaggtggtgccaacgctgtgttttaac    420
   421 ccggtcactaaacatccgcgagcatcctgtcagagctctcagctcattggcgaaagtaaa    480
   481 tacgccaaggaaaagcacctccctttttgggcgtggaaagatggcgtaaaaagccacaat    540
   541 acgcaggcgtcatcgctcactttccccctcccggcttctgctccacctgacgcctgcgca    600
   601 GTAAGTAAGCCTGCCAGACACACTGTGACGGCTGCCTGAAGCTAGTGAGTCGCGGCGCCG    660 exon 1
   661 CGCACTGGTGGTTGGGTCAGTGCCGCGCGCCGATCGGTCGTTACCGCGAGGCGCTGGTGG    720
   721 CCTTCAGGCTGGACGGCGCGGGTCAGCCCTGGTTCGCCGGCTTCTGGGTCTTTGAACAGC    780
   781 CGCGATGTCGATCTTCACCCCCACCAACCAGATCCGCCTAACCAATGTGGCCGTGGTACG    840
   841 GATGAAGCGTGCCGGGAAGCGCTTCGAAATCGCCTGCTACAAAAACAAGGTCGTCGGCTG    900
   901 GCGGAGCGGCGTgtgagtagccccctccctcgggcctgggcctgggcctgagccgtcacC    960
   961 tccgaggcggcctgtctctgcccaagtcgagtgaatgggccaggctggggtgttggccgg   1020
  1021 ggaggaaatggaacattcctgctgtgagcatgagacgtcgctgtccgagcttggcgccta   1080
  1081 agccaagggtttcttctttatttggttggttcggattgggttgttggtttggggttttgt   1140
  1141 tttgttggtgtcataaaagctgcagccaagaaatctcgtaattgtggtccttttcctaga   1200
  1201 ataatgatggctgagaacctagtcttacgaatactgtcatagttgtgggtacatctggtg   1260
  1261 tcatagatctcagtagccctagcagtttaaagtgcgtagtgtcttcactgctgccatcta   1320
  1321 gggactggcattccgtggcagcagctgtctgcaccccaccccaccccttgtgtttcttacg   1380
  1381 tcctcccatgacatttttctccagtgagcaaatggtaaggcaaatacggttctgagtttt   1440
  1441 gaaaatgttccctcaggccgatgcgggcagttcacttgaggccaggagttcgaggccagc   1500
  1501 ctggccaacatgaaaccccatctctactaaaaatacaaagttagccgggtgtggtggcgc   1560
  1561 atgcctgtaatcccagttactcaggaggctgaggcgggagaatcacttgaacccgggagg   1620
  1621 ctgaggttacagtgacccgagatcgcgccattgcactccagcctgggcaaaaacagtgaa   1680
  1681 attccatctaggggcgggggttgggggtaagaaaaagaaaactgccctctacactaaag   1740
  1741 gtcatcaggggatttgttgtgtcttgccgttcatgttgttgccatctcgtatttaaatg   1800
  1801 taaatgcatgtccaagtttcaagtatattcacataggactttctctcctgccctcacaag   1860
  1861 GGAAAAAGACCTCGATGAAGTTCTGCAGACCCACTCAGTGTTTGTAAATGTTTCTAAAGG   1920 exon 2
  1921 TCAGGTTGCCAAAAAGGAAGATCTCATCAGTGCGTTTGGAACAGATGACCAAACTGAAAT   1980
                ▼c.258+2T>C
  1981 CTGTAAGCAGgttgggtaacagctgcagcatagctaaccctaataaccatttataacgtat   2040
       del 8 bp
  2041 ttgtagatatattaaacattaaaggctgtttttctggaggaaagactaaccaagcaataa   2100
  2101 tgtgaactgcacagtgtcacttctaataataaagaacttggtggttttgtttgttttttg   2160
  2161 tggtttttttttttttttttttgccaaaacctcctgaaatcagattttctactaaattac   2220
  2221 ctcatttttctataaattgccccatttatagaatgtggtatacctgaaaactgaatttgt   2280
  2281 tttcaagtatttcatctttcagatccttttttttttgggtgggggggacagagtcttgctc   2340
  2341 tgttgcccaggctggagtgcagtgcacttcactgcactcagctcactgcaacctctgcct   2400
  2401 cctggattcaagcgattctcttgcctcagcttccagggtagctgggattacaggtgccca   2460
  2461 ccaccctgcctggctaatttttggatttttagtagagatggggtttcaccatgttggcca   2520
  2521 ggttggtctcaaactcctgaccttgggtgatatgcccgccttagccacccaaagtgctgg   2580
  2581 gattacagatgtgagccactgagcccagccaaaagattcttgcatcttttgggcaaagct   2640
  2641 caaaccattacttacatattgatagctggagaggatgaaatttaattttctctccatcca   2700
  2701 gttactcatttttatggttagttaataaatagtgtgtgatagagaaagatagtgatttc   2760
  2761 ttaaatgtgttggcatttttttagATTTTGACTAAAGGAGAAGTTCAAGTATCAGATAAA   2820 exon3
  2821 GAAAGACACACACAACTGGAGCAGATGTTTAGGGACATTGCAACTATTGTGGCAGACAAA   2880
  2881 TGTGTGAATCCTGAAACAAAGAGACCATACACCGTGATCCTTATTGAGAGAGCCATGAAG   2940
  2941 GACATCCACTATTCGGTGAAAACCAACAAGAGTACAAAACAGCAGgtgagtggtttctca   3000
```

(b)

```
WT        ATGTCGATCTTCACCCCCACCAACCAGATCCGCCTAACCAATGTGGCCGTGGTACGGATG exon1
258+2T>C  ATGTCGATCTTCACCCCCACCAACCAGATCCGCCTAACCAATGTGGCCGTGGTACGGATG
WT pep     M  S  I  F  T  P  T  N  Q  I  R  L  T  N  V  A  V  V  R  M
Alt pep    M  S  I  F  T  P  T  N  Q  I  R  L  T  N  V  A  V  V  R  M

WT        AAGCGTGCCGGGAAGCGCTTCGAAATCGCCTGCTACAAAAACAAGGTCGTCGGCTGGCGG
258+2T>C  AAGCGTGCCGGGAAGCGCTTCGAAATCGCCTGCTACAAAAACAAGGTCGTCGGCTGGCGG
Wt pep     K  R  A  G  K  R  F  E  I  A  C  Y  K  N  K  V  V  G  W  R
```

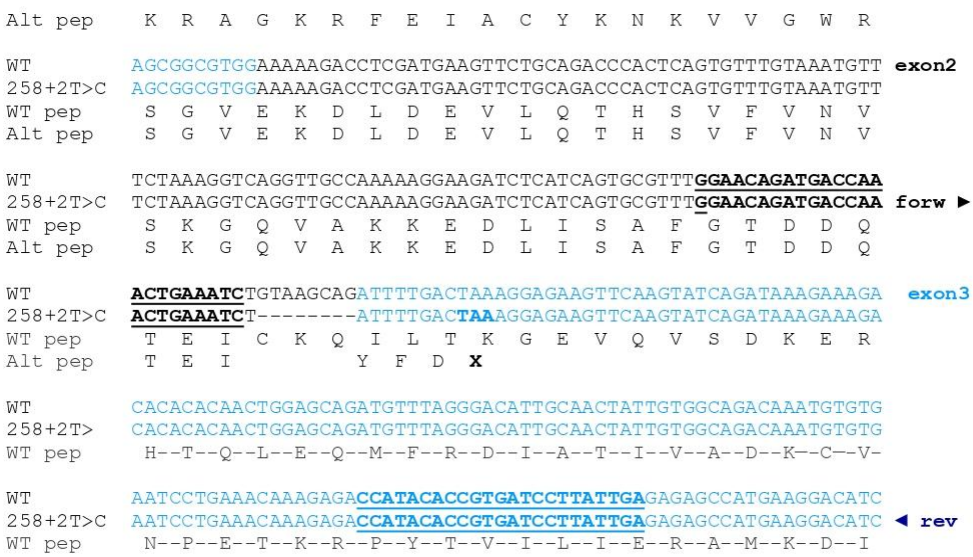

Figure S1.
(a) Genomic sequence of the gene SBDS showing the first 3 exons (capital letters) and introns (lowercase letters). It is indicate the position of the mutation c.258+2T>C (▼)that abrogates the classical 3' splice site GT and creates the mutated and weak splice site GC, and the position (▼)of the alternative splice site used in the alternative transcript, resulting in the deletion of 8 nucleotides.
(b) The alignment of wild type (WT), mutated (258+2T>C) nucleotide sequences and the amino acids sequence of the alternative transcript (alt pep) and the wild type protein at the mutation level (WT pep).
Primer sequences (forward and reverse) used for the RT-PCR are underlined and in bold.

RESULTS (SECTION 5)

Evaluation of ataluren as a therapeutic option for Shwachman Diamond syndrome

12.1. Introduction

Shwachman Diamond syndrome (SDS) is a complex genetic disorder, for which no drug based treatment option is available currently. *SBDS* gene, which was identified as the first causative gene (apart from the recently identified genes) for this syndrome, accumulates deleterious mutations in approximately 90% SDS patients (Valli et al. 2017a). Exon 2 region of *SBDS* is responsible for two key mutations, c.183_184TA>CT and c.258+2T>C (Boocock et al. 2003). The c.258+2T>C is considered a hypomorphic mutation due to the production of minimal wild type SBDS protein in its presence (Valli et al. 2017a). On the contrary, the c.183_184TA>CT is a severe mutation that can trigger a premature termination codon (PTC) signal, consequently resulting in a truncated nonfunctional protein that can immensely affect the normal cellular activities. Due to the deficiency of SBDS protein, patients with SDS show high propensity toward myelodysplastic syndrome (MDS) and/or acute myeloid leukemia (AML) (Dror 2005).

There are multiple genetic disorders where the phenomenon of PTC can give rise to the diseased condition (Atkinson et al. 1999). In few such genetic disorders, the PTC has been suppressed successfully by a counter strategy called nonsense suppression (Morais et al. 2020). By nonsense suppression, the stop codon that contributes to PTC can be substituted by a sense codon to fix the mutation and ensure normal protein synthesis. Welch and colleagues in the year 2007 described a novel molecule, PTC124 (commonly called ataluren or translarna) that can enhance nonsense suppression in dose-dependent manner (Welch et al. 2007). Although the mechanism of action of ataluren is still not fully understood, it is believed that ataluren enhances the integration of near-cognate tRNAs at the position of nonsense codon that can result in the production of full length functionally active protein (Welch et al. 2007). Presently,

ataluren is used for the treatment of Duchenne Muscular Dystrophy (Ryan et al. 2014) while it is still under investigation for the treatment of cystic fibrosis (Kerem et al. 2014; Zainal Abidin et al. 2017). Considering the apparent potential of ataluren to repair PTC, we designed a small scale study to evaluate the effect of ataluren on patient derived lymphoblastoid cell lines (LL) for the restoration of c.183_184TA>CT mutation in the absence of an effective therapy for SDS to analyze its capacity as a future therapeutic option for SDS patients.

13. Material and Methods

13.1. Cell culture

Patient-derived lymphoblastoid cells (LL) were grown in complete RPMI media in the presence of 10 % FBS and 2 mM L-glutamine at 37 °C in humidified Co_2 incubator. Cultures were maintained for at least three passages before any treatment was applied. A total of six samples (45, 90, 39, 100, 75, 46) were used in two different experiments for SBDS protein examination by western blot while two samples (100 and 45) were utilized for ribosomal profiling.

13. 2. Ataluren treatment

Approximately 48 hours before harvesting the cells, ataluren treatment was applied to cell cultures at a concentration ranging from 2.5 µM-5 µM. Ataluren was applied in the form of a solution dissolved in dimethyl sulfoxide.

13. 3. Cell lysate for SBDS protein western blot

Following ataluren treatment, about 1 million cells were collected in microcentrifuge tube and pelleted at 2200 RPM for 10 minutes at 4 °C. Subsequently, the pellet was subjected to a wash with PBS followed by a second centrifugation at 2200 RPM at 4 °C. The pellet was dried completely and re-suspended in about 50 µL of RIPA buffer mix that comprised of 47.5 µL RIPA buffer (Sigma®), 2 µL phosphatase inhibitor (Roche®) and 0.5 µL protease inhibitor (Sigma®). The solution was incubated on ice for 30

minutes with periodic pulse vortexing after every 5 minutes. Finally, the homogenized solution was centrifuged for 10 minutes at 10,000 RPM and 4 °C, thereby obtaining the clear lysate for western blot which was stored at -80 °C until the next use. The remaining steps of western blot were performed according to the protocol described with slight modifications (Bezzerri et al. 2017).

13. 4. Cell lysate preparation for ribosome profiling

Approximately 50 million cells in T75 flask were treated with cycloheximide (CHX) at a final concentration of 100 µg/mL and incubated for 20 minutes at 37 °C before harvesting. The same concentration of CHX was maintained in all the solutions throughout the harvesting process and all the following steps were performed on ice or 4 °C (inside the centrifuge). Briefly, cells were pelleted and washed twice with ice cold PBS at 300 x g at 4 °C for 5 minutes. Cells pellets were re-suspended in adequate volume of detergent buffer (1.2% Nonidet P-40, 0.2 M Sucrose and 0.004 U/µL RNAse inhibitor) and lysis buffer (20 mM Tris PH 7.5, 10 mM Nacl and 3 mM $Mgcl_2$) followed by incubation on ice for 10 minutes that involved occasional vortexing and mixing. Finally, the cloudy solution was centrifuged at 14000 x g for 10 minutes to obtain the clear cell lysate.

13. 5. Sucrose gradient centrifugation, fractionation and ribosomes peak detection

Cell lysates with a quantity of about 800 µg - 1.5 mg total proteins were poured on the top of sucrose gradient (15%-50%) and after balancing they were ultra-centrifuged at 36000 RPM for 2 hours at 4 °C in ultracentrifuge (Beckman Coulter). Subsequently, gradient fractions were monitored at 254nm UV absorbance for various ribosomal peaks by UV detector (Brandel) and about 13 fractions were retrieved per sample using the Foxy Jr. gradient collector (Teledyne Isco). Ribosomal profiling was performed before and after ataluren treatment to judge the effect of ataluren on ribosomal assembly.

14. Results

14.1 Positive response of LL cells to ataluren

We analyzed the effect of ataluren on LL cells in two discrete experiments and levels. In the first small scale experiment ataluren was applied to one million of cells (Fig. 1) while in another similar experiment, we applied ataluren to approximately 50 million cells to evaluate our findings at larger scale (Fig. 2). In both experiments the response of patients samples to ataluren was apparently positive by all patients' samples carrying c.183_184TA>CT (samples 45, 46 and 100). The only patient sample that lacked the c.183_184TA>CT was 90 (contains c.258+2T>C only) which did not show response to ataluren (Fig 1) and hence was excluded from the following experiment as shown in Fig 2. Samples 39 and 75 being controls were also not influenced by ataluren as expected (Fig 1 and Fig 2). Further, we were also interested to record the trickled down effect of ataluren at the ribosomal level to assess the change in ribosomal assembly in patients' samples. Knowing that ataluren would have apparently no effect on ribosomal assembly of healthy individuals and 90 patient as demonstrated in Fig 1 and Fig 2, they were not considered for ribosomal profiling. Although we included patient 46 for ribosomal evaluation initially, however, later due to some ambiguity we excluded it in the final result. Generally, our results of ribosomal profiling demonstrated the effect of ataluren treatment also at the ribosomal level. We observed an apparent increase in the ribosomal biogenesis (Fig 3B, 3C and Fig 4B and 4C), which validated our proposed hypothesis. However, due to time stringency we could not expand the spectrum of this experiment to a larger scale.

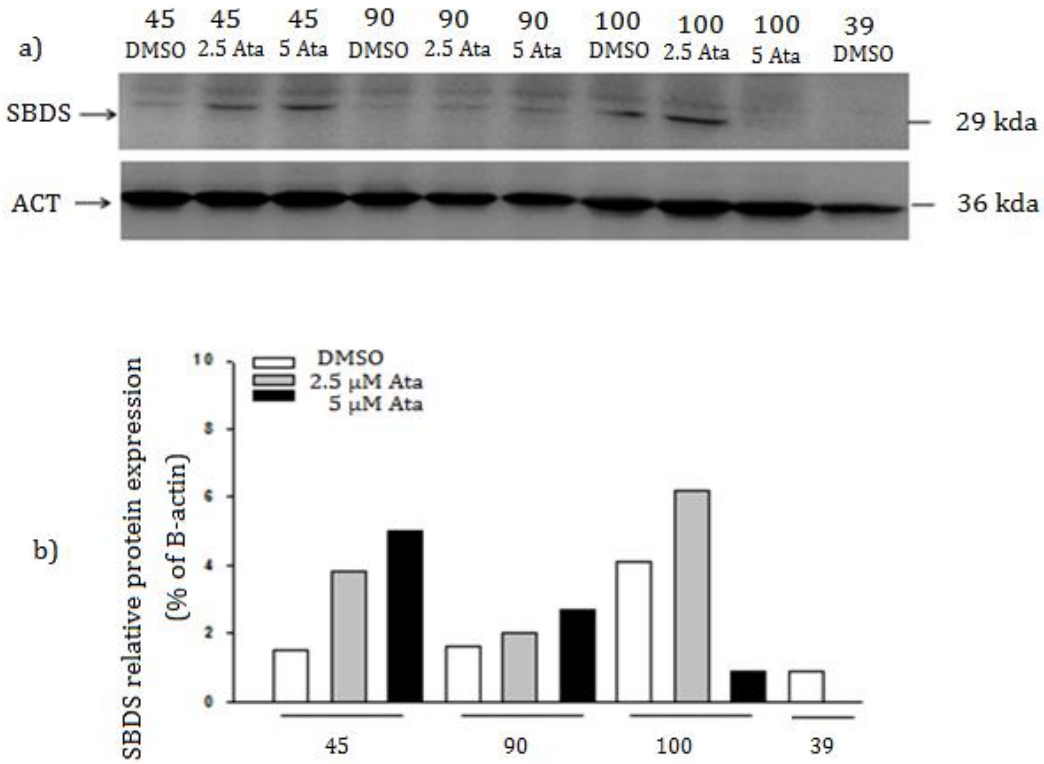

Figure 1. a) Western blot image of SBDS compared to β-actin at two concentrations of ataluren (2.5 µM and 5 µM) in LL cells. Numbers 45, 90, 100 and 39 describe various samples. Samples 45 and 100 contain c.183_184TA>CT mutations, sample 90 is homozygous for c.258+2T>C mutation while sample 39 is healthy control. b). SBDS relative protein expression.

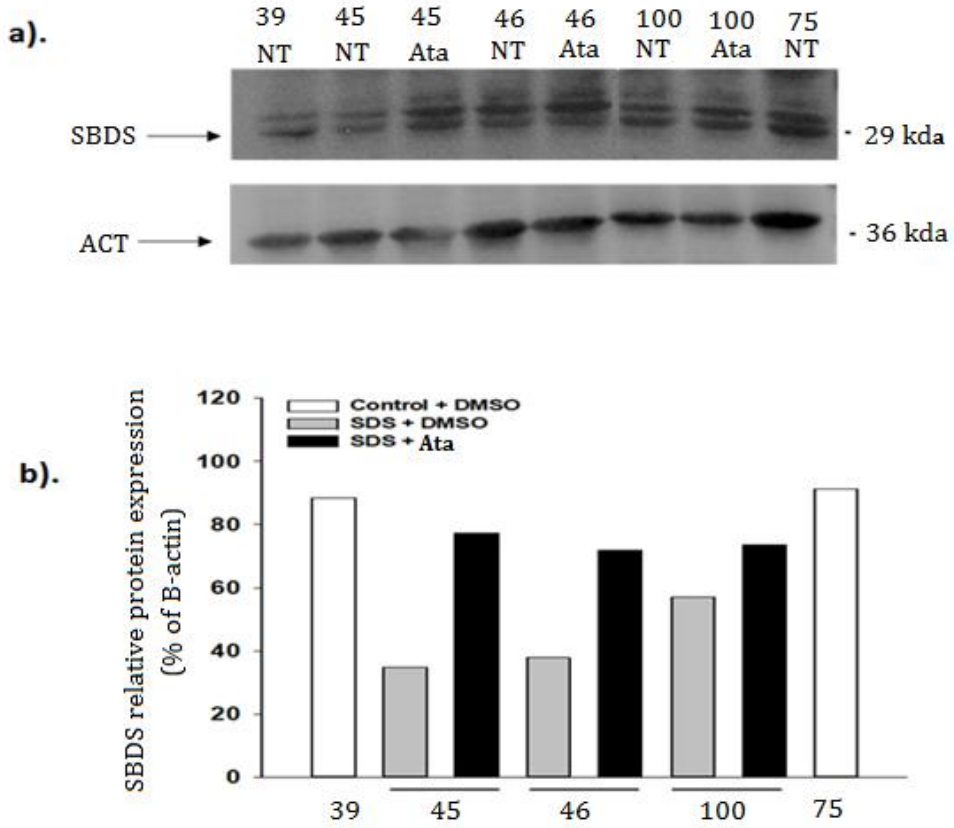

Figure 2. Western blot image of SBDS compared to β-actin at 5 μM concentration. a). Numbers 45, 46 and 100 indicate patients samples while 39 and 75 are healthy controls. "Ata" stands for ataluren treated samples while "NT" means not treated. b). SBDS relative protein expression.

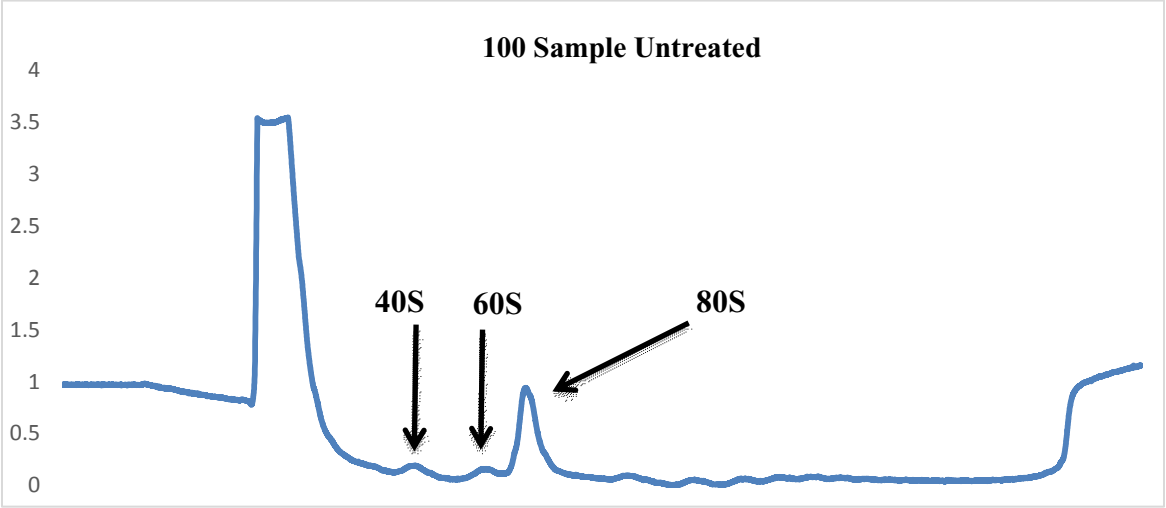

Figure 3A. Ribosomal profile of 100 sample (100/07/LL) before ataluren treatment.

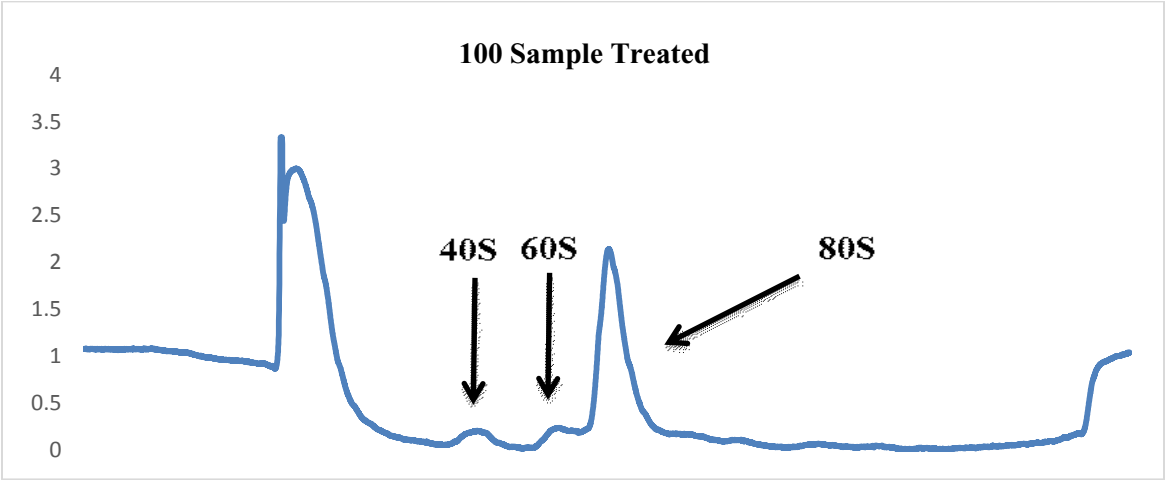

Figure 3B. Ribosomal profile of 100 sample (100/07/LL) after ataluren treatment.

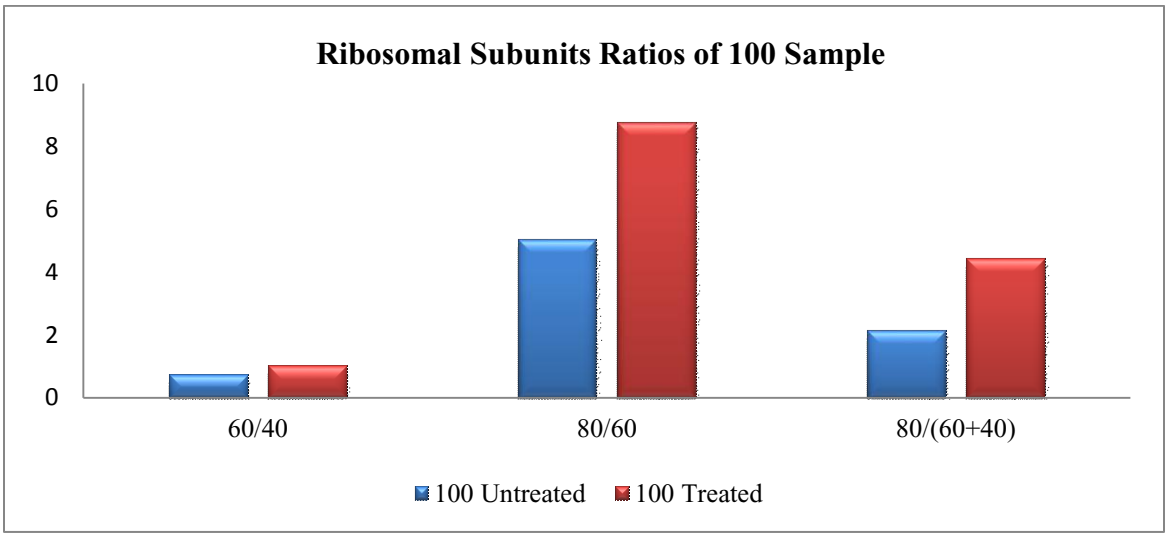

Figure 3C. Ribosomal subunits ratios of 100 sample (100/07/LL) in untreated and ataluren treated conditions.

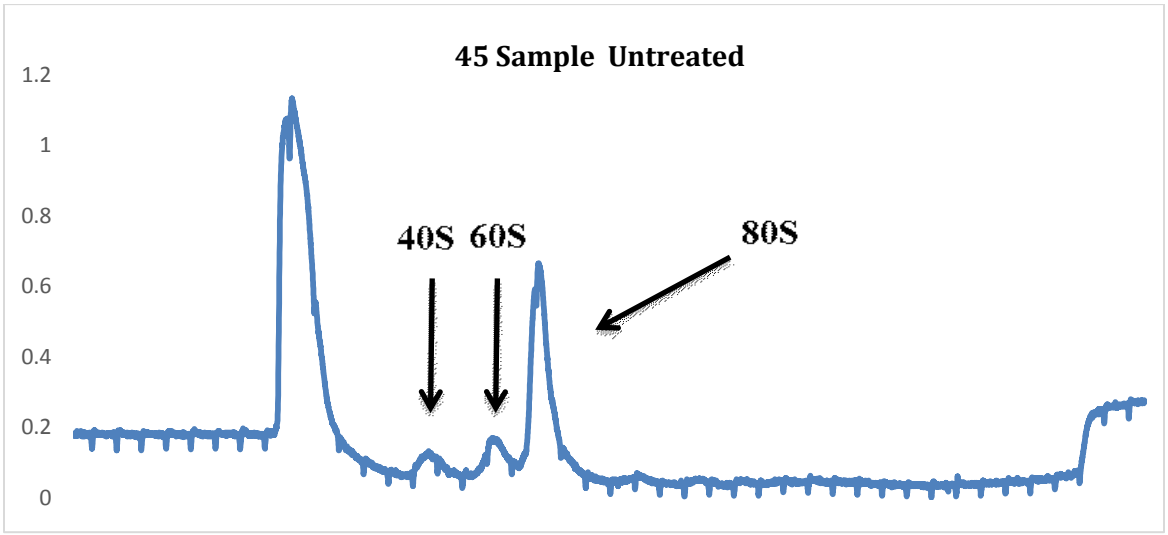

Figure 4A. Ribosomal profile of 45 sample (45/07/LL) before ataluren treatment.

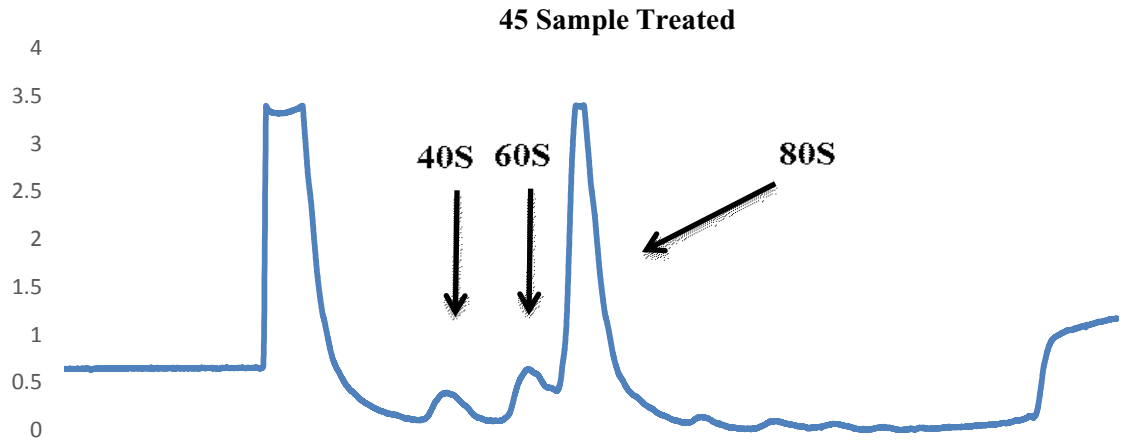

Figure 4B. Ribosomal profile of 45 sample (45/07/LL) after ataluren treatment.

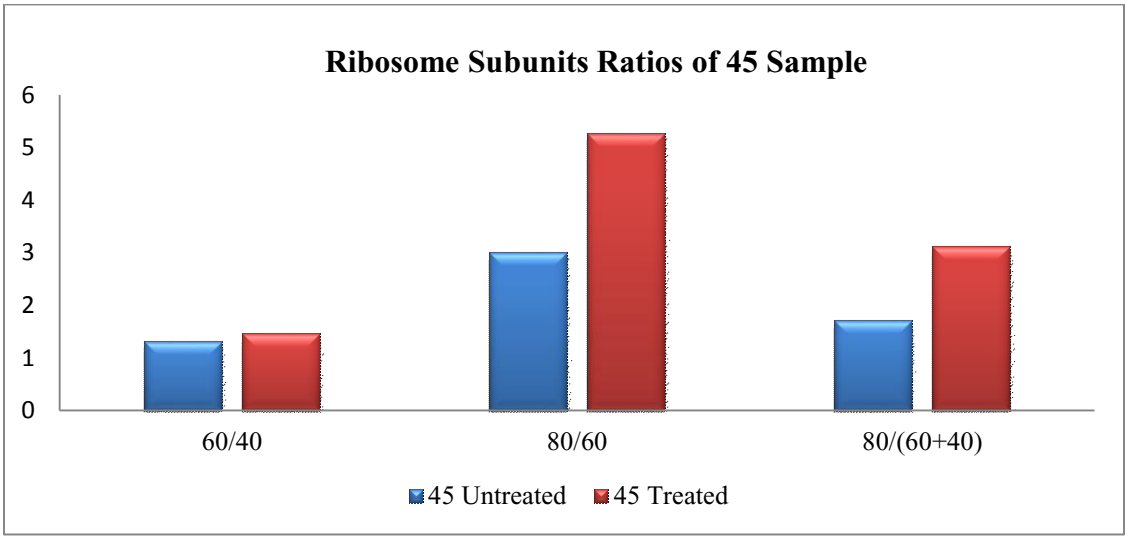

Figure 4C. Ribosomal subunits ratios of 45 sample (45/07/LL) in untreated and ataluren treated conditions.

15. Discussion

The role of ataluren to rectify PTC by nonsense suppression (Welch et al. 2007) is a ray a hope for those genetic disorders where PTC can severly impair the production of a functionally vital protein. Morais et al. (2020) has mentioned multiple counter strategies along with ataluren to be considered for PTC-triggered genetic disorders. Due to its ease of use and past precedence, we formulated a pilot scale study to evaluate the effects of ataluren on LL cells. Our results revealed that the nonsense mutation c.183_184TA>CT that triggers the PTC of SBDS protein in SDS patients was restored in the our LL samples (Fig 1 and Fig 2). Similarly, the utimate effect of this mutation restoration was also demonstrated in the form of increased ribosomal assembly (Fig 3B, 3C and Fig 4B, 4C), which authenticate the capability of ataluren to revert PTC signals and promote ribosomal biogenesis of 80S particle in accordance with the mechanism highlighted by Finch et al. (2011). Our study outcomes are in accordance with a recent report that applied ataluren in SDS and obtained positive results (Bezzeri et al. 2017). Many other past and recent studies have highlighted the scope of ataluren as a potential drug for PTC triggered genetic conditions (Lentini et al. 2014; Samanta et al. 2019; Tutone et al. 2019; Morias et al. 2020). Similarly, in Duchenne Muscular Dystrophy, the increased expression of dystrophin due to ataluren treatment was noticed in 61% of patients (Finkel et al. 2013), whereas between 40%-70% response was estimated in the case of cystic fibrosis patients (Kerem et al. 2008). However, response to ataluren is attributed to a variety of factors (Finkel et al. 2012) and may also vary among various tissue types as observed in mice (Thada et al. 2016). Therefore, although we apparently demonstrated that ataluren has restoring efficacy to rectify *SBDS* nonsense mutation and partially justify its scope for treatment of SDS in the future. Nevertheless, there are muliple factors that need our attention i. e. limitation of our sample size, authentication of ataluren in various cell types, evaluation of its toxicity and side effects, association between ataluren and patients demographic parameters etc. are some known factors that leave sufficient

space to challenge its efficiency in different cellular environments and circumstances before concluding the ultimate potential of ataluren in the case of SDS.

16. THESIS DISCUSSION

The discovery of *SBDS* gene by Boocock and colleagues (2003) was a breakthrough event in determining the genetic and molecular basis of Shwachman Diamond Syndrome (SDS). Earlier studies (Mack et al. 1996; Ginzberg et al. 1999a; Ginzberg et al. 1999b) and subsequent reports (Dror 2005) on SDS demonstrated its multifactorial dimensions and diverse clinical phenotypes in the SDS patients. Today, SDS is known to be a rare autosomal recessive disorder that demonstrates heterogeneous symptoms including exocrine pancreatic deficiency, hematological disorders, bone irregularities and neurodevelopmental abnormalities (Dror 2005). Patients with SDS tend to develop myelodysplastic syndrome (MDS) and/or acute myeloid leukemia (AML) (Dror 2005). SDS patients contain biallelic hypomorphic mutations in the *SBDS* gene (Shwachman–Bodian–Diamond syndrome) in 90% of clinically diagnosed patients (Boocock et al. 2003). Recent reports on SDS have revealed the association of other genes such as *DNAJC21* (Dhanraj et al. 2017), *EFL1* (Stepensky et al. 2017), *SRP54* (Carapito et al. 2017) and *EIF6* (Koh et al. 2020) to this syndrome which can trigger SDS or SDS like phenotype in the affected individuals. *SBDS* gene itself is functionally highly versatile which has key role in regulation of cell division (Austin et al. 2008), DNA replication (Ball et al. 2009), ribosomal biogenesis (Finch et al. 2011; Wong et al. 2011) and probably other cellular processes that mostly remain unknown till now. Due to the multifarious role of SBDS, it is understandable that in the case of its depletion, the affected individuals have to bear multipronged effects and complications both at cellular and overall phenotype level. Taking into consideration the aforementioned scenario, we devised the central idea of this PhD project to illustrate the pathogenesis, pathophysiology and clinical aspects of SDS for better understanding of this disorder by the use of advanced and state of the art molecular techniques.

The initial goal of the project comprised of the evaluation of karyotype instability and clonal chromosomal aberrations that take place in SDS patients' bone marrow (BM) cells (Pressato et al. 2012). Conventional cytogenetic techniques like karyotyping and fluorescent in situ hybridization (FISH) have been used in the past for examining

various chromosomal aberrations. Nevertheless, due to the limitation of karyotyping to identify small aberrations and FISH to detect only specific known regions, we used them in conjunction with comparative genomic hybridization array (aCGH). The use of aCGH technique gives a superior advantage over conventional cytogenetic approaches to evaluate micro deletions, micro duplications and loss of heterozygosity (LOH) along with its suitability to be utilized easily for various cell types without their prerequisite of going through division phase. Generally, different type of chromosomal aberrations may accumulate in the BM Of SDS patients, however, due to their hypothesized prognostic value and frequent occurrence in SDS (Pressato et al. 2012; Valli et al. 2013; Pressato et al. 2015), we were primarily focused on del(20)(q) and, i(7)(q10).

To assess clonal chromosomal anomalies in SDS, we analyzed a total of twenty five SDS patients BM in two batches (twelve in 2018 and thirteen in 2020). Interesting, in all BM samples carrying del(20)(q), *EIF6* was lost unanimously and the deletion was always interstitial (Results section 1 and Results section 2). Similar results have been reported in a study by Pressato et al. (2012). Moreover, the proximal ends of breakpoints were conserved between bands q11.211-q11.22. These results were accomplished through aCGH in twenty three patients, whereas, in two cases informative probes based FISH was applied for this purpose. In most cases (18/25), interstitially deleted fragments with a size ranging from 14-26.9 Mb, were visible by chromosome analysis. Conversely, relatively smaller deletions were identified by aCGH or FISH in few cases. The size of lowest deletion was recorded as 1.7 Mb (patient 13). Two patients (SDS1-000050 and UPN 68) were identified with two separate del(20)(q) (Results section 2, unpublished data).

Chromosomal anomalies, i(7)(q10) and del(20)(q) are known to be the most predominant clonal anomalies that are acquired by the BM of SDS patients (Pressato et al. 2012; Valli et al. 2013). The locus of *SBDS* gene is positioned on the chromosome 7, so, the i(7)(q10) is a way of augmenting the reduced quantity of SBDS protein by giving rise to duplication of hypomorphic *SBDS* allele. The EIF6 protein (Eukaryotic initiation factor 6) is an anti-association factor whose removal from the 60S ribosomal

subunit is essential for the association of 60S and 40S subunits to ensure the formation of 80S ribosomal particle (Finch et al. 2011). Therefore, del(20)(q) which contains the locus of *EIF6* gene, is an indirect mechanism to reduce the quantity of ribosomal anti-association factor by *EIF6* haploinsufficiency and hence, to enhance the ribosomal assembly in the absence of sufficient SBDS quantity. Our study regarding karyotype instability in SDS, particularly the presence of i(7)(q10) and del(20)(q) is testimony of the fact that SDS depleted clones strive to use this phenomena as a rescue mechanism for the deficiency of the SBDS protein to evolve and reach better fitness level.

The second part of our study comprised of understanding the BM gene expression pattern of SDS patients. The comparative analysis of SDS patients and healthy controls using expression arrays highlighted that the gene expression pattern of the SDS patients was quite different than the healthy individuals (Results section 3). This difference was obvious both at the level of whole transcriptome (WT) analysis as well as in the selected gene sets that are considered vital in normal BM functioning. Previously, few studies (Rujkijyanont et al. 2008; Nihrane et al. 2009; In et al. 2016) have been carried out in this domain that reported similar results, however, the scope of those studies remain confined to few gene sets only. Similarly, another study by Frattini and colleagues also discussed this gene expression pattern (Frattini et al. 2015). However, due to the choice of selected hela cell line by them, the obtained results may not be plausible as hela cell line shows high genetic unstability and variability and expression profiling among various batches may lack accuracy. More detailed studies supporting our findings on this topic have been published (Rujkijyanont et al. 2007; Rujkijyanont et al. 2009) which have used BM or better cell lines but they did not consider the clonal chromosomal changes in the BM of SDS patients in their studies. In our study, the differential expression pattern was more pronounced in those SDS patients with normal karyotype (SDS-NK) that lacked clonal chromosomal anomalies (Results section 3, Fig 2). On the contrary, patients with clonal anomalies (particularly in high proportion) behaved similar to the healthy

controls. Out of the total examined samples, only eight patients showed chromosomal anomalies, whereas, nine samples did not exhibit any chromosomal anomaly at the time of RNA extraction for transcriptome study. By evaluating the WT via the principal component analysis (PCA) for all the samples (both patients and controls), a pattern highlighting the stratification of patients in groups was seen. Similarly, WT based dendogram, also revealed clustering pattern bifurcating into two major groups indicating variable gene expression impression in the SDS-NK patients (Results section 3, Fig 3). Keeping in mind the importance of EIF6 and its deletion in case of del(20)(q), it was intriguing to ascertain the expression level of EIF6 in various samples. The extrapolated array raw data to assess EIF6 levels of RNA showed that of del(20)(q) containing the interstitial deletion of EIF6 expressed low EIF6 RNA similar to the healthy controls, especially when high proportion of clones containing del(20)(q) were present (Results section 3, Fig 1). The sole i(7)(q10) case i.e. UPN 24 showed normal EIF6 levels as anticipated, while patient suffering from AML and with complex karyotype (UPN 92) revealed elevated EIF6 levels. High expression of EIF6 has been linked to human cancer in a previous report (Zhu et al. 2017). These outcomes enlighten the role of clonal chromosomal changes and particularly the significance of *EIF6* in the del(20)(q) due to its prognostic importance (Pressato et al. 2012). One notable limitation of the study includes the scarcity of whole BM material used in expression array experiments for confirmation of the achieved results for important genes by real time PCR and western blot. Moreover, we could not figure out the wide spread distribution among the control individuals on PCA plot and were unable to mention the reason for lack of a coherent behaviour. Nevertheless, the most convincing rationale which justifies this aspect is the type of study samples used. Since whole bone marrow is composed of a heterogeneous population of cells and therefore, may not behave in a homogeneous manner.

Similarly, as a continuation of gene expression pattern examination in SDS by expression array, SDS patient derived osteoblast cells (SDS-OBs) also endorsed the findings of our work on whole bone marrow samples indicating altered gene

expression pattern compared to healthy controls (Results section 4). Thanks to the availability of sufficient material this time, we were able to carry out confirmatory experiments. Surprisingly, SDS-OBs lacked chromosomal anomalies and showed normal expression of EIF6 (data not shown). Further, the quantity of SBDS protein was highly compromised in SDS patients as expected. The impaired production of SBDS in osteoblasts was noticeably correlated to compromised expression of key osteoblastogenesis genes (Results section 4, Fig 3b and 3c) such as Runx2, BGP, BSP, ALP, COL1A and OPN etc. (except OSX) that are considered crucial in the maturation and differentiation process of osteoblasts (Lian et al., 1982; Holm et al. 2014; Singh et al. 2018; Komori, 2019) attributing to reduced mineralization potential and low bone mass. In accordance with these results, low levels of mineralization has been seen in the past in a study involving SDS patients biopsies (Toiviainen-Salo et al. 2007). Elevated levels of P53 were also recorded, hence, highlighting its inhibitory role in the overall ossification process (Elgetany and Alter, 2002). As a consequence of these altered cellular activities in osteoblasts, stunted bone phenotype may be observed in SDS patients. Therefore, it was deduced that SBDS is imperative for the regulation of differentiation and normal function of osteoblasts.

The third portion of our project was focused on the hunt for therapeutic agent for SDS. Till date, no drug is available to cure SDS. However, by exploiting the known capability of ataluren to revert nonsense mutations (Linde et al. 2008), it was proposed to assess the restoring potential of ataluren in SDS patient derived lymphoblastoid cell lines (LL) for restoration of *SBDS* gene nonsense mutation c.183_184TA>CT, that causes premature termination of the SBDS protein. Our results revealed that nonsense mutation was restored in the LL cells. The trickled down effect of this restoration was observed in the form of increased SBDS quantity as seen in both pilot and high scale experiments (Results section 5, Fig 1 and Fig 2). These finding are in line with the outcomes of Bezzerri et al. (2017), indicating the potency of ataluren in SDS. Likewise, the therapeutic capability of ataluren has been validated by various other studies (Lentini et al. 2014; Samanta et al. 2019; Tutone et al. 2019; Morias et al. 2020). In

Duchenne Muscular Dystrophy, the increased expression of dystrophin due to ataluren treatment was noticed in 61% of patients (Finkel et al. 2013), whereas between 40%-70% response was estimated in the case of cystic fibrosis patients (Kerem et al. 2008). As an extension of our work and knowing the role of SBDS in ribosomal biogenesis, we also demonstrated an increased quantity of 80S subunit in ataluren treated cells (Results section 5, Fig 3B, 3C and Fig 4B, 4C), indicating improved ribosomal assembly to form 80S particle in accordance with the mechanism proposed by Finch et al. (2011). Nevertheless, response to ataluren is attributed to a variety of factors (Finkel et al. 2012) and may also vary among various tissue types as observed in mice (Thada et al. 2016). Apparently, it was demonstrated that ataluren has restoring efficacy to rectify *SBDS* nonsense mutation and justify its scope for treatment of SDS in the future. However, considering the small sample size of our study, validation of ataluren in various cell types, evaluation of toxicity and side effects, correlation between ataluren and patients demographic parameters are some of the aspects that leave sufficient room to challenge its efficiency in different cellular environments and conditions prior to reach a firm conclusion.

Cumulatively, despite our study limitations, the outcomes of our study enhance the existing knowledge about SDS and advance it one step further. In the absence of an appropriate animal model for SDS, our studies on patient derived samples lay the foundation for future studies to pursue the aspects of pathogenesis, clinical repercussions and quest for potential therapy for SDS in the future.

Future perspective

SDS is a complex genetic disorder that is not very well understood till date. Our current study on SDS can be further extended to improve multiple other hidden aspects of the disorder. In the future, we intend to evaluate more samples from various global partners for cytogenetic monitoring and to assess the genomic instability in more detail, especially to ascertain the del(20)(q), always observed to retain the *EIF6* gene, which is a very fascinating finding exclusively associated to SDS.

In addition, it would be also of immense interest to examine the role of *EIF6* in-vitro in cell culture studies. The quantity of *EIF6* in cell culture could be regulated by knockdown effect using an appropriate cell line and proper knockdown strategy to mimic the haploinsufficiency. By this mean, we would be able to compare the obtained results with our existing studies on patient derived samples. Therefore, we would be in a better situation to give remarks about our existing findings and importance of *EIF6* in SDS. Similar proposal is also under consideration for the duplication of the *SBDS* hypomorphic mutation c.258+2T>C to achieve i(7)(q10) like condition.

Lastly, taking into consideration the apparently positive outcome of ataluren in LL cell line, it would be amazing to enhance the spectrum of these experiments by including more samples and other relevant cell lines to reach a firm conclusion regarding our preliminary work.

17. REFERENCES

Aggett PJ, Cavanagh NP, Matthew DJ, et al. Shwachman's syndrome. A review of 21 cases. Archives of Disease in Childhood. 1980; 55(5):331–347.

Atkinson J, Martin R. Mutations to nonsense codons in human genetic disease: Implications for gene therapy by nonsense suppressor tRNAs. Nucleic Acids Research. 1994;22:1327–1334. doi: 10.1093/nar/22.8.1327

Austin KM, Gupta ML Jr, Coats SA, et al. Mitotic spindle destabilization and genomic instability in Shwachman-Diamond syndrome. Journal of Clinical Investigation. 2008; 118 (4): 1511–1518.

Ball HL, Zhang B, Riches JJ, et al. Shwachman-Bodian Diamond syndrome is a multi-functional protein implicated in cellular stress responses. Human Molecular Genetics. 2009; 18(19): 3684–3695.

Bannon SA, DiNardo CD. Hereditary predispositions to myelodysplastic syndrome. International Journal of Molecular Sciences. 2016. https://doi.org/10.3390/ijms17060838.

Bench AJ, Nacheva EP, Hood TL, et al. Chromosome 20 deletions in myeloid malignancies: reduction of the common deleted region, generation of a PAC/BAC contig and identification of candidate genes. Oncogene. 2000; 19: 3902-13.

Bezzerri V, & Cipolli M. Shwachman–Diamond syndrome: molecular mechanisms and current perspectives. Molecular Diagnosis and Therapy. 2019; 23: 281–290.

Bidou L, Allamand V, Rousset JP, et al. Sense from nonsense: therapies for premature stop codon diseases. Trends in Molecular Medicine. 2012; 18: 679-688.

Bodian M, Sheldon W, Lightwood R. Congenital hypoplasia of the exocrine pancreas. Acta Paediatrica. 1964; 53: 282-293.

Boocock GR, Morrison JA, Popovic M, et al. Mutations in SBDS are associated with Shwachman-Diamond syndrome. Nature Genetics. 2003; 33(1): 97–101.

Bykov, VJN, Eriksson SE, Bianchi J, et al. Targeting mutant p53 for efficient cancer therapy. Nature Reviews Cancer. 2018; 18: 89–102.

Carapito R, Konantz M, Paillard C, et al. Mutations in signal recognition particle SRP54 cause syndromic neutropenia with Shwachman-Diamond-like features. Journal of Clinical Investigation. 2017; 127(11): 4090-4103.

Celik, A, Kervestin S, & Jacobson A. NMD: At the crossroads between translation termination and ribosome recycling. Biochimie. 2015; 114: 2-9.

Cesaro S, Pegoraro A, Sainati L, et al. A Prospective Study of Hematologic Complications and Long-Term Survival of Italian Patients Affected by Shwachman-Diamond Syndrome. Journal of Pediatrics. 2020; 219: 196-201.

Cipolli M, D'Orazio C, Delmarco A, et al. Shwachman's syndrome: pathomorphosis and long-term outcome. Journal of Pediatric Gastroenterology and Nutrition. 1999; 29: 265-272.

Dalle JH, De Latour RP. Allogeneic hematopoietic stem cell transplantation for inherited bone marrow failure syndromes. International Journal of Hematology. 2016; 103: 373–379.

Delaporta P, Sofocleous C, Economou M, et al. The Greek registry of Shwachman Diamond-Syndrome: Molecular and clinical data. Pediatric Blood Cancer.
2017; 64: e26630.
Dhanraj S, Matveev A, Li H, et al. Biallelic mutations in DNAJC21 cause Shwachman - Diamond syndrome. Blood. 2017; 129(11): 1557–1562.

Donadieu J, Leblanc T, Meunier BB, et al. Analysis of risk factors for myelodysplasias, leukemias and death from infection among patients with congenital neutropenia. Experience of the French Severe Chronic Neutropenia Study Group. Haematologica. 2005; 90: 45-53.

Donadieu J, Fenneteau O, Beaupain B, et al. Classification of and risk factors for hematologic complications in a French national cohort of 102 patients with Shwachman-Diamond syndrome. Haematologica. 2012; 97(9): 1312–1319.

Dror Y. Shwachman-Diamond syndrome. Pediatric Blood Cancer. 2005; 45: 892-901.

Dror Y, Donadieu J, Koglmeier J, et al. Draft consensus guidelines for diagnosis and treatment of Shwachman-Diamond syndrome. Annals of New York Academy of Science. 2011; 1242: 40–55.

Dror Y, Freedman MH. Shwachman-Diamond syndrome: an inherited preleukemic bone marrow failure disorder with aberrant hematopoietic progenitors and faulty marrow microenvironment. Blood. 1999; 94(9): 3048–3054.

Elghetany MT, Alter BP. p53 protein overexpression in bone marrow biopsies of patients with Shwachman-Diamond syndrome has a prevalence similar to that of patients with refractory anemia. Archives of Pathology and Laboratory Medicine. 2002; Apr;126(4):452-5. doi: 10.1043/0003-9985.

Fanen P, Wohlhuter-Haddad A, Hinzpeter A. Genetics of cystic fibrosis: CFTR mutation classifications toward genotype-based CF therapies. International Journal of Biochemistry and Cell Biology. 2014; 52: 94–102.

Finch, AJ, Hilcenko C. Basse N, et al. Uncoupling of GTP hydrolysis from eIF6 release on the ribosome causes Shwachman-Diamond syndrome. Genes & development. 2011; 25: 917-929.

Finkel RS, Flanigan KM, Wong B, et al. Phase 2a study of ataluren-mediated dystrophin production in patients with nonsense mutation Duchenne muscular dystrophy. PloS one. 2013; 8, e81302, doi:10.1371/journal.pone.0081302.

Ginzberg H, Shin J, Ellis L, et al. Shwachman syndrome: exocrine pancreatic dysfunction and variable phenotypic expression. Journal of Pediatrics. 1999a; 135: 81-88.

Ginzberg H, Shin J, Ellis L, et al. Shwachman syndrome: phenotypic manifestations of sibling sets and isolated cases in a large patient cohort are similar. Journal of Pediatrics. 1999b; 135(1): 81–88.

Goobie S, Popovic M, Morrison J, et al. Shwachman-Diamond syndrome with exocrine pancreatic dysfunction and bone marrow failure maps to the centromeric region of chromosome 7. American Journal of Human Genetics. 2001;68(4):1048–54.

Ip WF, Dupuis A, Ellis L, et al. Serum pancreatic enzymes define the pancreatic phenotype in patients with Shwachman-Diamond syndrome. Journal of Pediatrics. 2002; 141(2): 259–265.

Kerem, E. et al. Effectiveness of PTC124 treatment of cystic fibrosis caused by nonsense mutations: a prospective phase II trial. Lancet. 2008; 372: 719-727, doi:10.1016/S0140-6736(08)61168-X.

Kerr EN, Ellis L, Dupuis A, Rommens JM, et al. The behavioral phenotype of school-age children with shwachman diamond syndrome indicates neurocognitive dysfunction with loss of Shwachman-Bodian-Diamond syndrome gene function. Journal of Pediatrics. 2010; 156: 433-438.

Koh AL, Bonnard C, Lim JY, et al. Heterozygous missense variant in EIF6 gene: A novel form of Shwachman–Diamond syndrome? American Journal of Medical Genetics Part A. 2020 ;182(9): 2010-2020.

Lentini, L, Melfi R, Di Leonardo, et al. Toward a rationale for the PTC124 (Ataluren) promoted readthrough of premature stop codons: A computational approach and GFP-reporter cell-based assay. Molecular Pharmaceutics. 2014; 11: 653–664.

Linde, L. & Kerem, B. Introducing sense into nonsense in treatments of human genetic diseases. Trends in Genetics. 2008; 24, 552-563.

Mack DR, Forstner GG, Wilschanski M, et al. Shwachman syndrome: exocrine pancreatic dysfunction and variable phenotypic expression. Gastroenterology. 1996; 111(6):1593–1602.

Makitie, O. et al. Skeletal phenotype in patients with ShwachmanDiamond syndrome and mutations in SBDS. Clinical Genetics. 2004; 65, 101-112.

Mercuri A, Cannata E, Perbellini O, Cugno C, Balter R, Zaccaron A, et al. Immunophenotypic analysis of hematopoiesis in patients suffering from Shwachman-Bodian-Diamond Syndrome. European Journal of Haematology. 2015; 95(4): 308–15.

Morais P, Adachi H and Yu Y. Suppression of nonsense mutations by emerging technologies. International Journal of Molecular Sciences . 2020; 21(12): 4394.

Morini J, Nacci L, Babini G, et al. Whole exome sequencing discloses heterozygous variants in the DNAJC21 and EFL1 genes but not in SRP54 in 6 out of 16 patients with Shwachman-Diamond Syndrome carrying biallelic SBDS mutations. British Journal of Haematology. 2018. https ://doi.org/10.1111/bjh.15594.
Mort, M.; Ivanov, D.; Cooper, D.N.; Chuzhanova, N.A. A meta-analysis of nonsense mutations causing human genetic disease. Human Mutation. 2008; 29: 1037–1047.

Myers KC, Bolyard AA, Otto B, et al. Variable Clinical Presentation of Shwachman Diamond Syndrome: Update from the North American Shwachman–Diamond Syndrome Registry. The Journal of Pediatrics. 2014; 164 (4): 866-870

Myers KC, Furutani E, Weller E, et al. Clinical features and outcomes of patients with Shwachman-Diamond syndrome and myelodysplastic syndrome or acute myeloid leukaemia: a multicentre, retrospective, cohort study. Lancet Haematology. 2019; 7(3): E238-E246.

Neuhaus C, Eisenberger T, Decker C, et al. Next-generation sequencing reveals the mutational landscape of clinically diagnosed Usher syndrome: Copy number variations, phenocopies, a predominant target for translational read-through, and

PEX26 mutated in Heimler syndrome. Molecular Genetics and Genomic Medicine. 2017; 5: 531–552.

Nicolis E, Bonizzato A, Assael BM, et al. Identification of novel mutations in patients with Shwachman-Diamond syndrome. Human Mutation. 2005; 25, 410.

Perobelli S, Alessandrini F, Zoccatelli G. Diffuse alterations in grey and white matter associated with cognitive impairment in Shwachman–Diamond syndrome: evidence from a multimodal approach. Neuro Image Clinical. 2015; 7: 721–731.

Pichler J, Meyer R, Koglmeier J, et al. Nutritional status in children with Shwachman-Diamond syndrome. Pancreas. 2015; 44: 590–5.

Pressato B, Valli R, Marletta C, et al. Deletion of chromosome 20 in bone marrow of patients with Shwachman-Diamond syndrome, loss of the EIF6 gene and benign prognosis. British Journal of Haematology. 2012; 157: 503-505.

Pressato B, Valli R, Marletta C, et al. Cytogenetic monitoring in Shwachman-Diamond syndrome: a note on clonal progression and a practical warning. Journal of Pediatrics Hematology and Oncology. 2015; 37(4): 307–310.

Rothbaum R, Perrault J, Vlachos A, et al. Shwachman-Diamond syndrome: report from an international conference. Journal of Pediatrics. 2002; 141(2): 266–270.

Roy B, Friesen WJ, Tomizawa Y, et al. Ataluren stimulates ribosomal selection of near-cognate tRNAs to promote nonsense suppression. Proceedings of the National Academy of Sciences of the United States of America. 2016; 113: 12508-12513, doi:10.1073/pnas.1605336113.

Ryan N J. Ataluren: first global approval. Drugs. 2014; 74: 1709-1714, doi:10.1007/s40265-014-0287-4.

Sakuru, R, Bollu, PC. Hurler Syndrome. StatPearls Publishing: Treasure Island, FL, USA, 2020.

Samanta A, Stingl K, Kohl S, et al. Ataluren for the Treatment of Usher Syndrome 2A Caused by Nonsense Mutations. International Journal of Molecular Sciences. 2019; 20, 6274.

Shammas C, Menne TF, Hilcenko C, et al. Structural and mutational analysis of the SBDS protein family. Insight into the leukemia-associated Shwachman-Diamond Syndrome. Journal of Biological Chemistry. 2005; 280(19): 19221–9.

Shwachman H, Diamond LK, Oski FA, et al. The syndrome of pancreatic insufficiency and bone marrow dysfunction. Journal of Pediatrics. 1964; 65: 645-663.

Stepensky P, Chacón-Flores M, Kim KH, et al. Mutations in EFL1, an SBDS partner, are associated with infantile pancytopenia, exocrine pancreatic insufficiency and skeletal anomalies in a ShwachmanDiamond like syndrome. Journal of Medical Genetics. 2017; March 22. Doi: 10.1136/jmedgenet-2016-104366.

Tan S, Kermasson L, Hoslin A, et al. EFL1 mutations impair eIF6 release to cause Shwachman-Diamond syndrome. Blood. 2019 Jul 18; 134(3): 277-290. doi: 10.1182/blood.2018893404.

Toiviainen-Salo S, Mayranpaa MK, Durie PR, et al. Shwachman-Diamond syndrome is associated with low-turnover osteoporosis. Bone. 2007; 41: 965-972.

Toiviainen-Salo S, Makitie O, Mannerkoski M, et al. Shwachman-Diamond syndrome is associated with structural brain alterations on MRI. American Journal of Medical Genetics Part A. 2008; 146A: 1558-1564.

Thada V, Miller JN, Kovacs AD, et al. Tissue-specific variation in nonsense mutant transcript level and drug-induced read-through efficiency in the Cln1(R151X) mouse model of INCL. Journal of cellular and molecular medicine. 2016; 20, 381-385, doi:10.1111/jcmm.12744.

Tutone M, Pibiri I, Lentini L, et al. Deciphering the Nonsense Readthrough Mechanism of Action of Ataluren: An in Silico Compared Study. ACS Medicinal Chemistry Letter. 2019; 10: 522–527.

Valli R, Frattini A, Minelli A. Shwachman-Diamond syndrome: diagnosis, pathogenesis and prognosis, Expert Opinion on Orphan Drugs. 2017a; 5: 10: 753-767

Valli R, De Paoli E, Nacci L, et al. Novel recurrent chromosome anomalies in Shwachman-Diamond syndrome. Pediatr Blood Cancer. 2017b; 64: 8.

Welch EM, Barton ER, Zhuo J, et al. PTC124 targets genetic disorders caused by nonsense mutations. Nature. 2007; 447: 87-91, doi:10.1038/nature05756.

Woloszynek JR, Rothbaum RJ, Rawls AS, et al. Mutations of the SBDS gene are present in most patients with Shwachman-Diamond syndrome. Blood. 2004; 104(12): 3588–3590.

Wong TE, Calicchio ML, Fleming MD, et al. SBDS protein expression patterns in the bone marrow. Pediatric Blood Cancer. 2010; 55(3): 546-549

Wong, CC, Traynor D, Basse N, et al. Defective ribosome assembly in Shwachman–Diamond syndrome. Blood. 2011; 118: 4305–4312.

Zainal Abidin N, Haq IJ, Gardner AI, et al. Ataluren in cystic fibrosis: development, clinical studies and where are we now? Expert Opinion in Pharmacotherapy. 2017; Sep; 18(13): 1363-1371. doi: 10.1080/14656566.2017.1359255.

Zhang S, Shi M, Hui CC, et al. Loss of the mouse ortholog of the Shwachman-Diamond syndrome gene (Sbds) results in early embryonic lethality. Molecular Cell Biology. 2006; 26(17): 6656–6663.

Zhu W, Li GX, Chen HL, et al. The role of eukaryotic translation initiation factor 6 in tumors (review). Oncology Letters. 2017; 14: 3–9.